Norges miljø- og biovitenskapelige universitet

Master's Thesis 2019 60 ECTS
Faculty of Chemistry, Biotechnology and Food Science

Synthesis of the Methyl Ester of $MaR2_{n\text{-}3\ DPA}$

Jeanne Sønderskov Rasmussen
Master's degree in Chemistry and Biotechnology

Acknowledgements

The master's degree was performed as collaboration between the Faculty of Chemistry, Biotechnology and Food Science at the Norwegian University of Life Sciences and the Department of Pharmacy, University of Oslo. The practical work as part of this thesis was conducted in the LIPCHEM group at the Section of Pharmaceutical Chemistry.

First, I would like to thank my two supervisors, Professor Trond Vidar Hansen and Professor Yngve Stenstrøm for excellent guidance, encouragement and especially, for sharing long-time experience.

Also, thanks to Dr. Jørn Tungen and Associate professor Anders Vik for solid guidance and teaching, especially during the time in the laboratory. I would also like to thank the rest of the LIPCHEM group. It has been a great experience to be a part of a research group and witness the impressive work that is carried out.

Also, I am very grateful for sharing this challenging period with the four master students in pharmaceutical chemistry, Amalie Føreid Reinertsen, Marie Hermansen Mørk, Aina Kristin Pham and Margrethe Kristiansen. It has been nice to get to know you and follow your progress as well.

Finally, an enormous thank to my lovely boyfriend, family and friends. Thanks for fantastic support and cheering through my six years of education.

Blindern, May 2019

Jeanne Sønderskov Rasmussen

Abstract

This master thesis presents the first synthesis of the methyl ester of the specialized pro-resolving mediator named $MaR2_{n\text{-}3\ DPA}$. The stereoselective synthesis is based on a *Z*-selective Lindlar reaction, a Sonogashira coupling reaction and a Takai olefination, as the key steps. These efforts resulted in a satisfactory synthesis of the methyl ester of $MaR2_{n\text{-}3\ DPA}$ in 12 steps and in 95% purity, affording multi milligrams of the material. Synthesis of the free acid of $MaR2_{n\text{-}3\ DPA}$ was achieved, however, due to limited time period not in an acceptable degree of purity.

Graphic abstract

The Wittig salt

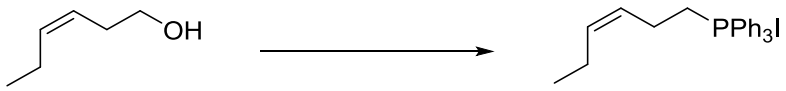

The middle fragment

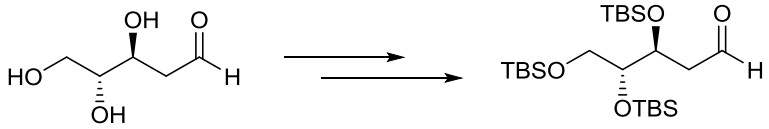

The alpha-fragment

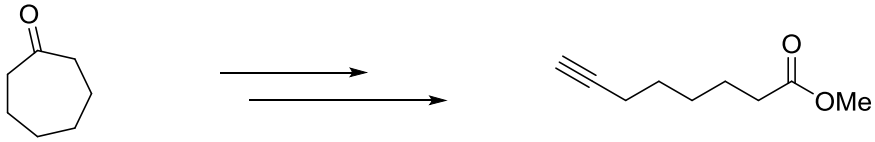

Assembly of the fragments

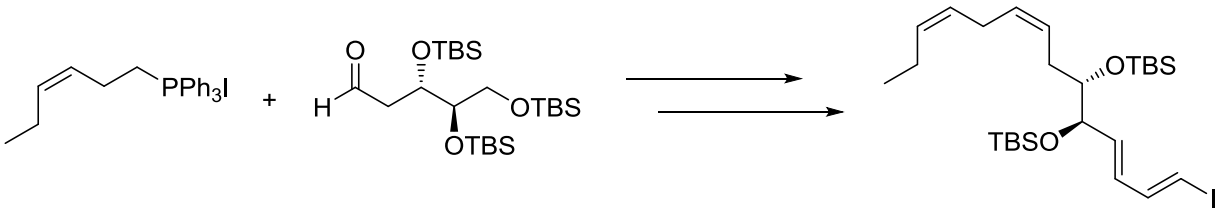

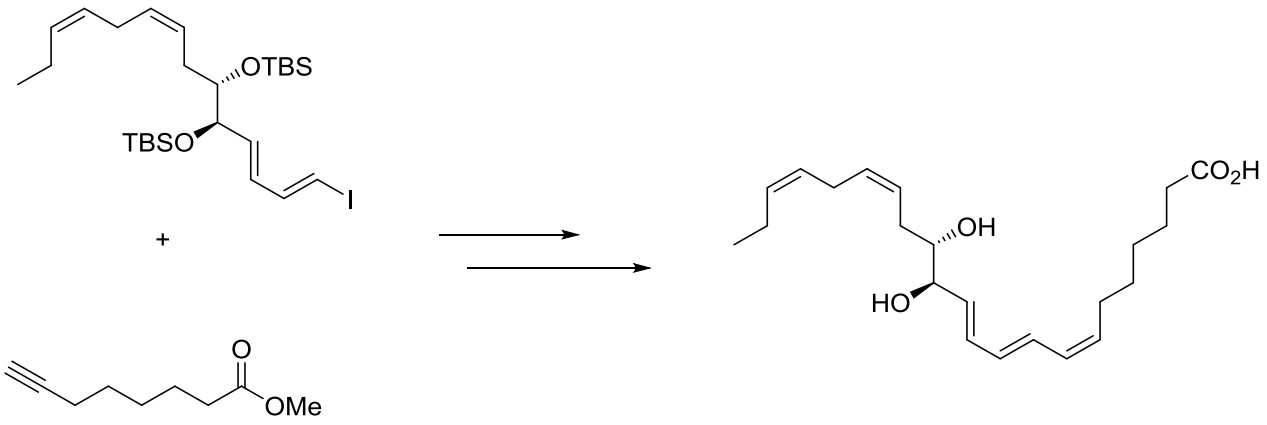

List of abbreviations

AA	Arachidonic acid ((5*Z*,8*Z*,11*Z*,14*Z*)-eicosatetraenoic acid)
CAM	Cerium ammonium molybdate
COX	cyclooxygenase enzyme
DHA	Docosahexaenoic acid ((4*Z*,7*Z*,10*Z*,13*Z*,16*Z*,19*Z*)-docosahexaenoic acid)
DMP	Dess-Martin periodinane
n-3 DPA	Docosapentaenoic acid ((7*Z*,10*Z*,13*Z*,16*Z*,19*Z*)-docosapentaenoic acid)
EPA	Eiocosapentaenoic acid ((5*Z*,8*Z*,11*Z*,14*Z*,17*Z*)-eicosapentaenoic acid)
GPCR	G protein-coupled receptor
KHMDS	Potassium *bis*(trimethylsilyl)amide
LC/MS-MS	Liquid chromatography - tandem mass spectra
LOX	lipoxygenase enzyme
LT	Leukotriene
LX	lipoxin
MaR	Maresin
*m*CPBA	*meta*-chloroperbenzoic acid
MCTR	Maresin conjugated in tissue regeneration
NaHMDS	Sodium *bis*(trimethylsilyl)amide
NBS	N-bromosuccinimide
PCTR	Protectin conjugated in tissue regeneration
PD	Protectin
PG	Prostaglandin

PMN	Polymorphonuclear neutrophil
PTSA	*p*-toluenesulfonic acid
PUFA	Polyunsaturated fatty acid
RCTR	Resolvins conjugated in tissue regeneration
RvD	D-series Resolvins
RvE	E-series Resolvins
TBSOTf	*tert*-butyldimethylsilyl trifluoromethanesulfanoate
TBAF	Tetrabutylammonium fluoride
TBS	*tert*-butyldimethylsilyl
THF	Tetrahydrofuran

Table of Contents

1 Introduction

1.1 Background

1.1.1 Inflammation

All living organisms depend on an efficient defense system to protect itself against exogenous pathogens and repair damaged tissue after infection, physical or chemical stress. Inflammation is an important innate defense mechanism which is activated when tissue is damaged or invaded by pathogens. The main purpose of the inflammatory response is limiting tissue damage, neutralize and eliminate pathogens as well as clearing and restoring the function and structure of the affected tissue.[1,2] Inflammation is divided into acute or chronic inflammation, where acute inflammation is a self-resolving initial response, while chronic inflammation is defined by an unresolved reaction and occurs over an extended period of time (**Fig. 1**).[1]

Acute inflammation involves a complex orchestration of events.[1,3] Among these events are initiate the response by releasing chemical signal molecules which in turn increases the permeability of endothelium cells. Consequently, it leads to edema and infiltration of polymorphonuclear leukocytes (PMN), inflammatory lymphocytes and macrophages to the sites of infection or injury (**Fig. 1**).[1] As one of the triggering responses the omega-6 polyunsaturated fatty acid (PUFA), arachidonic acid (AA) (**1**), is converted to pro-inflammatory lipid mediators such as leukotrienes (LTs) and prostaglandins (PGs) by the enzymes lipoxygenases (LOXs) and cyclooxygenases (COXs).[4] The potent bioactive compounds interact with individually G protein-coupled receptors (GPCRs), which promote recruitments of PMNs.[4] Then the PMNs neutralize and clear foreign invaders by phagocytosis, ingesting microorganisms or particles.[1,3] Lipoxins (LXs) are also biosynthesized from AA (**1**), but dissociate from LTs and PGs due to their anti-inflammatory and pro-resolving properties as signals for the resolution phase.[5,6]

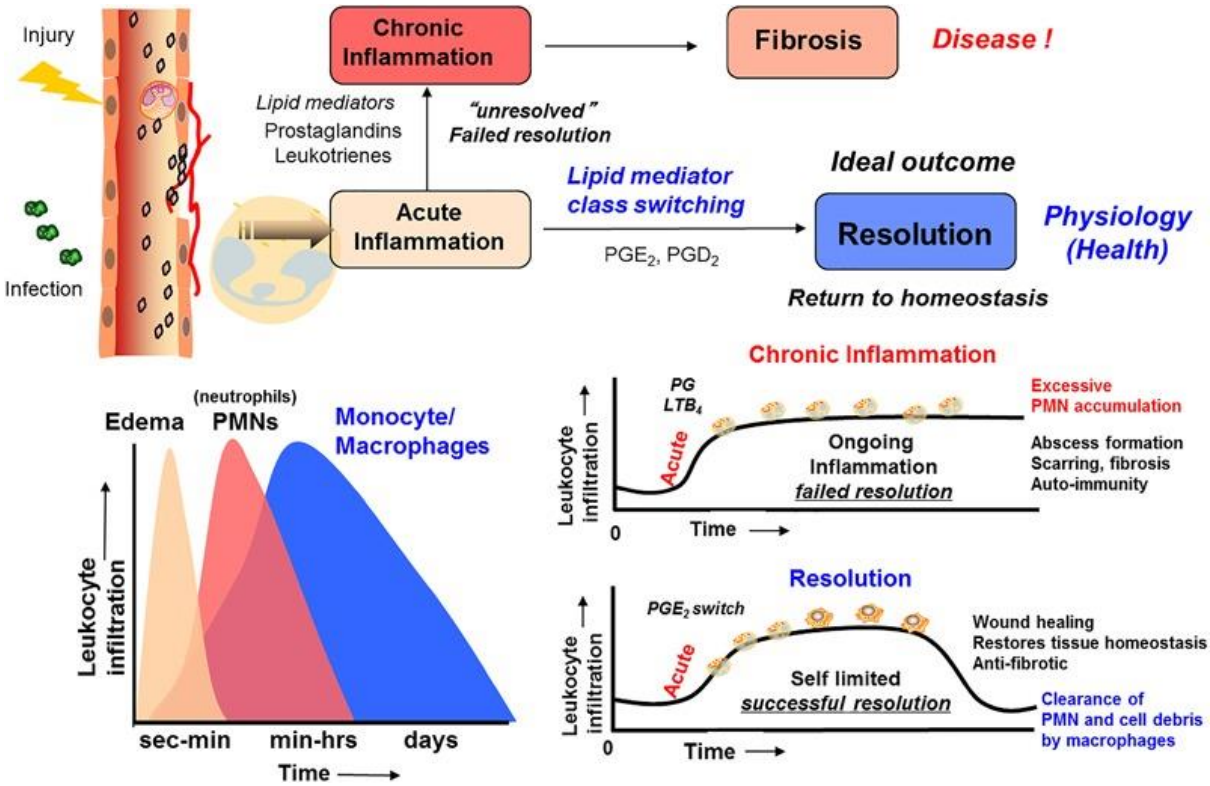

Figure 1. Illustration of the inflammatory response leading to resolution, the ideal outcome of inflammation, or fails resolution leading to chronic inflammation.[7]

1.1.2 Resolution of inflammation and specialized pro-resolving mediators

Unresolved acute inflammation can result in excessive accumulation of PMNs, LTs, PGs and debris, leading to a condition of chronic inflammation (**Fig. 1**).[3] This in turn can lead to fibrosis of the affected tissue and is linked to a number of chronic diseases such as cardiovascular disease, cancer, rheumatoid arthritis and neurological disorders.[2,8] This highlights the essential purpose of the resolution phase.[1,9] Resolution of inflammation is characterized by cessation of neutrophil influx and clearance of neutrophils and cell debris by macrophages, which, in ideal outcome, result in return to homeostasis.[1,10]

The resolution phase is a complex and not fully understood mechanism. However, studies have revealed various endogenous lipid mediators with the ability to initiate and resolve the acute inflammatory response. Hence, a lipid mediator class switch has been suggested (**Fig. 1** and **Fig. 3**).[3,11] In details, the initial actions, controlled by pro-inflammatory lipid mediators, i.e. leukotriene and prostaglandins, switch to the anti-inflammatory and pro-resolving actions of specialized pro-

resolving mediators (SPMs). In the presence of COX and LOX enzymes, SPMs are biosynthesized from oxygenated PUFAs, and involve families of lipoxins, resolvins, protectins and maresins.[9,12] As shown in **Figure 2**, the E-series resolvins (RvE) are produced from eicosapentaenoic acid (EPA) (**2**),[13] while the D-series resolvins (RvD),[14] protectins (PD),[14-16] maresins (MaR),[17-19] and the recently found sulfido-conjugates, resolvins conjugated in tissue regeneration (RCTRs), protectins conjugated in tissue regeneration (PCTRs) and maresins conjugated in tissue regeneration (MCTRs), are biosynthesized from docosahexaenoic acid (DHA) (**3**).[20-23] Series of SPMs biosynthesized from docosapentaenoic acid (n-3 DPA) (**4**), e.g. $RvD1_{n\text{-}3\ DPA}$, $PD1_{n\text{-}3\ DPA}$ and $MaR1_{n\text{-}3\ DPA}$ have also been reported.[24]

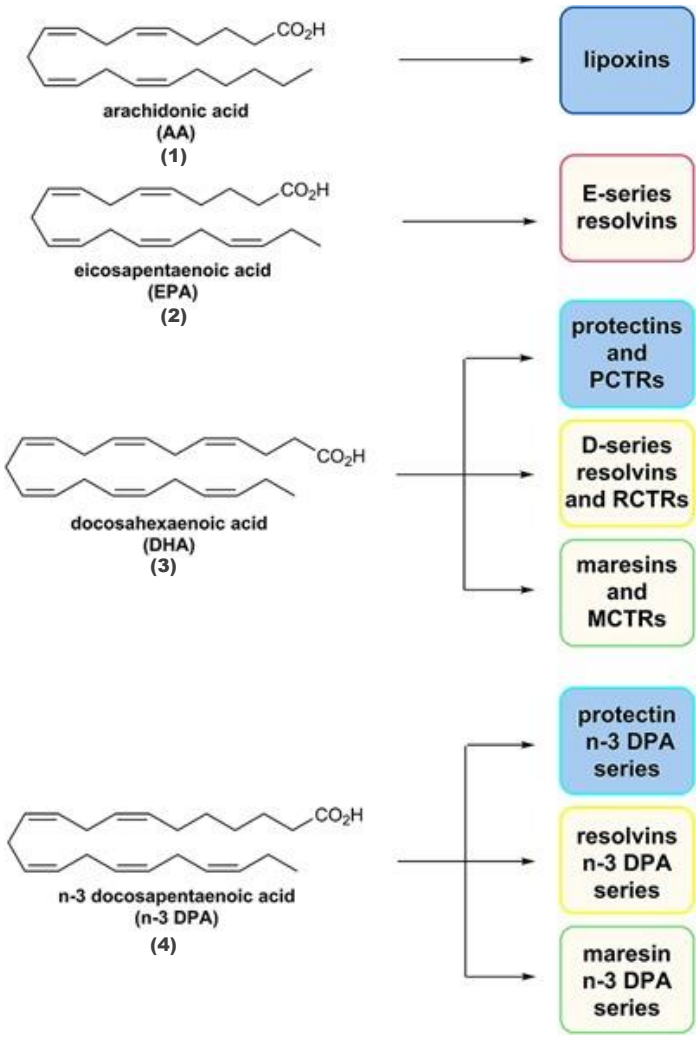

Based on an excess of biological activities in promoting the termination of ongoing inflammation, individual families of SPMs have attracted interest from the biomedical, pharmacological and synthetic organic communities.[12,25] SPMs act on individual GPCRs as potent agonists, where studies have observed reduction of further PMNs recruitment to the inflammatory site, accelerated termination of resolution time *in vivo* as well as increasing clearance of bacteria and apoptotic cells.[3,14,26,27] SPMs have also shown capabilities of protecting the host from bacterial infections[28] and controlling the re-generation of the tissue.[22,29]

Figure 2. The chemical structures of the oxygenated PUFAs and the associated SPMs families biosynthesized by the outlined PUFAs.[7]

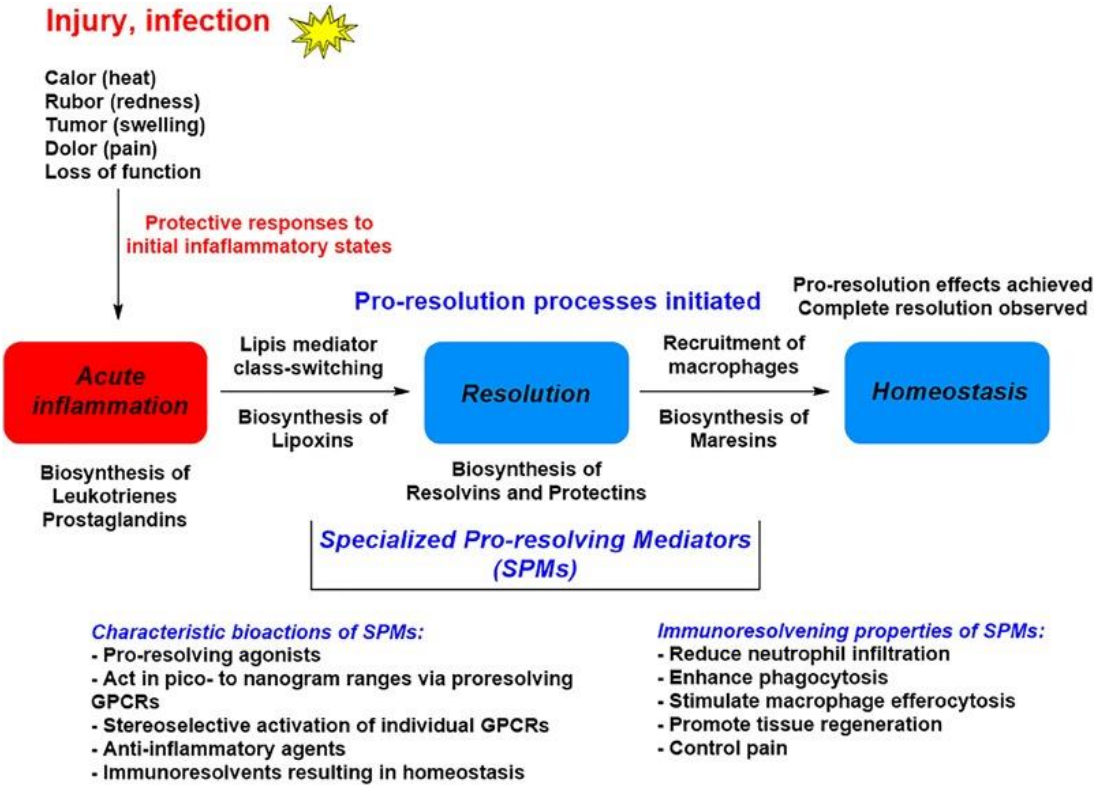

Figure 3. Overview of the lipid mediator class switch and SPMs characteristic bioactions and immunoresolving properties.[7]

1.1.3 Maresin 1 and Maresin 2

Maresin 1 (MaR1) (**7**) was the first identified molecule of the maresin family of SPMs biosynthesized from DHA (**3**). The name maresin was given since it was reported as a *ma*crophage mediator in *re*solving *in*flammation.[19] D-series resolvins and protectins were already known to be biosynthesized from DHA (**3**) via 17*S*-hydroxydocosa-4*Z*,7*Z*,10*Z*,13*Z*,15*E*,19*Z*-hexaenoic acid (17*S*-HDHA). Using self-resolving inflammatory exudates and lipid mediator metabolomics, a new possible precursor, 14*S*-hydroxydocosa-4*Z*,7*Z*,10*Z*,12*E*,16*Z*,19*Z*-hexaenoic acid (14*S*-HDHA), was found formed in the resolution phase. Further analysis using LC/MS-MS-based mediator lipidomics, MaR1 (**7**) was identified as one of the products biosynthesized from DHA (**3**). Later, an additional maresin, MaR2 (**8**), from DHA (**3**) was identified.[18]

In the biosynthesis of MaR1 (**7**), DHA (**3**) is converted by human macrophage 12-lipoxygenase to 14*S*-HpDHA (**5**). The peroxide intermediate **5** is then converted into 13*S*,14*S*-epoxy-DHA (**6**) followed by enzymatic hydrolysis to give MaR1 (**7**).[30] The biosynthesis for MaR1 (**7**) is shown in

Scheme 1. The proposed biosynthetic pathway of MaR2 (**8**) is comparable to the biosynthesis of MaR1 (**7**) but the 13*S*,14*S*-epoxy-maresin intermediate **6** is converted via the enzyme soluble epoxide hydrolase to MaR2 (**8**) as shown in **Scheme 1**. [18]

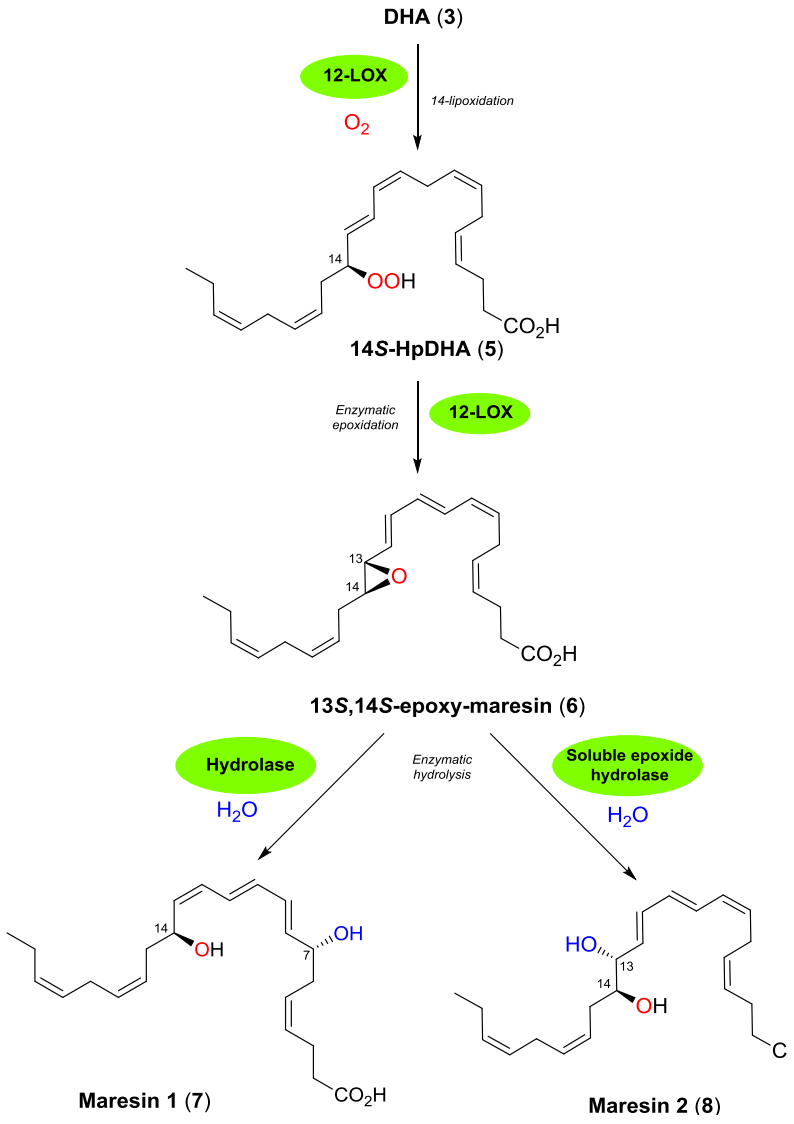

Scheme 1. Biosynthetic pathway for MaR1(**7**) and the proposed biosynthesis of MaR2 (**8**).

The first reported total synthesis of MaR1 (**7**) was achieved in 17 steps which also was used to confirm the absolute configuration of MaR1 (**7**), 7*R*,14*S*-dihydroxydocosa-4Z,8*E*,10*E*,12*Z*,*16Z*,*19Z*-hexaenoic acid.[17,31] Follow-up studies have accomplished more efficient and selective synthetic pathways for MaR1 (**7**).[32,33] An highly stereoselective and efficient synthesis of MaR1 (**7**) was reported by the LIPCHEM group in 2015, using an Evans-Nagao aldol reaction as one of the key

reactions. This synthesis gave MaR1 (**7**) in 10 steps.[34] The retrosynthesis for this synthesis is shown in **Scheme 2**.

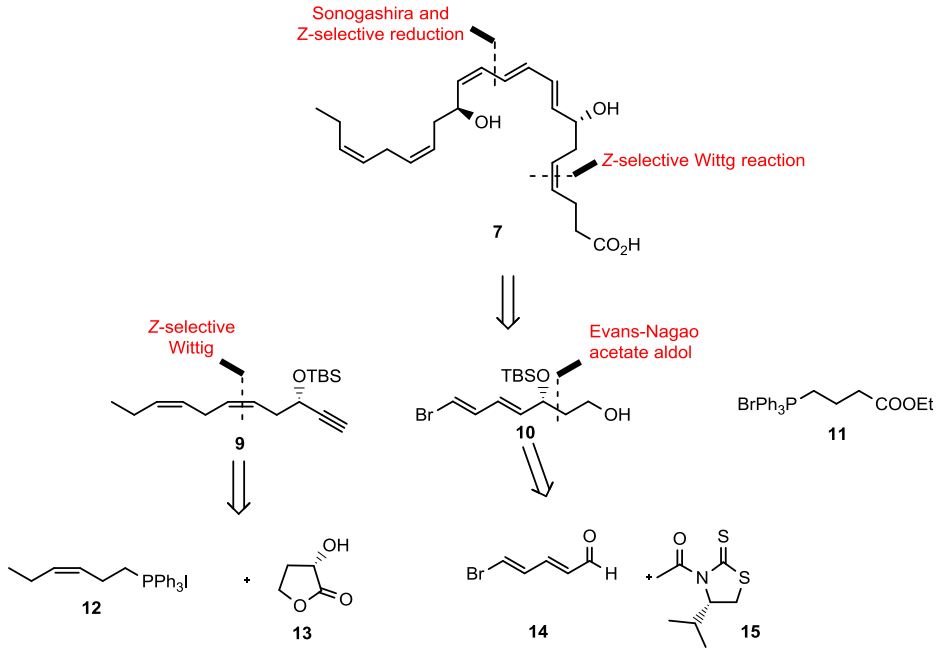

Scheme 2. Retrosynthesis analysis of MaR1 (**7**) using the Evans-Nagao aldol reaction.[34]

MaR1 (**7**) displays several interesting biological effects *in vitro* and *in vivo*, such as reducing PMN infiltration,[19] stimulate macrophage phagocytosis and efferocytosis,[19] regulate tissue regeneration and pain resolution[17] as well as mitigate lipopolysaccharide-induced lung injury in mice.[35] MaR2 (**8**) has also displayed potent actions, e.g. reducing neutrophil infiltration and enhancing human macrophage phagocytosis.[18]

1.1.4 Maresins biosynthesized from n-3 DPA

In 2013 Dalli and coworkers reported several new series of SPMs biosynthesized from n-3 DPA (**4**).[24] n-3 DPA (**4**), consisting of 22 carbons and five double bonds, is an elongated product of EPA (**2**) and an intermediate in the biosynthesis of DHA (**3**).[36] Using a self-limited model of inflammation and targeted metabololipidomics during onset and resolution of acute inflammation, they uncovered the novel n-3 DPA products, $MaR1_{n\text{-}3\ DPA}$ (**19**), $MaR2_{n\text{-}3\ DPA}$ (**20**) and $MaR3_{n\text{-}3\ DPA}$ (**17**) as well as $RvD1_{n\text{-}3\ DPA}$, $RvD2_{n\text{-}3\ DPA}$, $RvD5_{n\text{-}3\ DPA}$, $PD1_{n\text{-}3\ DPA}$ and $PD2_{n\text{-}3\ DPA}$.

A proposed biosynthesis of the n-3 DPA maresin family is shown in **Scheme 3**. First, n-3 DPA (**4**) is converted by 12-LOX to 14*S*-hydroperoxy-7*Z*,10*Z*,12*E*,16*Z*,19*Z*-docosapentaenoic acid (14*S*-H*p*DPA) (**16**). Subsequently, it is converted to epoxide 13,14*S*-epoxy-MaR$_{n\text{-}3\ DPA}$ (**18**) which is enzymatically hydrolyzed to MaR1$_{n\text{-}3\ DPA}$ (**19**) and MaR2$_{n\text{-}3\ DPA}$ (**20**).[24] A second oxidation at the omega-2 position of 14*S*-HpDPA (**16**) can also occur to form MaR3$_{n\text{-}3\ DPA}$ (**17**). Results obtained from chiral lipidomics analysis indicated the *S* configuration for the epoxy intermediate, as the major isomer in inflamed tissue. Therefore, the *S* configuration at position 14 was assumed to be maintained in the biosynthesis of the maresins.[24] The configuration of C-13 is not yet confirmed.

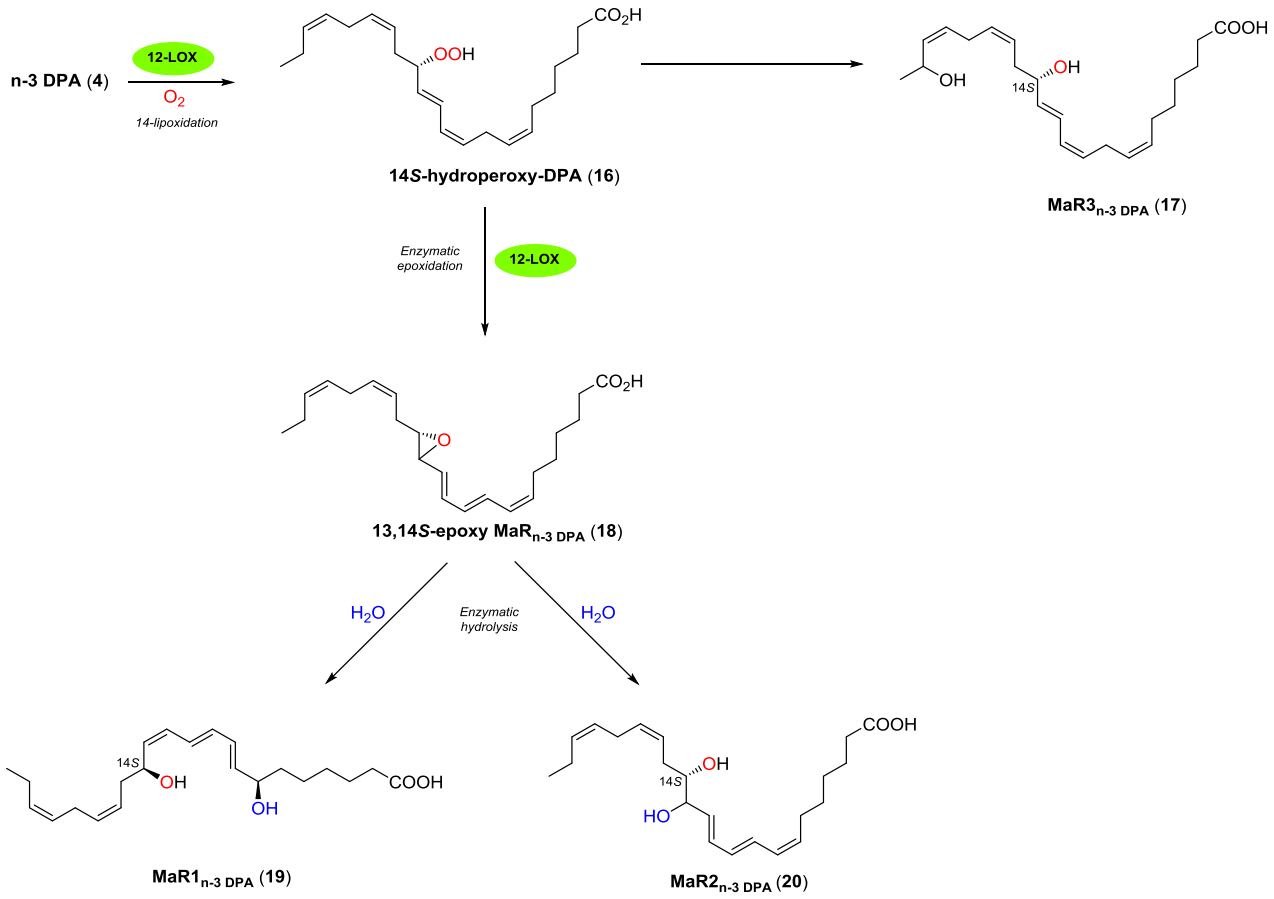

Scheme 3. Proposed biosynthesis of MaR1$_{n\text{-}3\ DPA}$ (**19**), MaR2$_{n\text{-}3\ DPA}$ (**20**) and MaR3$_{n\text{-}3\ DPA}$ (**17**), where known, the absolute configuration is included.

The complete stereochemical configuration of MaR1$_{n\text{-}3\ DPA}$ (**19**) was achieved by matching the biological actions of the synthetic material and the biologically formed MaR1$_{n\text{-}3\ DPA}$ (**19**), being (7*S*,8*E*,10*E*,12*Z*,14*S*,16*Z*,19*Z*)-7,14-dihydroxydocosa-8,10,12,16,19-pentaenoic acid.[37] MaR2$_{n\text{-}3\ DPA}$

(**20**) and MaR3$_{n\text{-}3\ DPA}$ (**17**) have never been prepared or subjected to biological investigations before and their exact configurational assignments are still elusive.

The only published total synthesis of MaR1$_{n\text{-}3\ DPA}$ (**19**) is reported by Hansen and coworkers in 12% overall yield in 11 steps with a sp^3-sp^3 Negishi cross-coupling reaction as one of the key reactions (**Scheme 4**).[37] Total syntheses of either MaR2$_{n\text{-}3\ DPA}$ (**20**) or MaR3$_{n\text{-}3\ DPA}$ (**17**) have not been reported.

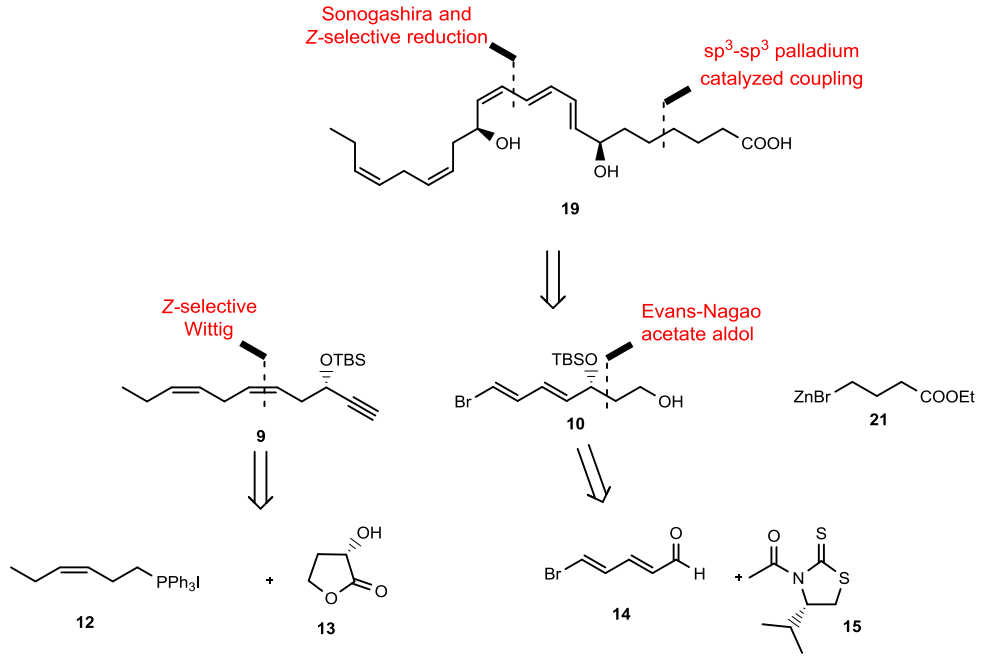

Scheme 4. Retrosynthetic analysis of MaR1$_{n\text{-}3\ DPA}$ (**19**).[37]

In vitro bioaction studies of synthesized MaR1$_{n\text{-}3\ DPA}$ (**19**) revealed potent anti-inflammatory and pro-resolving effects in nanomolar range, as potent stimulation of macrophage efferocytosis of apoptotic human neutrophils, as shown in **Figure 4**.[37] This is very similar potency and activity as for DHA-derived maresin 1 (**7**). The ethyl ester of MaR1$_{n\text{-}3\ DPA}$ showed capability to stimulate macrophage efferocytosis too, but in a lower extent. A mixture of MaR1$_{n\text{-}3\ DPA}$ (**19**) and MaR2$_{n\text{-}3\ DPA}$ (**20**) (ratio 4:1) have shown significantly reduction in PMN recruitment and pro-inflammatory cytokine exudate levels *in vivo* (**Fig. 5**).[24]

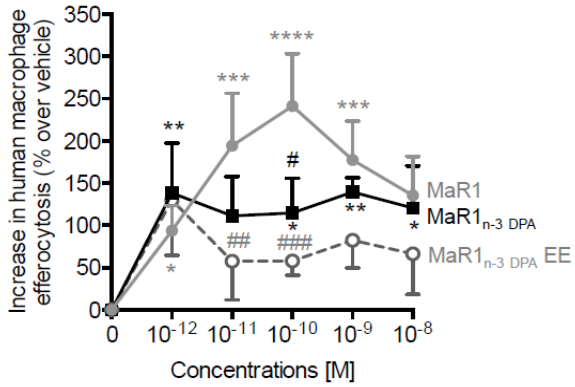

Figure 4. *In vitro* data of $MaR1_{n\text{-}3\ DPA}$ (**19**), its ethyl ester and MaR1 (**7**).[37]

1.1.5 Sulfido-conjugated maresins

Dalli and coworkers reported in 2014 a new series of bioactive mediators in planaria, mouse and human tissues, which promoted repair and regeneration during infection.[23] They identified two sulfido-conjugated mediators, called maresins conjugates in tissue regeneration, MCTR1 (**22**) and MCTR2 (**23**). In 2016 they reported another maresin conjugates in tissue regeneration called MCTR3 (**24**).[38]

Dalli and coworkers suggested a biosynthesis of MCTR1 (**22**) and MCTR2 (**23**).[23] The proposed biosynthesis is shown in **Scheme 5**. Like for MaR1 (**7**), DHA (**3**) is converted by LOX to 13*S*,14*S*-HpDHA (**5**), which further is transformed into the epoxide (**6**). Further it is enzymatically converted to MCTRs (**22**-**24**).

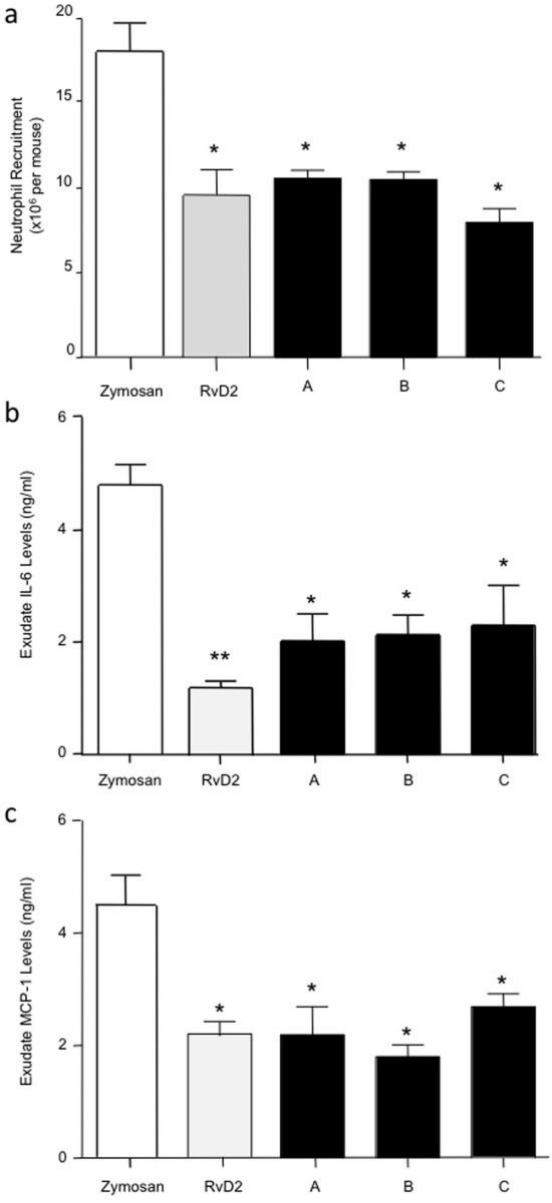

Figure 5. SPMs biosynthesized from n-3 DPA display anti-inflammatory actions *in vivo* as similar levels as RvD2. (A) is a mixture of $RvD1_{n\text{-}3\ DPA}$ and $RvD2_{n\text{-}3\ DPA}$ in ratio ~3:1, (B) is a mixture of $MaR1_{n\text{-}3\ DPA}$ and $MaR2_{n\text{-}3\ DPA}$ in ratio ~4:1 and (C) is a mixture of $RvD5_{n\text{-}3\ DPA}$ and $PD1_{n\text{-}3\ DPA}$ in ratio ~9:1.[24]

The exact structures of MCTRs (**22**-**24**) were established using LC/MS-MS on MCTRs isolated from human macrophages and murine infectious exudates, and synthetic prepared MTCRs.[38,39] The synthetic MCTRs (**22**-**24**) were prepared by Rodriguez and Spur.[39] The key steps were Wittig reactions, selective epoxide formation and epoxide opening with glutathione (**25**), L-cysteinylglycine (**27**) or L-cystein methyl ester hydrochloride (**28**). The retrosynthesis analysis is shown in **Scheme 6**.

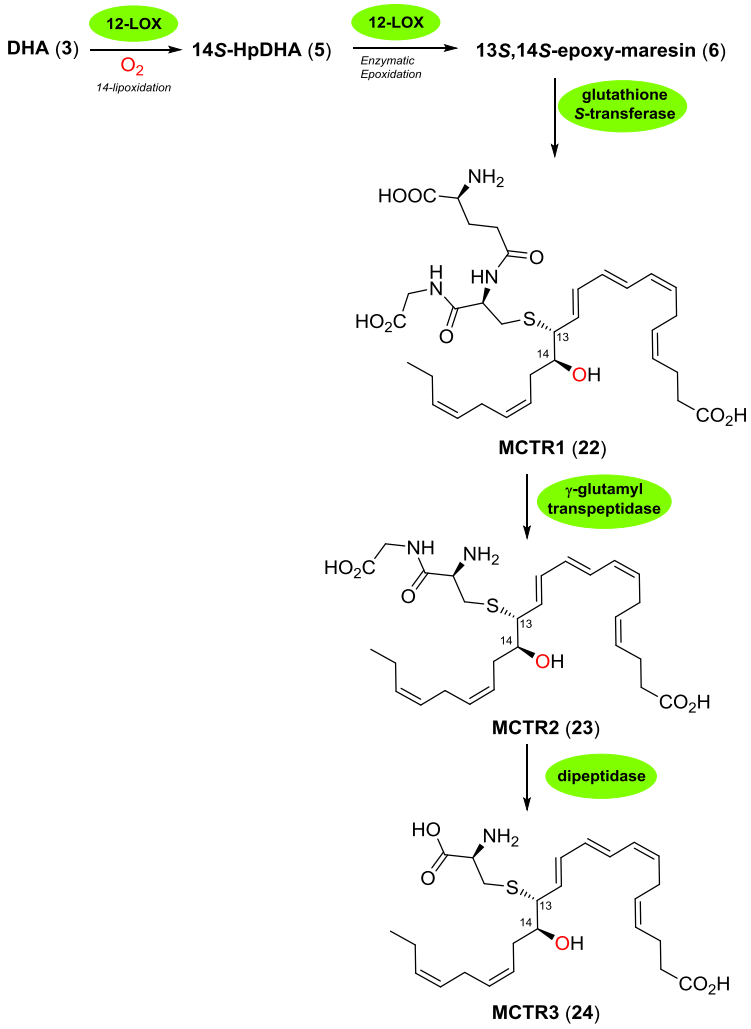

Scheme 5. Proposed MCTR (**22**-**24**) biosynthetic pathway.[23,38]

The MCTRs (**22**-**24**) have shown several interesting bioactions. They promote resolution of *E. coli* infections in mice by regulating host responses to clear infections and promote tissue regeneration.[23,38] Administered at onset or peak inflammation, MCTRs increase bacterial phagocytosis and clearance, limiting neutrophil infiltration, promoting efferocytosis of apoptotic cells and reducing eicosanoids.[38]

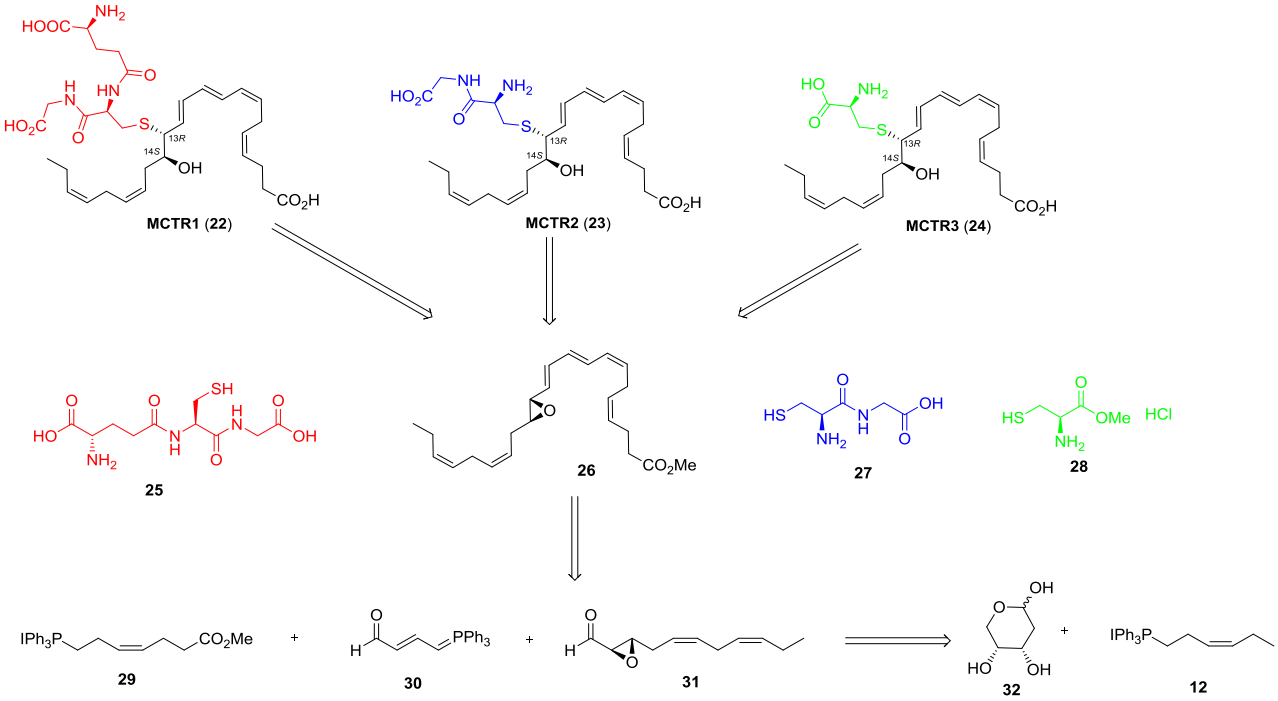

Scheme 6. Retrosynthetic approach to 13*R*,14*S*-MCTR1 (**22**), 13*R*,14*S*-MCTR2 (**23**) and 13*R*,14*S*-MCTR3 (**24**).[39]

1.2 Synthetic methods

1.2.1 Aim of synthesis

The resolution phase was once believed to be a passive process, but today it is known as a biosynthetically active process, regulated and controlled by chemical mediators.[10,40] The new way of understanding the resolution phase has resulted in an interest in developing new classes of anti-inflammatory drugs, where the endogenously formed SPMs are used as lead compounds. Hence, detailed information on the chemical structures, cellular functions and distinct biosynthetic pathways of specialized pro-resolving lipid mediators are necessary, whereby stereoselective syntheses of SPMs are essential.

The aim for this master thesis is to synthesize the SPM MaR2$_{n\text{-}3\ DPA}$ (**20**) which never has been prepared before. The exact configurational assignment is still elusive. However, based on biosynthetic considerations and experience from other structures of SPMs, the MaR2$_{n\text{-}3\ DPA}$ (**20**) is envisioned as the structure shown in **Figure 6**. A highly stereoselective synthesis of the presented configuration is therefore the aim of the synthesis.

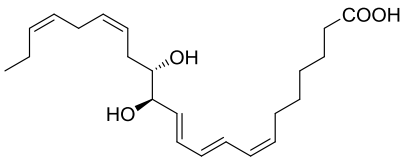

(7*Z*,9*E*,11*E*,13*R*,14*S*,16*Z*,19*Z*)-13,14-dihydroxydocosa-7,9,11,16,19-pentaenoic acid (**20**)

Figure 6. Anticipated structure of MaR2$_{n\text{-}3\ DPA}$ (**20**).

The synthetic strategy for the synthesis of MaR2$_{n\text{-}3\ DPA}$ (**20**) is based on the convergent strategy of the published synthesis of RvD1$_{n\text{-}3\ DPA}$ reported by the LIPCHEM group in 2019.[41] The retrosynthetic analysis of MaR2$_{n\text{-}3\ DPA}$ (**20**) is showed in **Scheme 7**. It reveals three fragments, **33**, **34** and **40**, prepared from the commercially available molecules, 2-deoxy-D-ribose (**32**), cycloheptanone (**36**) and *(Z)*-hex-3-en-1-ol (**41**). The key reactions in the synthesis of MaR2$_{n\text{-}3\ DPA}$ (**20**) will be further discussed in the below sections.

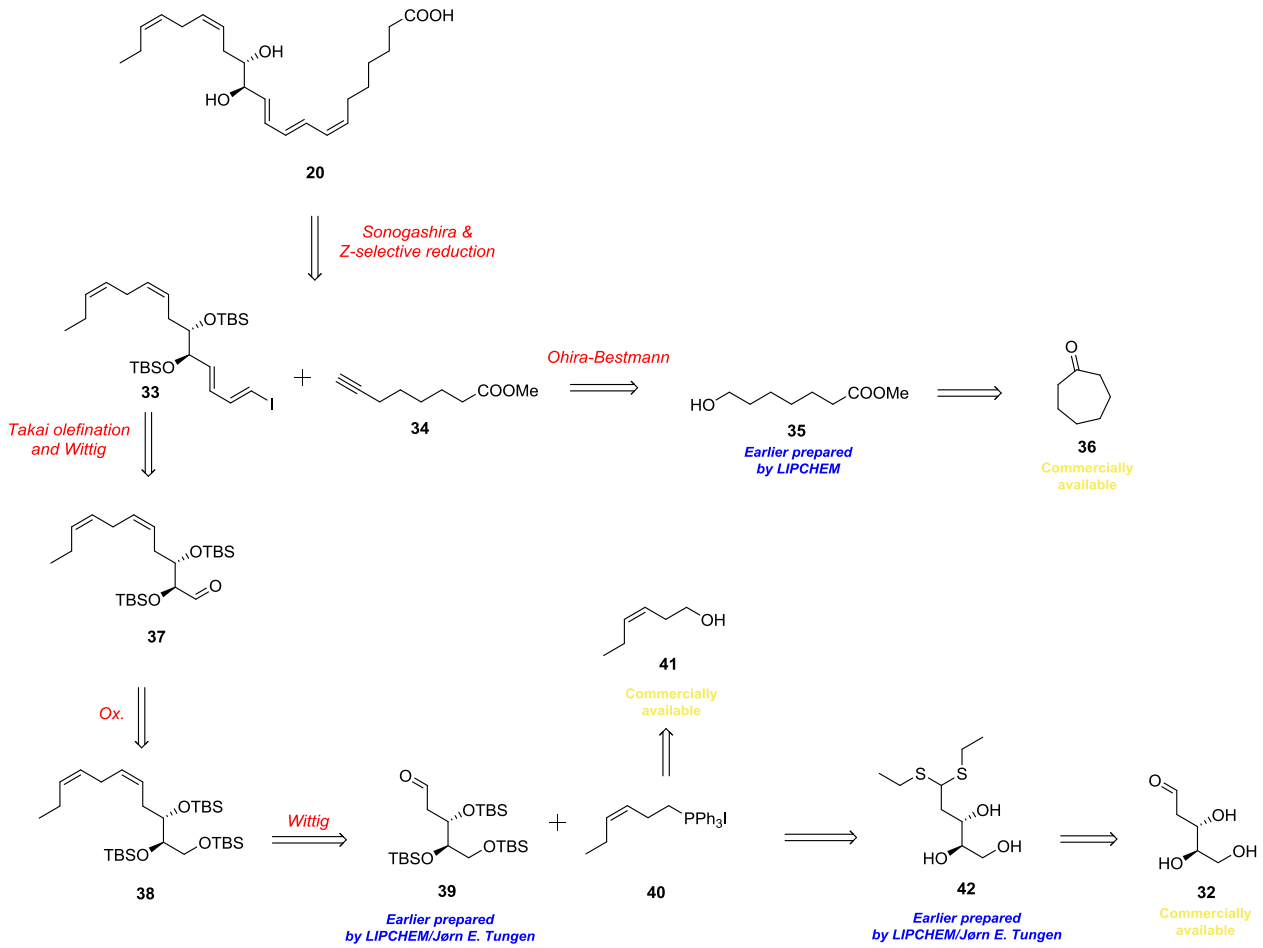

Scheme 7. Retrosynthetic analysis of MaR2$_{n\text{-}3\ DPA}$ (**20**)

1.2.2 The Wittig reaction

The Wittig reaction, discovered by Georg Wittig in 1954, is a widely used procedure for preparing alkenes from aldehydes and ketones.[42,43] The aldehyde or ketone reacts with a triphenyl phosphonium ylide to provide alkene and triphenylphosphine oxide. An ylide has positive and negative charges on adjacent atoms. From the nature of the used ylide the geometry of the formatted double bond can be predicted. Stabilized ylides result in *E*-alkenes formed with a high selectivity while non-stabilized ylides give *Z*-alkenes in a moderate to highly selectivity.[43] A stabilized ylide has an anion-stabilizing substituent (e.g. a ketone or ester group) which stabilizes the negative charge. When the substituent is an alkyl group, the ylide is characterized as non-stabilized due to the lack of possibility for resonance stabilization. Semi-stabilized ylides are classified as ylides with conjugated substituents, such as phenyl or allyl groups, but often provide low selectivity.

The mechanism for the Wittig reaction has not yet been established and is still open for discussion.[44,45] A proposed mechanism for the *Z*-selective Wittig reaction is shown in **Scheme 8**.[46] The first step is the preparation of the ylide **46**. Alkyl halide **43** reacts in a S_N2 reaction with triphenylphosphine (**44**) to form phosphonium salt **45**. The acidic proton of phosphonium salt **45** is easily removed by a base, often NaHMDS or KHMDS, to form a resonance-stabilized phosphorus ylide **46**. When ylide **46** reacts with an aldehyde **47**, the carbon anion of ylide **46** attacks the electrophilic carbonyl carbon of **47** to form the betaine **48**, which cyclizes to a four-membered ring **49**. After fragmentation of the ring, the product alkene **50** and triphenylphosphine (**51**) are established. The byproduct **51** is typical removed by chromatography.

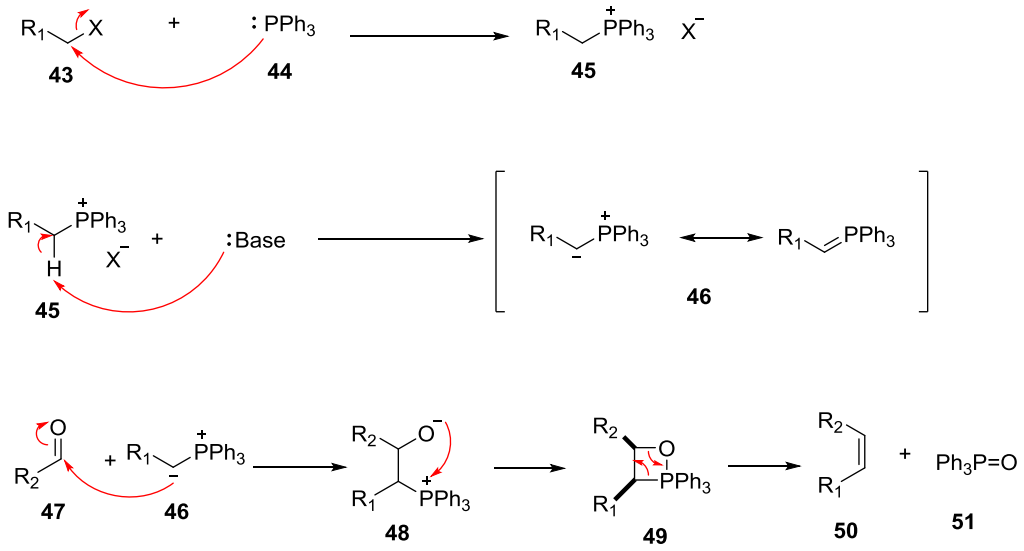

Scheme 8. Proposed mechanism for Wittig reaction.

1.2.3 The Ohira-Bestmann reaction

Acetylenes are useful building blocks in organic synthetic chemistry due to their effective abilities in coupling reactions, selective synthesis of alkenes etc. Therefore, practical protocols for acetylene synthesis are required. The Ohira-Bestmann reaction is a well-established protocol, where alkynes are obtained in good to excellent yields from aldehydes.[47,48] The procedure is an one-pot reaction which gives the product in analytic pure form after aqueous work-up using the Ohira-Bestmann reagent, dimethyl (1-diazo-2-oxopropyl) phosphonate (**53**).

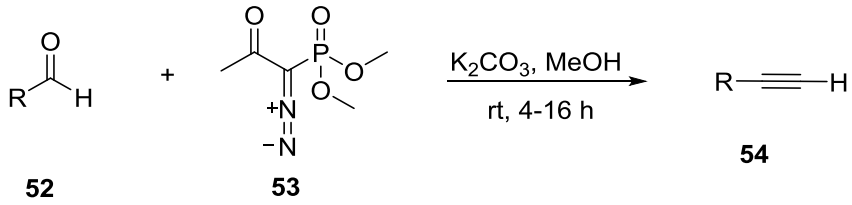

Scheme 9. Ohira-Bestmann reaction.

Before the Ohira-Bestmann reaction was reported, the Seyferth–Gilbert homologation was one of the most applied protocols for synthesis of alkynes. Due to some challenges with the Seyferth-Gilbert reagent (**55**), dimethyl (diazomethyl) phosphonate (DAMP), which should be prepared freshly, scientists needed a better protocol for preparing alkynes.[49,50]

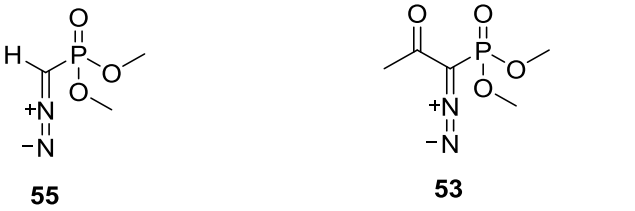

Figure 7. The Seyferth-Gilbert reagent (**55**) and the Ohira-Bestmann reagent (**53**).

A proposed mechanism of the Ohira-Bestmann reaction is shown in **Scheme 10** based on the proposed mechanism for the Seyferth-Gilbert reaction.[49] First, deprotonated methanol reacts with the Ohira-Bestmann reagent **53** to form the anion **57**. It then attacks the electrophilic carbonyl carbon of the aldehyde **52** to form the oxaphosphetane **59**. Elimination of dimethylphosphate gives resonance-stabilized vinyl diazo-intermediate **60**. Nitrogen gas is then eliminated, resulting in alkyne **54** via 1,2-migration from carben **61**.

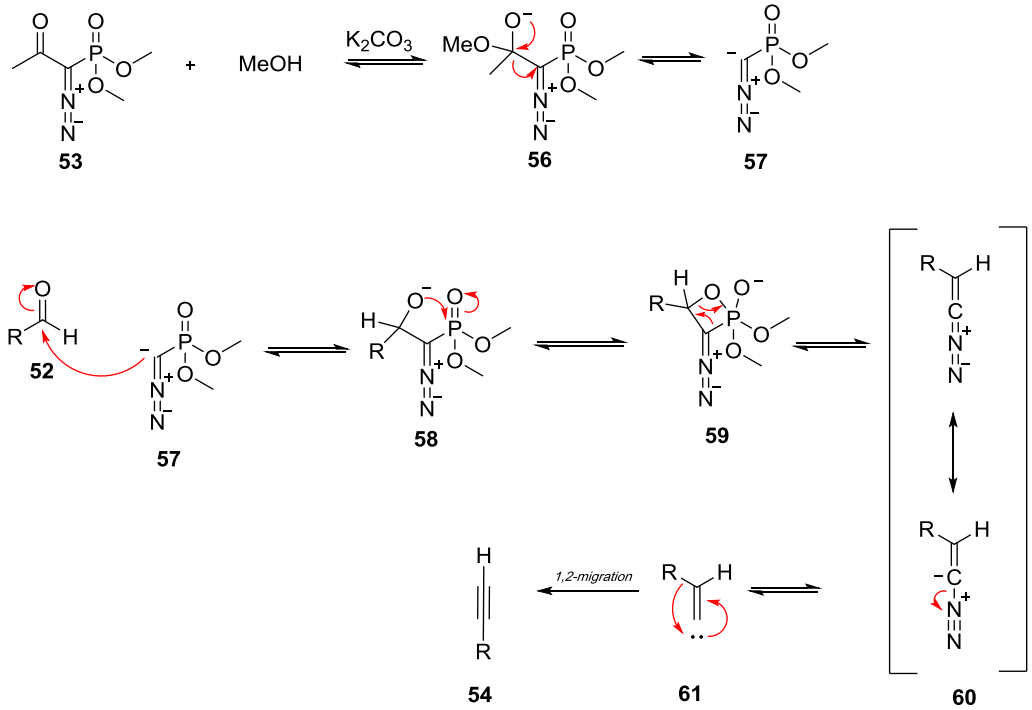

Scheme 10. Proposed mechanism for Ohira-Bestmann reaction.

1.2.4 The Takai reaction

In 1986 Takai and coworkers reported the *E*-selective monohalido-olefination of aldehydes by an *in situ* generated organochromium specie.[51] This was a great discovery for the development of

olefination chemistry, especially due to the relative ease of the reaction. In **Scheme 11** the Takai reaction is shown.

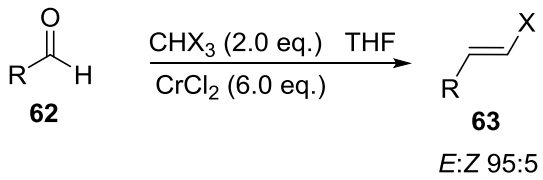

Scheme 11. The Takai olefination.

The mechanism for the Takai olefination has not yet been fully established. However, Takai proposed two possible pathways in his report in 1986 (**Scheme 12**).[51] Iodoform **64** reacts with $Cr^{II}Cl_2$, which is oxidized to Cr^{III}, creating complex **65**. For pathway *a*, complex **66** is formed and reacts with aldehyde **62** giving the *trans* product **63** through intermediate **67**. For pathway *b*, complex **65** is proposed to be the active specie, and therefore will directly react with aldehyde **62**, giving the *trans* product **63** via intermediate **68**.

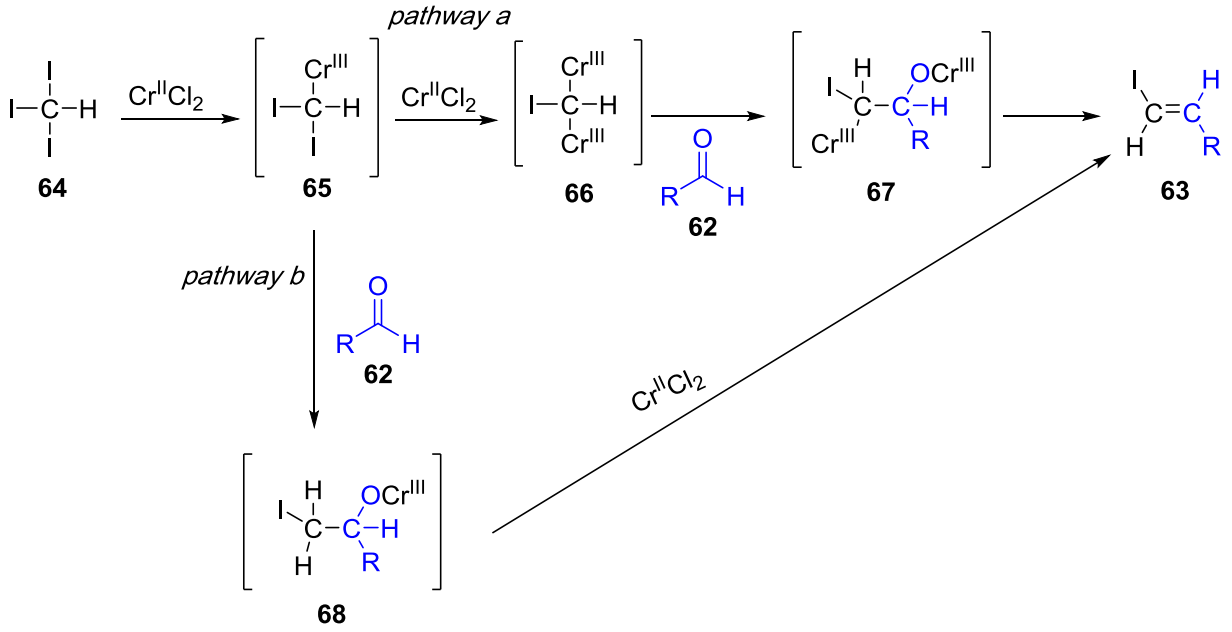

Scheme 12. Proposed mechanism for Takai olefination.

In 2018 Werner and Anwander reported that they had tested the two possible pathways. They concluded that the active specie of the Takai olefination was the iodo-methylidene complex **66**, hence pathway *a* being the most probable route.[52] When testing complex **65** with aldehydes, *cis* products were mostly obtained.

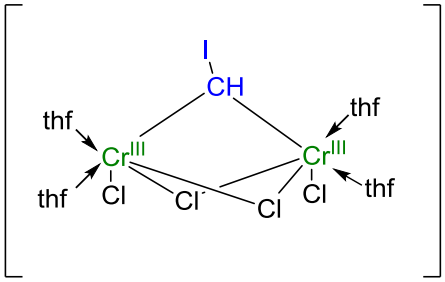

66

Figure 8. The isolated and active complex of Takai olefination. Please note the thf was used by the authors.[52]

1.2.5 The Sonogashira coupling reaction

A widely used coupling reaction is the Sonogashira reaction and it is utilized in numerous synthesis of natural products, including several SPMs.[37,41,53] It allows cross-coupling between terminal alkynes **70** and either a vinyl or an aryl halides **69** in the presence of a palladium catalyst and a copper co-catalyst.[54,55] In 1975 Kenkichi Sonogashira and Nobue Hagihara reported the palladium-catalyzed coupling reaction where they had added copper as a co-catalyst to the reactions of Heck[56] and Cassar.[57] This improvement caused milder conditions of the reaction. Also, the reaction rate was observed increased significantly.[54]

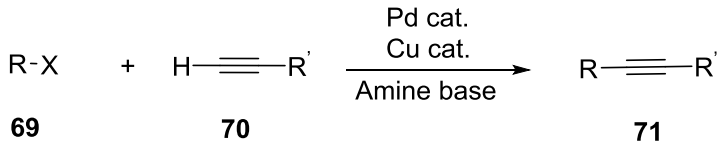

69 **70** **71**

Scheme 13. The Sonogashira coupling.

A generally accepted mechanism for the Sonogashira coupling is shown in **Scheme 14**.[54,55] It is only a proposed mechanism since the isolation and characterization of the organometallic intermediates are challenging to perform. The proposed mechanism involves a palladium cycle and a copper cycle.

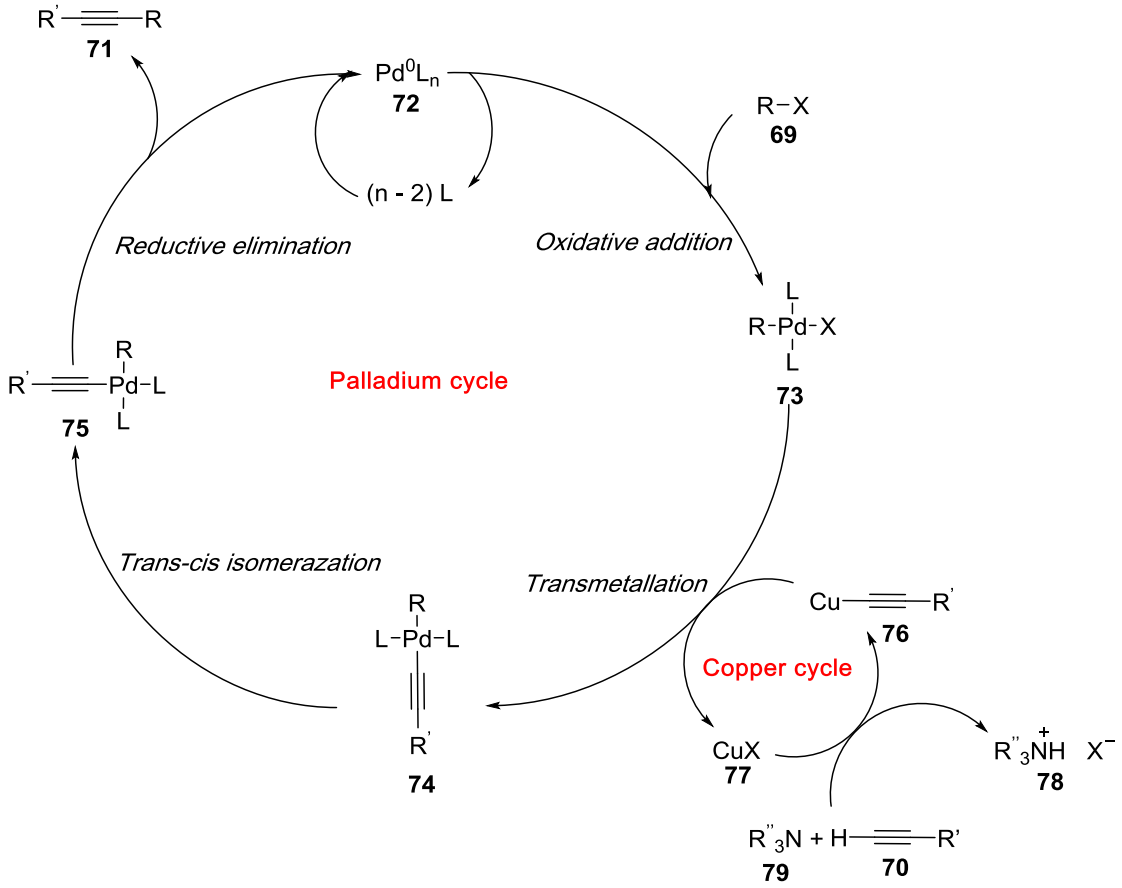

Scheme 14. Proposed mechanism for Sonogashira coupling reaction.

The palladium cycle starts with the active Pd(0) **72** bonded with two ligands (L), often PPh_3. In an oxidative addition the Pd(0) reacts with e.g. a vinyl or an aryl halide **69**, creating Pd(II) catalytic intermediate **73**. Then the two cycles are connected by the copper acetylide **76** from the copper cycle and intermediate **73** from the palladium cycle. The two intermediates are connected in a transmetallation reaction creating the Pd(II) acetylide intermediate **74** and regenerates the copper halide **77** to the copper cycle. If the substrate motifs of **74** are in *trans*-orientation, a *trans-cis* isomerization is conducted to give intermediate **75**. Reductive elimination reduces the palladium to Pd(0) and thereby regenerates it, while the alkyne cross-coupling product **71** is eliminated.

In the copper cycle the terminal alkyne **70** reacts with the copper halide to make the acetylene proton more acidic. An amine base **79** deprotonates the alkyne, resulting in copper acetylide **76**. Compound **76** reacts then with the Pd(II) intermediate **73** from the palladium cycle, as descried earlier, and the copper halide **77** is regenerated.

1.2.6 Lindlar reaction

A widely used procedure for *Z*-selective reduction of alkynes is the Lindlar reaction, reported by Herbert Lindlar in 1952.[58] Using a palladium catalyst, called the Lindlar catalyst, alkynes **80** are reduced to alkenes **81** under hydrogen atmosphere with a highly dominance of the *Z*-configuration. The Lindlar reaction has been used in many SPM-syntheses e.g. $RvD1_{n\text{-}3\ DPA}$, $PD1_{n\text{-}3\ DPA}$ and MaR1.[34,41,59]

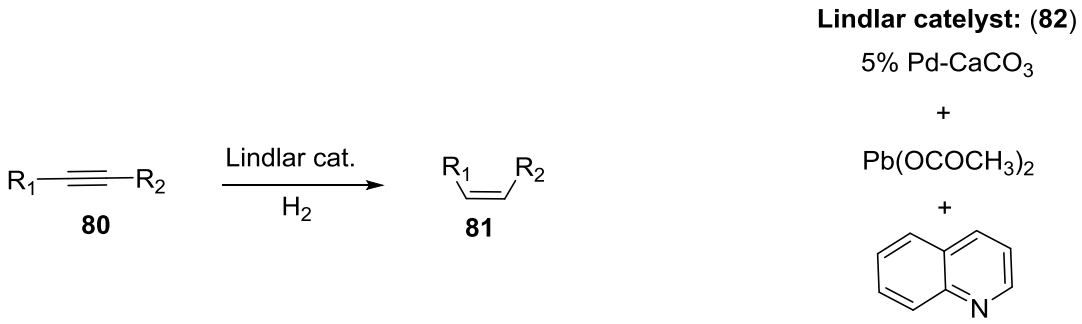

Scheme 15. The Z-selective reduction of alkyne **80** to alkene **81** by using Lindlar catalyst (**82**).

The Lindlar catalyst (**82**) is based on palladium deposited on calcium carbonate. For lowering the risk of overreduction and better the selectivity, palladium is poisoned with lead acetate and quinoline.[60]

2 Results and discussion

A summary of the synthetic strategy has been given in section 1.2.1 page 11.

2.1 Synthesis of the middle fragment 39

2.1.1 Synthesis of compound 42

The first step in preparing the middle-fragment **39** required protection of 2-deoxy-D-ribose (**32**) to maintain the open-ring structure.[41] The aldehyde **32** was dissolved in concentrated HCl, before adding ethanethiol. The reaction mixture was stirred at room temperature for three hours. Basic work-up was followed by purification through column chromatography affording thioacetal **42** in 70% yield.

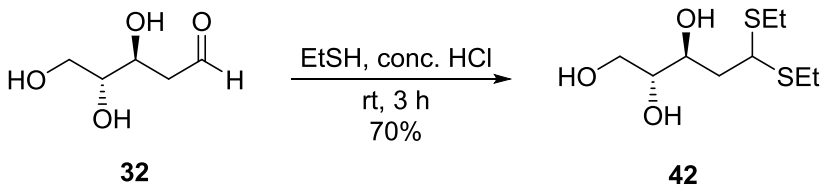

32 **42**

Scheme 16. Synthesis of compound **42**.

2.1.2 Characterization of compound 42

NMR characterization of compound 42

The recorded ^{1}H NMR spectrum shows peaks integrating for twenty hydrogens which correspond to the number of hydrogens in the compound. The two ethyl groups of the thioacetal appear together at 2.68 ppm (4H), as a multiplet. The thioacetal methyl hydrogens appear as a multiplet at 1.27 ppm (6H), which can seem like two overlapping triplets due to the diastereometry of the thioacetal. The three hydroxyl groups appear as a broad singlet at 2.26 ppm (3H). The hydrogens of the alkoxy carbons emerge as two multiplets at 4.07 (2H) and 3.79 ppm (2H). Hydrogens of primary alkoxy groups have higher electron density compared to secondary alkoxy groups. Therefore, the peak at 3.79 ppm indicates the hydrogens of the primary alkoxy group and the hydrogens of the two secondary alkoxy groups are indicated by the peak at 4.07 ppm. The sulfur atoms are expected to give a deshielding effect on the hydrogen at C-5 resulting in a downfield

appearance in the spectrum. Therefore, the hydrogen matches the multiplet at 3.61 ppm (1H). The remaining hydrogens are two hydrogens at C-4 which appear as a multiplet at 2.04 ppm (2H). Hereby, all of the hydrogens of the compound have been accounted for. A singlet at 5.30 ppm may indicate residue of the solvent dichloromethane.

The ^{13}C NMR spectrum displays nine signals, in agreement with the molecular formula ($C_9H_{20}O_3S_2$) of the compound. The secondary alcohols match the two most downfield signals at 73.8 and 72.2 ppm while the primary hydroxyl carbon matches the peak at 63.6 ppm. The C-5 is indicated by the signal at 48.7 ppm. The ethyl groups give signals at 24.5 and 24.2 ppm, for the methylene groups, and two signals at 14.6 ppm for the methyl groups. The remaining carbon, C-4, matches the signal at 39.0 ppm. This accounts for all of the nine carbon atoms in the compound.

The obtained NMR spectra for **42** are in accordance with the previously reported data.[41]

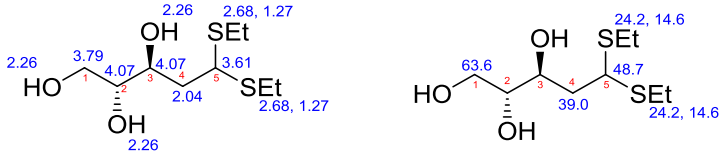

Figure 9. Assignment of ^{1}H and ^{13}C NMR signals for compound **42**.

Specific optical rotation of compound 42

The calculated specific optical rotation of compound **42** was $[\alpha]_D^{20}$ = -14.5 (c = 2.9, MeOH), which is similar to the previously reported value $[\alpha]_D^{20}$= -19.2 (c = 1.0, MeOH).[41] The measured optical rotation is sensitive to the compound concentration. Small error measurements of the solvent's volume or when weighing the compound can have significant impacts on the calculated specific optical rotation. The temperature has also an effect on the optical rotation. Since the previously reported and the calculated value are measured with the same temperature-controlled polarimeter, this should not induce the difference. Even though the values are not exactly the same, the sign of the values and the order's magnitude of the values are the same. Therefore, the difference is acceptable for this project.

2.1.3 Synthesis of compound 83

The next step was protection of the alcohol groups in **42** to maintain these for following reactions.[41] The unprotected **42** was dissolved in dichloromethane, cooled and added TBSOTf and 2,6-lutidine. The reaction mixture was slowly warmed to room temperature overnight. After acidic work-up, the crude product was purified by column chromatography giving the TBS-protected **83** in 90% yield.

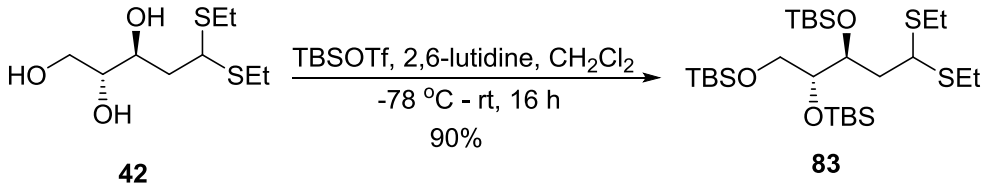

42 **83**

Scheme 17. Synthesis of compound **83**.

2.1.4 Characterization of compound 83

NMR characterization of compound 83

In the recorded ^{1}H NMR spectrum the TBS-groups appear as two intensive multiplets at 0.89 (27H) and 0.07 ppm (18H). Since silicon has a lower electronegativity than carbon, it will affect the surrounding hydrogens to appear at lower chemical shift than ordinary alkyl hydrogens. Consequently, the six methyl groups, attached directly to silicon, appear most upfield in the spectrum as the multiplet at 0.07 ppm (18H). The multiplet at 0.89 ppm (27H) matches the *tert*-butyl hydrogens of the TBS-groups. Five peaks appear in the region of hydrogens affected by electronegative atoms. The two doublets of doublets at 3.51 (1H) and 3.44 ppm (1H) match the two diastereomer hydrogens of the primary alkoxy group at C-1 based on the equal coupling constant (J = 10.1 Hz). The peak at 4.17 ppm (1H) appears as a doublet of doublets of doublets. The form as a doublet of doublets of doublets matches the hydrogen at C-3 since it is split by three different hydrogens. The large and middle coupling constants (J = 9.4 and 2.6 Hz) indicate coupling with the peaks at 2.07 (1H) and 1.78 ppm (1H). The doublet of doublets, emerging at 3.93 ppm, matches the hydrogen at C-5. This assumption is based on the expectation of the hydrogen will couple with the two diastereomer hydrogens at C-4, therefore appearing as a doublet of doublets. Also, the peak gives the coupling constants (J = 11.0 and 3.8 Hz) which match the coupling

constants of the two peaks at 2.07 and 1.78 ppm. These two doublet of doublets of doublets at 2.07 (1H) and 1.78 ppm (1H) have equal coupling constants with each other (J = 14 Hz), the doublet of doublets of doublets at 4.17 ppm (J = 9.8 and 2.6 Hz) and the doublet of doublets at 3.93 ppm (J = 11.0 and 3.7 Hz). Based on this, the two doublets of doublets of doublets match the two diastereomer hydrogens at C-4. The multiplet at 3.69 ppm matches the hydrogen at C-2. The ethyl groups of the thioacetal appear as a multiplets at 2.62 (4H) and 1.24 ppm (6H). The number of hydrogens in the spectra is in accordance with the compound's total of 62 hydrogens.

In the obtained ^{13}C NMR spectrum the three peaks at 77.8, 72.2 and 64.5 ppm can be assigned to the three alkoxy carbons. The peak at 48.2 ppm matches the tertiary carbon C-5 and the peak at 39.0 ppm matches C-4, based on comparing to the spectrum for the previously compound **32**. The methyl carbons of the ethyl groups are indicated by the peaks at 14.8 and 14.5 ppm. The sixteen remaining peaks are not consistent with the twenty carbons left. However, the likenesses of the TBS-carbons can result in appearances in equal signals. This is for instance proposed in more intensive signals at 26.2 and 2 x 26.1 ppm, which can indicate the signals represent more than one carbon. For studying this suggestion, a HMQC spectrum will be needed. The signals at 26.2 to 18.3 ppm are expected to appear from the two thioacetal methylene carbons as well as the nine methyl carbons and the three tertiary carbons of the *tert*-butyl groups. The six methyl carbons directly bonded to silicon match the peaks most upfield in the spectrum at -3.5 to -5.3 ppm. Thus, all of the carbons of the molecule have been accounted for. The signal at 2.8 ppm seems a little odd on account of the low intensity and not suitable appearance compared to previously reported data.[41] Beside this observation, the obtained NMR spectra for **83** are in good accordance with the previously reported data.[41]

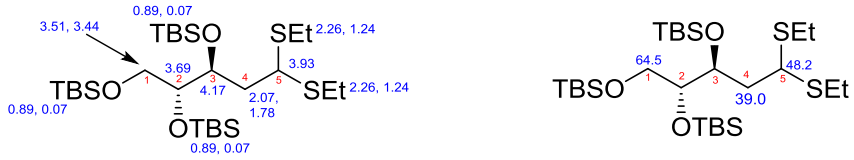

Figure 10. Assignment of ^{1}H and ^{13}C NMR signals for compound **83**.

Specific optical rotation of compound 83

The specific optical rotation of compound **83** was calculated to be $[\alpha]_D^{20}$= -4.3 (c = 0.31, MeOH), which is similar to the previously reported value of $[\alpha]_D^{20}$stated to be -8.9 (c = 1.0, MeOH).[41] As described in section 2.1.2, small error measurements of the concentrations can have significant impact on the value of the calculated specific optical rotation. The two calculated values have after all the same operational sign and are in the same order of magnitude therefore suggesting the same molecule considering the different concentrations.

2.1.5 Synthesis of middle fragment 39

For deprotection of the thioacetal **83** the compound was dissolved in a mixture of acetone and water, and 2,6-lutidine and NBS were added the cooled mixture.[41] After 3 hours and aqueous work-up, the crude product was purified by column chromatography to give the aldehyde **39** in 70% yield.

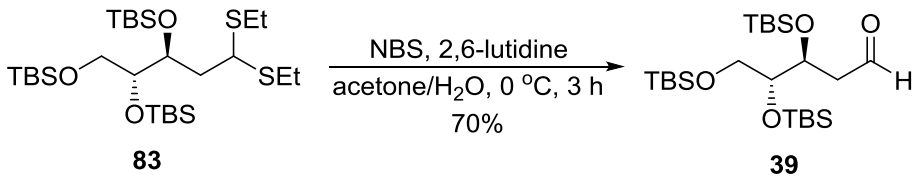

83 **39**

Scheme 19. Synthesis of middle fragment **39**.

2.1.6 Characterization of middle fragment 39

NMR characterization of middle fragment 39

The characteristic hydrogen of the aldehyde appears in the ^{1}H NMR spectrum at 9.85 ppm (1H) as a doublet of doublets. The coupling constants (*J* = 3.4 and 1.7 Hz) indicate coupling with the two doublets of doublets of doublets at 2.59 (1H) and 2.46 ppm (1H). These peaks match the two diastereomer hydrogens at C-2 which is supported by their mutual coupling constant (*J* = 16.3 Hz) indicating geminal coupling. A doublet of triplets appears at 4.35 ppm (1H). This appearance matches the hydrogen at the alkoxy C-4 due to coupling with the hydrogen at C-3 and the two hydrogens of C-5. The coupling constant (*J* = 5.2 Hz) of this peak (4.35 ppm) indicates coupling with the doublet of doublets at 3.49 ppm. This doublet of doublets also couples with doublet of doublets at 3.41 ppm (*J* = 10.3 Hz). Consequently, the hydrogens of C-5 match the two doublets of

doublets at 3.49 and 3.41 ppm and the hydrogen at C-3 matches the multiplet appearing at 3.77 ppm (1H). Most upfield the 45 hydrogens of the TBS-groups emerge as two multiplets at 0.89 and 0.08 ppm.

In the obtained ^{13}C NMR spectrum the aldehyde carbonyl carbon emerges at 202.7 ppm. The three peaks at 77.3, 69.7 and 64.5 ppm indicate the three alkoxy carbons. The signal at 45.8 ppm matches the methylene carbon C-2, since it is affected by the electron-withdrawing carbonyl group. The remaining eleven peaks indicate the carbons of the three TBS-groups. The six methyl carbons directly attached to a silicon atom may be indicated by the six peaks at -4.2 to -5.3 ppm. The three peaks at 18.4, 18.3 and 18.2 ppm indicate the nine methyl carbons of the *tert*-butyl-groups while the two peaks at 26.0 ppm may indicate the three tertiary carbons of the *tert*-butyl-groups. Thus, all of the carbons in the compound have been accounted for.

The obtained NMR spectra for **39** are in accordance with the previously reported data.[41]

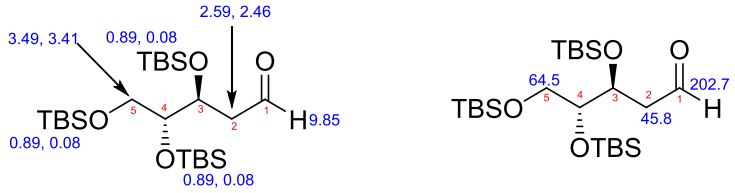

Figure 12. Assignment of ^{1}H and ^{13}C NMR signals for the middle fragment **39**.

Specific optical rotation of middle fragment 39

The specific optical rotation of compound **39** was calculated to be $[\alpha]_D^{20}$ = -11.8 (c = 0.42, MeOH). Previously reported calculated value of the specific optical rotation is -5.9 (c = 0.1, MeOH).[41] Both of the values have negative operational sign but are different in magnitude. This can be based on differences in concentrations, as mention earlier (see section 2.1.2). Even though it should not be such great difference for the values, the variation is acceptable for this project.

2.2 Synthesis of Wittig salt 40

2.2.1 Synthesis of Wittig salt 40

Over two steps the Wittig salt **40** was prepared from commercially available (*Z*)-hex-3-en-1-ol (**41**).[61] In the first step, alcohol **41** was reacted in a mixture of dichloromethane, triphenylphosphine, imidazole and iodide affording the intermediate (*Z*)-1-iodohex-3-ene (**84**) after aqueous work-up. The oil **84** was dissolved in acetonitrile and triphenylphosphine was added. After reflux over night the mixture was purified by chromatography and the Wittig salt **40** was obtained in overall 51% yield in the two steps.

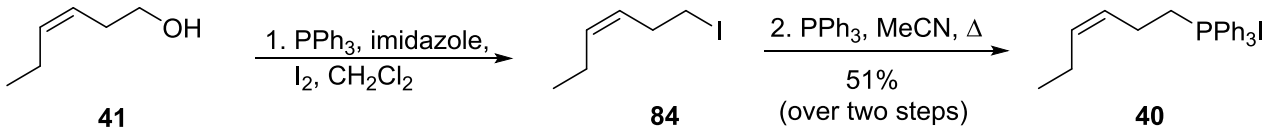

Scheme 18. Synthesis of Wittig salt **40**.

2.2.2 Characterization of Wittig salt 40

NMR characterization of Wittig salt 40

The fifteen phenyl hydrogens are presented in the recorded ^{1}H NMR spectrum as two multiplets at 7.80 (9H) and 7.70 ppm (6H). At 5.47 (1H) and 5.35 ppm (1H), two multiplets appear, indicating the two hydrogens of the double bond. The methyl hydrogens appear as a triplet at 0.82 ppm (3H). The remaining peaks appear as multiplets at 3.67 (2H), 2.42 (2H) and 1.78 ppm (2H) which are in correlation with the six alkyl hydrogens at C-1, C-2 and C-5. Total 26 hydrogens show up in the spectrum which also is in accord with the total number of hydrogens in compound **40**.

The phosphorus isotope ^{31}P has a spin I = ½ which will participate in spin-spin coupling interactions with nearby ^{13}C nuclei. Therefore, carbons close to phosphorus will appear as doublets in the recorded ^{13}C NMR spectrum. In the typical area of aromatic carbons and alkenes, six signals emerge. At 135.3 ppm (3C) a doublet appears. The integral and relatively low coupling constant ($^{4,}J_{CP}$ = 3.0 Hz) indicate the carbons in the *para* position in the aromatic rings. The six *meta* positioned carbons emerge as a doublet at 133.7 ppm (6C) with a larger coupling constant ($^{3,}J_{CP}$ = 10.2 Hz). The doublet at 130.7 ppm (6C) indicates the carbons in the *ortho* positions ($^{2,}J_{CP}$ = 12.6

HZ). The last aromatic carbons emerge as a doublet at 118.0 ppm where the large coupling constant ($^{1}J_{CP}$ = 86.2 Hz) indicates directly attachment to phosphorus. The integral of the peak is not accurate with the three remaining aromatic carbons. However, the chemical shift and the coupling constant support the suggestion when comparing the spectrum to previously data.[61] The doublet at 134.4 ppm (1C) matches the carbon of the alkene longest from the phosphorus due to the small coupling constant ($^{4}J_{CP}$ = 1.1 Hz). The other alkene carbon appears as a doublet at 125.2 ppm with a coupling constant ($^{3}J_{CP}$ = 14.3). The methylene bonded with phosphorus emerges as a doublet at 23.3 ppm (1C) ($^{1}J_{CP}$ = 48.7 Hz). The peak at 20.7 ppm indicates the allylic carbon C-4 located longest from phosphorus while the doublet at 20.3 ppm matches the allylic carbon C-3 nearest phosphorus with coupling constant ($^{2}J_{CP}$ = 3.7 Hz). Most upfield the methyl carbon appears at 14.0 ppm. Thus, all of the carbons in the compound have been accounted for.

The obtained NMR spectra for **40** are in accordance with the previously reported data.[62]

Figure 11. Assignment of ^{1}H and ^{13}C NMR signals for Wittig salt **40**.

2.3 Assembly of the middle-fragment 39 and Wittig salt 40

2.3.1 Synthesis of compound 38

For the *Z*-selective Wittig reaction, the ylide **40** was dissolved in dichloromethane and cooled. Aldehyde **39** and NaHMDS in dichloromethane were added before the reaction mixture was stirred while slowly warmed to room temperature. After aqueous work-up and purification by column chromatography on silica gel, compound **38** was afforded in 84% yield. Two spots appeared on the TLC plate, which together with low peaks displayed in the 120-140 ppm range in the ^{13}C NMR spectrum, indicating that the *E* isomer also was formed. From the ^{13}C NMR spectrum the *E*:*Z* ratio was determined to 10:90. To achieve higher selectivity, an attempt to separate the isomers could have been done.

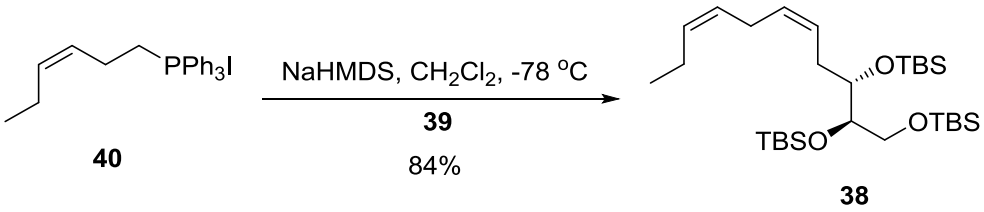

40 38

Scheme 20. Synthesis of compound **38**.

2.3.2 Characterization of compound 38

NMR characterization of compound 38

In the registered ^{1}H NMR spectrum the four alkene hydrogens appear as a multiplet at 5.39 ppm (4H). The two doublets of triplets at 3.80 (1H) and 3.70 ppm (1H) match the two hydrogens at C-2 and C-3, due to the complex splitting with the neighbor hydrogens. The peak at 3.70 ppm couples with the doublet of doublets appearing at 3.62 ppm (1H) (J = 6.2 Hz), which additionally couples with the doublet of doublets at 3.47 ppm (1H) (J = 10.0 Hz). Thereby, it is indicated that the peak at 3.70 ppm matches the hydrogen at C-2 and the peak at 3.80 ppm matches the hydrogen at C-3. Consequently, the two doublets of doublets at 3.62 and 3.47 ppm match the two diastereomer hydrogens at C-1. The multiplet at 2.78 ppm (2H) matches the hydrogens at C-7 due to the deshielding effect from the π-electrons. The three methyl hydrogens match the triplet at 0.97 ppm (3H) due to the chemical shift and the integral of three hydrogens. The multiplets at 2.28 (2H) and 2.07 ppm (2H) indicate the four hydrogens at C-4 and C-10. The 45 hydrogens of the TBS-groups emerge as two multiplets at 0.89 (27H) and 0.05 ppm (18H). Thus, all of the hydrogens in the compound are accounted for.

In the measured ^{13}C NMR spectrum the four carbons of the diene appear at 131.8, 129.4, 127.3 and 127.1 ppm. The two secondary alkoxy carbons emerge at 77.2 and 74.2 ppm while the primary alkoxy carbon appears at 64.8 ppm. The rest of the peaks emerge in the area expected for saturated carbons and are a bit more difficult to identify with an acceptable certainty for each carbon. When the spectrum is compared to previously spectra for compound **39** and **40**, the remaining peaks are in accordance with the rest of the carbons in compound **38**. For example, the peaks at -4.2 to -5.4 ppm indicate the six methyl carbons directly attached to silicon in the TBS-

groups, and the peak at 14.3 ppm indicates the methyl C-11. The peaks in the area at 30.6 to 18.2 indicate the remaining TBS-carbons as well as C-4, C-7 and C-10.

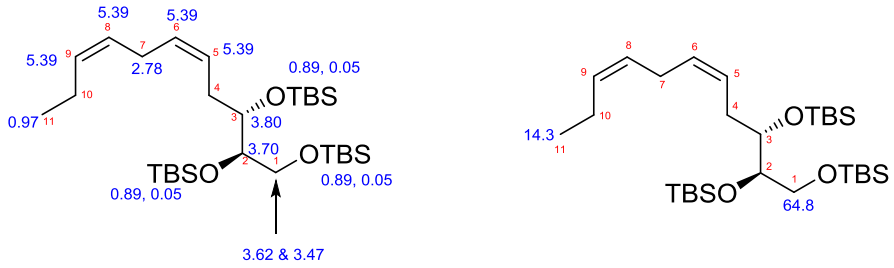

Figure 13. Assignment of ^{1}H and ^{13}C NMR signals for compound **38**.

Other characterizations of compound 38

In the recorded MS spectrum, the molecular ion peak, appears as the base peak at *m/z* 565.39, which corresponds with the calculated mass of the sodium adduct of compound **38**. The HRMS spectrum shows a peak at *m/z* 565.3899, which is the same as for the calculated exact mass of the sodium adduct of compound **38**.

The specific optical rotation of compound **38** was calculated to be $[\boldsymbol{\alpha}]_{\boldsymbol{D}}^{\boldsymbol{20}}$= 2.5 (c = 0.41, MeOH).

NMR and MS spectra confirm the formed structure is compound **38**.

2.3.3 Synthesis of alcohol 85

The next step was a selective deprotection of the primary TBS-group in fragment **38** with *p*-toluenesulfonic acid (PTSA). There is a risk of alcohols in alpha position to a TBS-group assist in deprotection. To prevent this, the reaction was stopped after 1.5 h when two spots, one from the starting material **38** and the other from the formed product **85**, were observed in similar extent on the TLC plate. Using column chromatography, separation of the formed product **85** and unreacted starting material **38** gave the product **85** in 51 % yield.

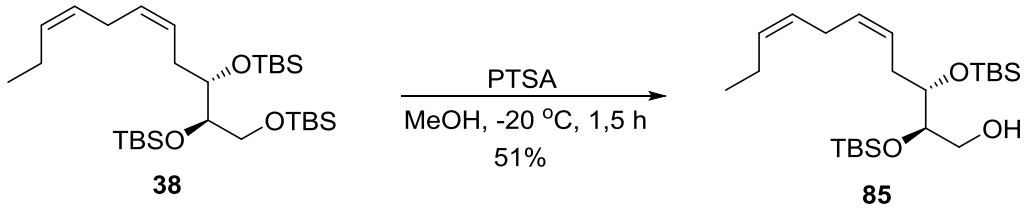

Scheme 21. Synthesis of alcohol **85**.

2.3.4 Characterization of alcohol 85

NMR characterization of alcohol 85

In the obtained ^{1}H NMR spectrum the integral for the multiplets at 0.90 (18H) and 0.08 ppm (12H) indicate successful deprotection. The four unsaturated hydrogens of the diene appear as a multiplet at 5.37 ppm (4H). The two secondary alkoxy hydrogens emerge as a multiplet at 3.76 ppm (2H), while the hydrogens of the primary alkoxy group match the multiplet at 3.63 ppm (2H). The remaining peaks are consistent with the remaining hydrogens in the compound. The multiplet at 2.77 ppm (2H) matches the hydrogens at C-7 based on deshielding from the π-bonds as mentioned earlier. The triplet at 0.97 ppm (3H) indicates the methyl hydrogens at C-11 based on the integral and chemical shift. The hydrogens at C-4 and C-10 are indicated by the multiplets at 2.06 (2H) and 2.31 ppm (2H). Between the multiplets, a broad singlet is noticeable which may indicate the hydrogen of the hydroxyl group. The number of hydrogens in the recorded ^{1}H NMR matches the total number of hydrogens in compound **85**.

The obtained ^{13}C NMR spectrum display fewer peaks upfield compared to the spectrum of compound **38**. This indicates well the absence of one TBS-group. The TBS-methyl carbons, directly attached to silicon, appear as only four signals at -4.3, -4.3 and 2 x -4.4 ppm, instead of six signals as previously in spectrum for compound **38**. The four unsaturated carbons emerge as four peaks at 132.3, 130.3, 127.0 and 125.6 ppm. The two secondary alkoxy carbons appear at 75.0 and 74.9 ppm and the primary hydroxyl carbon appears at 63.9 ppm. The peak at 14.4 ppm matches the methyl carbon at C-11. The carbons at C-4, C-7, C-10 and some of the carbons in TBS-groups fit with the signal at 32.1, 26.1, 26.0, 26.0, 20.7 18.3 and 18.2. Thus, all of the carbons in the compound have been accounted for.

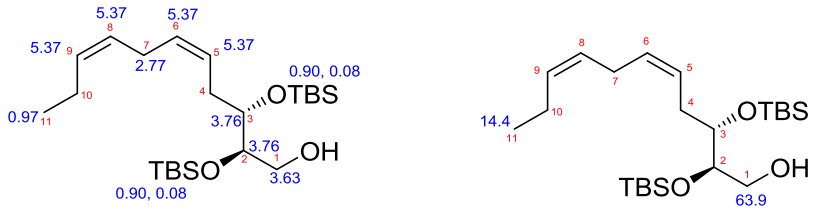

Figure 14. Assignment of ^{1}H and ^{13}C NMR signals for alcohol **85**.

Other characterizations of alcohol 85

The molecular ion peak in the recorded MS spectrum appears at *m/z* 451.303, which also corresponds with the calculated mass of the sodium adduct of compound **85**. The calculated exact mass of the sodium adduct of compound **85** is equal to the measured peak at *m/z* 451.3034 in the HRMS spectrum with an error of 0.1 ppm. This is an acceptable error within the 10 ppm error criteria for HRMS spectrums.

The calculated specific optical rotation of compound **85** was $[\alpha]_D^{20}$= 5.2 (c = 0.10, MeOH).

NMR and MS spectra confirm the formed structure is compound **85**.

2.3.5 Synthesis of aldehyde 37

For the oxidation of alcohol **85** to aldehyde **37**, Dess-Martin periodinane (DMP) was used as the oxidizing agent. A mixture of alcohol **85**, dichloromethane and $NaHCO_3$ were reacted with the oxidant and the mixture was stirred at room temperature overnight. The following day, some starting material **85** was still visible on the TLC plate. Consequently, further DMP was added to the mixture for complete conversion of the alcohol **85**. After aqueous work-up, the crude product was purified by flash chromatography to obtain the wanted aldehyde **37** in 80% yield. The abnormal long reaction time for this oxidation could be due to steric hindrance between the TBS-group and DMP.

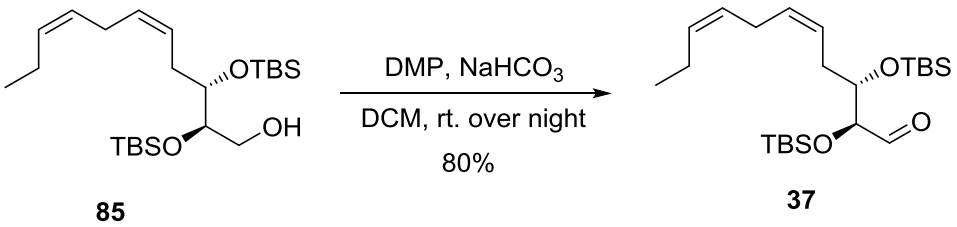

85 **37**

Scheme 22. Synthesis of aldehyde **37**.

2.3.6 Characterization of aldehyde 37

NMR characterization of aldehyde 37

The characteristic peak for the aldehyde appears in the measured ^{1}H NMR spectrum as a doublet at 9.56 ppm (1H). The four olefinic hydrogens emerge as two multiplets at 5.42 (2H) and 5.31 ppm (2H), as expected compared to the recorded spectra for the previously fragments **38** and **85**. The

multiplet at 3.94 ppm (2H) matches the hydrogens at C-2 and C-3. The methylene between the two alkenes appears aa a multiplet at 2.80 ppm (2H). The methyl group at C-11 matches the triplet at 0.97 ppm (3H). The 30 hydrogens of the TBS-groups emerge as two multiplets at 0.90 (18H) and 0.08 ppm (12H). The remaining three multiplets at 2.07 (2H), 2.46 (1H) and 2.25 ppm (1H) match the hydrogens at C-4 and C-10. Thus, the number of hydrogens in the spectrum is in accordance to the compound's total of 46 hydrogens.

In the recorded ^{13}C NMR spectrum the characteristic carbonyl emerges at 203.9 ppm. The signals of the four unsaturated carbons appear at 132.4, 131.6, 126.9 and 124.8 ppm. The two alkoxy carbons, C-2 and C-3, emerge at 81.1 and 76.1 ppm, more downfield than in previously recorded spectra. It may be due to the electron-withdrawing aldehyde, which affects the neighboring carbon to appear at a higher chemical shift. This suggests that the α-carbon matches the peak at 81.1 ppm while the β-carbon matches the peak at 76.1 ppm. Proposed by data from previously spectra of compounds **38** and **85**, the methyl carbon C-11 appears at 14.4 ppm. The peaks at 31.8, 26.0, 25.9, 20.7, 18.4 and 18.2 ppm indicate C-4, C-7 and C-10 and some carbons of the TBS-groups. The rest of the TBS-carbons emerge at -4.4, -4.5 and 2 x -4.6 ppm.

In comparison with spectra of previously fragments the NMR spectra are consistent with compound **37**.

Figure 15. Assignment of ^{1}H and ^{13}C NMR signals for aldehyde **37**.

Other characterizations of aldehyde 37

In the reported MS spectrum of compound **37** the molecular ion peak emerges as the base peak at *m/z* 481.314, which is consistent with the calculated mass of the sodium adduct of compound **37**. In the reported HRMS spectrum the calculated exact mass of the sodium adduct of compound **37** is equal to the measured peak at *m/z* 449.2878.

The specific optical rotation of compound **37** was calculated to be $[\boldsymbol{\alpha}]_{\boldsymbol{D}}^{\mathbf{20}}$= 9.3 (c = 0.37, MeOH).

NMR and MS spectra confirm the formed structure is compound **37**.

2.3.7 Synthesis of α,β-unsaturated aldehyde 86

For the Wittig reaction, aldehyde **37** was dissolved in toluene and the stabilized ylide (triphenylphosphoranylidene)acetaldehyde was added. The addition was dispersed in two portions over six hours to lower the risk of the ylide reacting with itself. The reaction temperature was 95 °C and the mixture was stirred over night before the solvent was removed. The α,β-unsaturated aldehyde **86** was obtained after purification by column chromatography in a 60% yield. A spot, possibly the double-added Wittig product, was observed on the TLC plate but eliminated in flash chromatography.

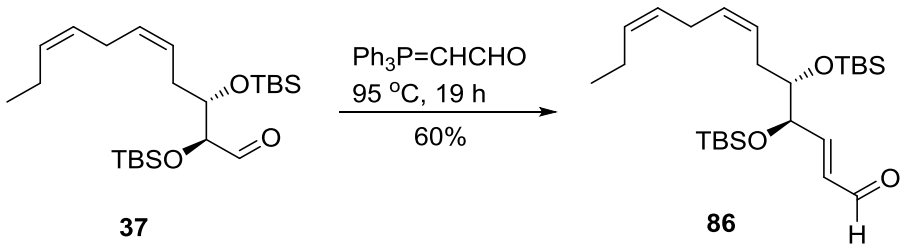

37 **86**

Scheme 23. Synthesis of α,β-unsaturated aldehyde **86**.

2.3.8 Characterization of α,β-unsaturated aldehyde 86

NMR characterization of α,β-unsaturated aldehyde 86

In the obtained ^{1}H NMR spectrum the formed *E*-double bond appears as two separated peaks. One of the hydrogens emerges at 6.88 ppm as a doublet of doublets while the other one appears at 6.25 ppm as a doublet of doublets of doublets. The coupling constant (*J* = 15.7 Hz) confirms the formed double bond has an *E*-configuration. The aldehyde appears at 9.58 ppm (1H) as a doublet. The doublet of doublets of doublets at 6.25 ppm indicates the hydrogen at the α-carbon based on the coupling constant (*J* = 8.0 Hz) is equal with the coupling constant for the doublet from the aldehyde. Hereby, the doublet of doublets at 6.88 ppm matches the hydrogen of the β-carbon. The four hydrogens of the two *cis*-double bonds emerge as a multiplet at 5.38 ppm (4H). The two hydrogens at the alkoxy carbons C-4 and C-5 appear as a multiplet at 4.31 ppm (1H) and a doublet of triplets at 3.75 ppm (1H). The doublet of triplets matches the hydrogen at C-5 based on the

complex coupling with the four neighbor hydrogens. Thereby, the hydrogen at C-4 matches the multiplet at 4.31 ppm. The triplet at 0.97 ppm (3H) matches the methyl group at C-13. The three methylenes at C-6, C-9 and C-12 are indicated by three multiplets at 2.77 (2H), 2.30 (2H) and 2.07 ppm (2H). The TBS-hydrogens match the multiplets at 0.90 and 0.05 ppm. The number of hydrogens in the spectra is in accordance with the compound's total of 48 hydrogens. Some singlets appear at 1.56, 1.33 and 1.28 ppm, which can indicate water or solvent remnants.

The aldehyde emerges in the obtained ^{13}C NMR spectrum at 193.5 ppm. The α-carbon matches the peak at 157.7 ppm. The rest of the unsaturated carbons, C-3, C-7, C-8, C-10 and C-11, appear at 132.3, 132.2, 130.6, 126.7 and 125.2 ppm. The peaks at 76.5 and 75.4 ppm match the alkoxy carbons, C-4 and C-5. The other peaks are consistent with the previously recorded spectrum of compound **37**. The peaks at 31.9, 25.9, 25.8, 20.6, 18.2 and 18.1 ppm indicate C-6, C-9 and C-12 as well as the TBS-*tert*-butyl carbons. The four peaks at -4.2, -4.4, -4.5 and -4.7 ppm appear from the TBS-methyl carbons directly attached to silicon. The methyl C-13 matches the peak at 14.2 ppm. There appear some small peaks around the unsaturated peaks which may be isomers. Since they are at quite lower intensity than the peaks for the main molecule, it is acceptable.

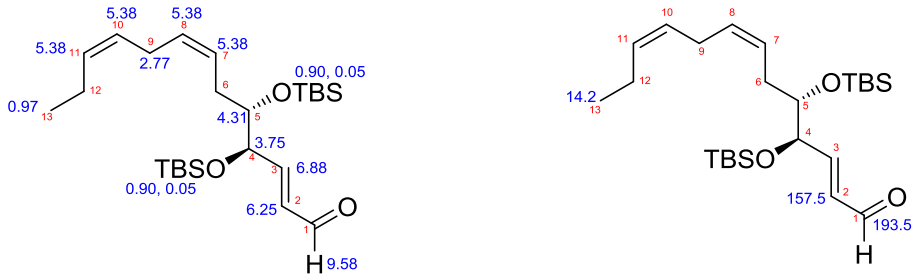

Figure 16. Assignment of ^{1}H and ^{13}C NMR signals for α,β-unsaturated aldehyde **86**.

Other characterizations of α,β-unsaturated aldehyde 86

In the recorded mass spectrum, the molecular ion peak appears at *m/z* 475.303 which is in accordance with the calculated mass of the sodium adduct of the compound **86**. The HRMS spectrum shows the measured *m/z* peak at 475.3034 which fits with the calculated exact mass of the sodium adduct of compound **86** with an acceptable error of 0.1 ppm.

The specific optical rotation of compound **86** was calculated as $[\alpha]_D^{20}$**=** 37.8 (c = 0.09, MeOH).

NMR and MS spectra confirm the formed structure is compound **86**.

2.3.9 Synthesis of vinyl-iodide 33

To complete the formation of fragment **33**, a Takai reaction was accomplished. $CrCl_2$ was dissolved in a mixture of dioxane and THF, cooled before aldehyde **86** and CHI_3 in a mixture containing dioxane and THF were added. After 30 minutes at 0 °C, the mixture was stirred at room temperature for another 1.5 hours. After acidic work-up the mixture was purified by column chromatography to give the vinyl-iodide **33** in 73% yield. The *Z*-isomer was not observed on either the TLC plate or in the obtained NMR spectra. When compound **33** was dissolved in solution, the color shifted from yellow to violet within a few hours at room temperature. This indicated formation of iodide, which could be residue from the reaction. However, differences in the ^{1}H NMR spectra obtained before and after the color change, confirmed the unstability of the compound **33**. Therefore, product **33** was stored at -20 °C until it was reacted in the next reaction within a few days.

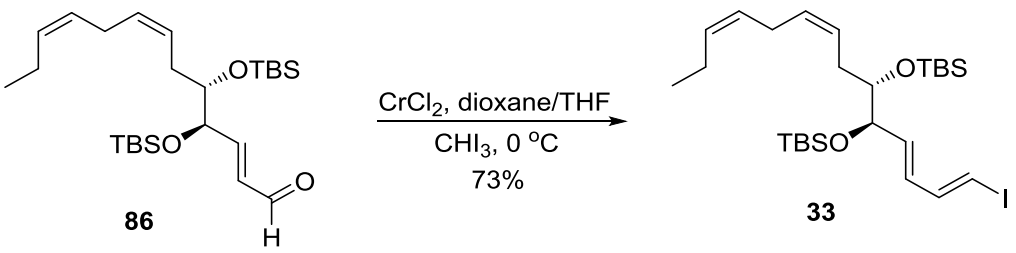

Scheme 24. Synthesis of vinyl-iodide **33**.

2.3.10 Characterization of vinyl-iodide 33

NMR characterization of vinyl-iodide 33

No peaks appear in the characteristic area for aldehydes in the recorded ^{1}H NMR spectrum for compound **33**, indicating conversion of the starting material. Five peaks, integrating for total eight hydrogens, emerge in the area for alkene hydrogens. The four hydrogens of the *E*-double bonds appear as separated peaks while the four hydrogens of the *Z*-double bonds appear in a multiplet at 5.35 ppm (4H). Based on the coupling patterns for the unsaturated hydrogens in *E*-configuration, it is indicated that the doublet of doublets at 7.03 ppm matches the hydrogen at C-2, the doublet at 6.28 ppm matches the hydrogen at C-1, the doublet of doublets at 6.06 ppm matches the hydrogen of C-3 and the doublet of doublets at 5.72 ppm matches the hydrogen at C-

4. The doublet of doublets at 3.98 ppm (1H) and doublet of triplets at 3.63 ppm (1H) indicate the hydrogens at C-5 and C-6. Based on the splitting form doublet of doublets and the equal coupling constant (J = 7.0 Hz) with the peak, indicating the hydrogen at C-4 (5.72 ppm), the doublet of doublets at 3.98 ppm matches the hydrogen at C-5. Thereby, the hydrogen at C-6 is indicated by the doublet of triplets at 3.63 ppm, which is also consistent with the expected splitting system for that hydrogen. The multiplet at 2.76 ppm (2H) matches the hydrogen at C-10 while the triplet at 0.97 ppm (3H) matches the methyl hydrogens at C-14. The TBS-hydrogens emerge as two multiplets at 0.88 (18H) and 0.03 ppm (12H), as in previously spectra. The remaining peaks at 2.23 (2H) and 2.06 ppm (2H) matches the hydrogens at C-7 and C-13. Thus, all of the 49 hydrogens of the compound have been accounted for.

In the obtained ^{13}C NMR spectrum seven peaks appear in the characteristic area of unsaturated carbons at 145.0 - 126.2 ppm, which indicate C-2, C-3, C-4, C-8, C-9, C-11 and C-12. The last unsaturated carbon, C-1, emerges as one of the peaks at 78.8, 76.5 or 76.5 ppm, probably due to the heavy atom effect from iodide. The two other mentioned peaks indicate the two alkoxy carbons, C-5 and C-6. The peaks at 31.8, 26.1, 26.0, 20.7, 18.4 and 18.3 ppm indicate C-7, C-10 and C-13, as well as the TBS-*tert*-butyl carbons. The methyl carbon C-14 matches the peak at 14.4 ppm. The most upfield signals at -4.0, -4.0, -4.2, -4.3 and -4.5 ppm indicate the TBS-methyl carbons directly attached to silicon. Thus, all of the 26 carbons of the compound are accounted for.

With comparison with previously NMR spectra of the fragments which comprise component **33**, the NMR spectra are consistent with the structure of compound **33**.

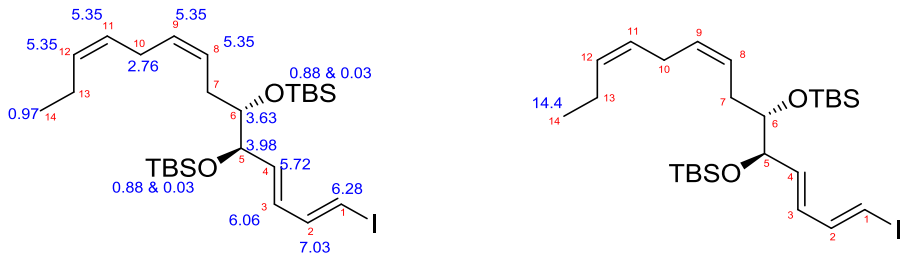

Figure 17. Assignment of ^{1}H and ^{13}C NMR signals for vinyl-iodide **33**.

Other characterizations of vinyl-iodide 33

The MS spectrum shows the molecular ion peak at *m/z* 599.221 which is in accordance with the calculated mass of the sodium adduct of compound **33**. In the HRMS spectrum the measured *m/z* peak appears at *m/z* 599.2207 which matches the calculated exact mass of the sodium adduct of compound **33** with an acceptable error of 0.2 ppm.

The specific optical rotation of fragment **33** was calculated to be $[\alpha]_D^{20}$= -12.8 (c = 0.05, MeOH).

NMR and MS spectra confirm the formed structure is compound **33**.

2.4 Synthesis of alpha-fragment 34

2.4.1 Synthesis of ester 35

The alcohol ester **35** was prepared after a previously reported protocol from the LIPCHEM group.[59] Commercially available cycloheptanone (**36**) was added to a solution of *m*-CPBA in dichloromethane at 0 °C and the mixture was stirred at room temperature for seven days. After aqueous work-up the intermediate was catalyzed by concentrated sulfuric acid and methanol. Purification by column chromatography on silica gave the alcohol ester **35** in 31% yield overall in the two steps. The reactions were not followed with spotting on TLC plates, which could be a reason for the poorly yield.

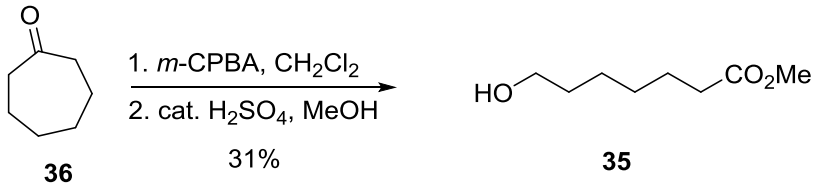

36 **35**

Scheme 25. Synthesis of ester **35**.

2.4.2 Characterization of ester 35

NMR characterization of ester 35

In the measured ^{1}H NMR spectrum the most intensive peak emerges at 3.64 ppm (3H) as a singlet. This is a characteristic appearance for a methyl ester due to the bonding with electronegative oxygen. Right next to the singlet a triplet emerges at 3.60 ppm (2H), which matches the two

hydrogens at C-7. A triplet appears more upfield at 2.29 ppm (2H). Based on the appearance at a relatively high chemical shift, compared to ordinary alkyl hydrogens, suggests that the peak indicating the two hydrogens at the α-carbon. The hydrogen of the alcohol appears as a singlet at 1.82 ppm (1H). The two multiplets, emerging at 1.66 (4H) and 1.40 ppm (4H), indicate the eight remaining hydrogens. Thus, the number of hydrogens in the spectrum is in accordance with the compound's total of 16 hydrogens.

The eight peaks in the ^{13}C NMR spectrum are consistent with the number of carbons in compound **35**. The carbonyl carbon appears at 174.4 ppm. The peak at 62.8 ppm matches the carbon of the primary alcohol. At 51.6 ppm a peak emerges, indicating the methyl carbon of the ester. In the interval for alkanes five peaks emerge quite close at 34.1 ppm, 32.6 ppm, 29.0 ppm, 25.5 ppm and 24.9 ppm. These peaks indicate the five carbons, C-2, C-3, C-4, C-5 and C-6. This accounts for all eight carbon atoms in the compound.

The obtained NMR spectra for **35** are in accordance with the previously reported data.[59]

Figure 18. Assignment of ^{1}H and ^{13}C NMR signals for ester **35**.

2.4.3 Synthesis of compound 87

For oxidation of the primary alcohol **35**, Dess-Martin periodinane was used as the oxidation agent. To a solution of alcohol **35** dissolved in dichloromethane, sodium bicarbonate and Dess-Martin oxidant were added. The desired product **87** was obtained in 92% yield after aqueous work up and purification by column chromatography on silica.

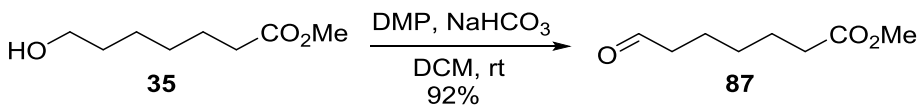

Scheme 26. Synthesis of compound **87**.

2.4.4 Characterization of compound 87

NMR characterization of compound 87

In the registered ^{1}H NMR spectrum a singlet at 9.72 ppm (1H) appears, indicating the hydrogen of the aldehyde. The methyl group in the ester matches the singlet at 3.62 ppm (3H). Two triplets, emerging at 2.41 (2H) and 2.28 ppm (2H), match the hydrogens at C-2 and C-6, due to the vicinal position to a carbonyl group. The remaining six alkyl hydrogens are indicated by two multiplets at 1.61 (4H) and 1.36 ppm (2H). The number of hydrogens in the spectrum is in accordance with the compound's total of 14 hydrogens.

In the obtained ^{13}C NMR spectrum eight peaks emerge which are in consistent with the structure of compound **87**. In the characteristic interval for ^{13}C signals for aldehydes and ketones (190-220 ppm), a peak appears at 202.5 ppm, indicating the aldehyde of the molecule. The carbonyl carbon of the ester emerges a little more upfield at 174.0 ppm. The peak at 51.6 ppm indicates the methyl carbon of the ester. The remaining five carbons appear at 43.7 ppm, 33.8 ppm, 28.6 ppm, 24.7 ppm and 21.7 ppm.

Figure 19. Assignment of ^{1}H and ^{13}C NMR signals for compound **87**.

2.4.5 Synthesis of alpha-fragment 34

In the last step in the synthesis of alpha-fragment **34**, an Ohira-Bestmann reaction was accomplished. The aldehyde **87** was dissolved in dry methanol before basic K_2CO_3 and the Ohira-Bestmann reagent were added. The reaction mixture was stirred at room temperature for 4 h before aqueous work-up. The crude product was purified by column chromatography on silica to give the product **34** in 43% yield.

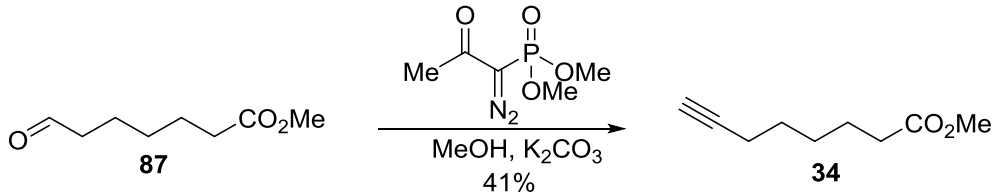

Scheme 27. Synthesis of alpha-fragment **34**.

2.4.6 Characterization of alpha-fragment 34

NMR characterization of alpha-fragment 34

In the obtained ^{1}H NMR spectrum the significant peak of the starting material aldehyde is absent. The singlet at 3.62 ppm indicates the methyl group of the ester. The acetylene hydrogen matches the triplet at 1.90 ppm (1H), due to the integral. The splitting to a triplet probably derives from long-range coupling (J = 2.7 Hz) with the two hydrogens across the triple bond. The doublet of triplets at 2.15 ppm has the same coupling constant (J = 2.7 Hz) which indicates that the peak matches the hydrogens at C-6. The splitting of the peak supports this. The triplet at 2.28 ppm matches the hydrogens at the α-carbon based on the (n+1) rule and effect from the electron-withdrawing carbonyl group. The remaining peaks are three multiplets at 1.60 (2H), 1.49 (2H) and 1.40 ppm (2H) for the hydrogens at C-3, C-4 and C-5. Thereby, all of the hydrogens of the compound have been accounted for.

In the obtained ^{13}C NMR spectrum the carbonyl carbon of the ester appears at 174.0 ppm, while the methoxy group emerges at 51.5 ppm. The alkyne appears as two peaks at 68.4 and 84.3 ppm. Since C-7 is more substituted than C-8, C-7 is expected to be indicated by the most downfield peak (84.3 ppm). Five peaks emerge in the area of saturated carbons, which match the remaining carbons of the molecule. Based on the impact from the electron-withdrawing carbonyl, the α-carbon appears as the peak most downfield in the alkane area (33.9 ppm). The rest of the saturated carbons are indicated by the peaks at 28.2, 28.1, 24.5 and 18.3 ppm. Thus, the number of carbons in the molecule is in accordance with the number of peaks in the reported spectrum.

Figure 20. Assignment of ^{1}H and ^{13}C NMR signals for alpha-fragment **34**.

2.5 Assembly of the vinyl-iodide 33 and the alpha-fragment 34

2.5.1 Synthesis of alkyne 88

In a Sonogashira coupling reaction the vinyl iodide **33** was dissolved in Et_2NH and benzene before the solution was added the catalyst $Pd(PPh_3)_4$. The mixture was stirred for 35 minutes protected

from light followed by adding a mixture of alkyne **34** and CuI in a small amount of Et_2NH. The mixture was stirred overnight at room temperature before acidic work-up. The crude product was purified on column chromatography affording the Sonogashira product **88** in 50% yield.

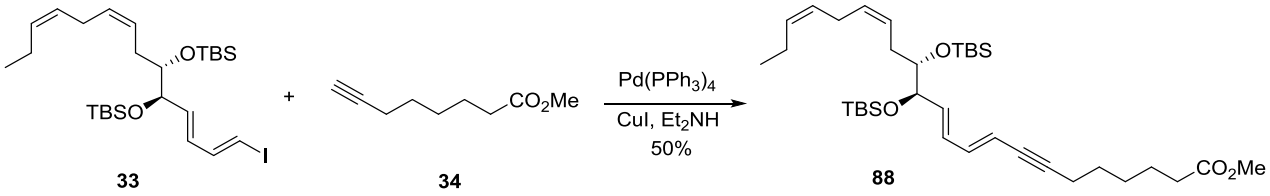

Scheme 28. Synthesis of alkyne **88**.

2.5.2 Characterization of alkyne 88

NMR characterization of alkyne 88

The ^1H spectrum shows signals integrating for total 62 hydrogens, corresponding with the molecular formula of the expected product ($C_{35}H_{62}O_4Si_2$). The four hydrogens of the two *Z*-double bonds from fragment **33** give a multiplet at 5.38 ppm (4H). The four hydrogens of the two *E*-double bonds match the disperse signals at 6.47, 6.21, 5.76 and 5.60 ppm, as a result of the *trans*-configuration. The doublet of doublets at 6.47 ppm couples with the doublet at 5.60 ppm (J = 15.5 Hz) and the doublet of doublets at 6.21 ppm (J = 10.9 Hz). The doublet of doublets at 6.21 ppm also couples with the doublet of doublets at 5.76 ppm (J = 15.3 Hz) which also couples with the doublet of doublets at 4.11 ppm (J = 7.2 Hz). Based on this, the peak at 6.47 ppm matches the hydrogen at C-10, while the doublet at 5.60 ppm matches the hydrogen of C-9. The doublet of doublets at 6.21 ppm matches the hydrogen at C-11 and the hydrogen of C-12 is indicated by the peak at 5.76 ppm. The mutual coupling constant (J = 7.2 Hz) for the doublet of doublets at 5.76 ppm and the doublet of doublets at 4.11 ppm indicating the peak at 4.11 ppm matches the hydrogen at C-13. The suggestion is supported by the expected splitting as a doublet of doublets caused by the complex coupling with the two non-identical hydrogens. Thereby, the multiplet at 3.71 ppm matches the hydrogen at the C-14. The methyl hydrogens of the ester appear as a singlet at 3.67 ppm (3H). By comparing the spectrum to the previously spectrum of fragment **33**, indicating the multiplet at 2.8 ppm (2H) matches the hydrogens at the skipped C-18. The hydrogens of the TBS-groups appear as two multiplets at 0.92 (18H) and 0.07 ppm (12H). The

methyl hydrogens at C-22 emerge as a triplet at 0.99 ppm (3H). The remaining peaks match the hydrogens at C-2, C-3, C-4, C-5, C-6, C-15 and C-21. Thus, all of the hydrogens in the compound have been accounted for.

The recorded ^{13}C NMR spectrum gives 31 signals, which corresponds with the molecular formula of the compound ($C_{35}H_{62}O_4Si_2$) considering the equivalent carbons from the TBS-groups. ^{13}C NMR spectra from the starting materials, the vinyl iodide **33** and the alkyne **34**, gave 22 and 9 signals, respectively, so the coupling product was expected to give 31 signals. The carbonyl carbon of the ester is found downfield at 175.8 ppm. There are eight alkene carbons of the compound, which give signals at 140.9, 136.5, 132.8, 132.5, 130.9, 128.2, 127.3 and 113.1 ppm, respectively. The acetylene carbons appear at 93.6 and 80.9 ppm. The two secondary alkoxy carbons emerge at 78.2 and 78.0 ppm. The methyl of the ester matches the peak at 52.0 ppm. The methyls in the TBS-groups are indicated by four peaks appearing at -3.7, -3.8, -4.1 and -4.3 ppm. The signal at 14.7 ppm indicates the carbon of the methyl at C-22. The remaining 12 signals are 34.7, 32.6, 29.5, 26.8, 26.6, 26.6, 26.5, 21.6, 20.1, 19.2 and 19.1 ppm. These signals indicate the carbons in position 2, 3, 4, 5, 6, 15, 18, 21 as well as the quaternary carbons and the equivalent methyl carbons of the *tert*-butyl moiety in the two TBS-groups. As such, all of the 35 carbon atoms in the compound have been accounted for.

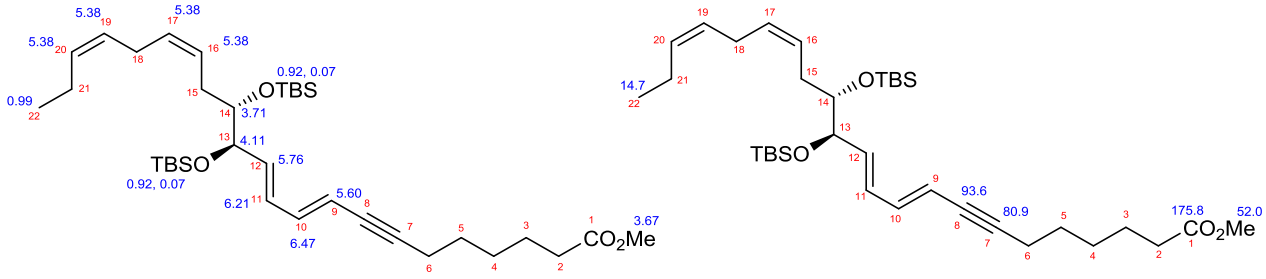

Figure 21. Assignment of ^{1}H and ^{13}C NMR signals for alkyne **88**.

Other characterizations of alkyne 88

In the recorded MS spectrum, the molecular ion peak emerges at *m/z* of 625.408. This corresponds with the calculated molecular mass of the sodium adduct of compound **88**. The HRMS spectrum show a peak at *m/z* 625.4077, close to the calculated exact mass of 625.4079 for the

sodium adduct. The error is 0.2 ppm, which is satisfactorily within the 10 ppm error criteria for HRMS spectra.

The specific optical rotation for compound **88** was calculated to be $[\alpha]_D^{20}$= -12.8 (c = 0.05, MeOH).

NMR and MS spectra confirm the formed structure is compound **88**.

2.5.3 Synthesis of compound 89

Before the selective reduction, deprotection of the alcohols was performed. TBS-protected **88** was dissolved in THF, cooled and TBAF was added. The reaction mixture was stirred overnight before neutralized with phosphate buffer. Brine was added followed by extraction with dichloromethane. Purification through column chromatography afforded the deprotected alcohol **89** in 77% yield.

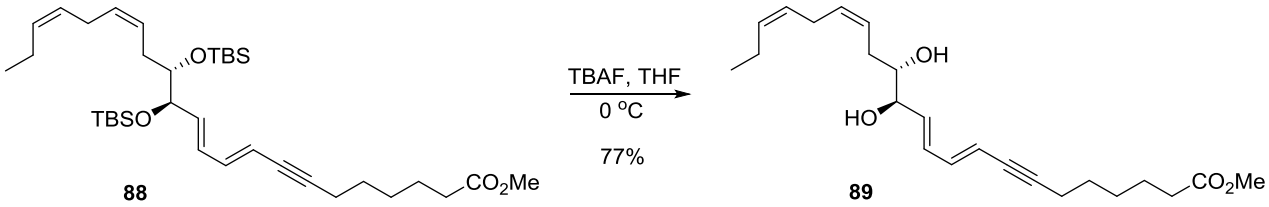

Scheme 29. Synthesis of compound **89**.

2.5.4 Characterization of compound 89

NMR characterization of compound 89

It emerges from the obtained ^{1}H NMR spectrum that the deprotection reaction was successful because of the absence of signals for the TBS-groups. Only the three methyl hydrogens at C-22 appear at 0.99 ppm, which is in the area where the hydrogens of the TBS-groups have appeared in previously spectra. There are some impurities around the triplet at 0.99 ppm, formed as another triplet, which can be some residue of the solvents, most likely hexane. The unsaturated hydrogens of the *trans*-double bonds appear, as previously for compound **88**, as three doublets of doublets at 6.52, 6.33 and 5.89 ppm and one doublet at 5.64 ppm. Based on the coupling patterns and splitting of these peaks; the doublet of doublets at 6.52 ppm (1H) matches the hydrogen at C-10, the doublet of doublets at 6.33 ppm (1H) matches the hydrogen at C-11, the doublet of doublets

at 5.89 ppm matches C-12 and the doublet at 5.64 ppm (1H) matches the hydrogen of C-9. The *cis*-double bonds appear as a multiplet at 5.42 ppm (4H). The two hydrogens at C-13 and C-14 emerge as a triplet at 4.02 ppm (1H) and a multiplet at 3.57 ppm (1H), respectively. The three hydrogens of the methyl ester appear at 3.68 ppm (3H) as a singlet. The hydrogens at the skipped carbon, C-18, are expected to match the multiplet at 2.82 ppm (2H) due to comparison with the previously spectrum of compound **88**. The remaining signals are multiplets at 2.36 (4H), 2.14 (4H), 1.66 (2H), 1.56 (2H) and 1.46 ppm (2H). These signals indicate the fourteen hydrogens at C-2, C-3, C-4, C-5, C-6, C-15 and C-21. Thus, all of the hydrogens in the compound have been accounted for beside the hydrogens of the two hydroxyl groups which are not appearing in the spectrum.

In the ^{13}C NMR spectrum 23 peaks appear which match the number of carbons in the compound. The carbonyl carbon of the ester emerges at 175.8 ppm while the methyl of the ester appears at 52.0 ppm. The eight carbons of the alkenes appear at 141.2, 135.4, 132.7, 132.5, 131.0, 128.3, 127.1 and 113.3 ppm. The two acetylene carbons emerge at 93.5 ppm and 80.9 ppm. The peaks at 76.0 and 75.8 ppm indicate the two alkoxy carbons of the secondary alcohols. The methyl at C-22 matches the peak at 14.7 ppm where it has appeared in previously spectra for similar compounds. The eight remaining peaks, appearing in the alkane region, are equivalent with the remaining carbons of the compound. Some impurities show up in the spectrum which may be resulted by trace amount of solvents. To remove the residual solvents, evaporation under a high vacuum pressure could have been done.

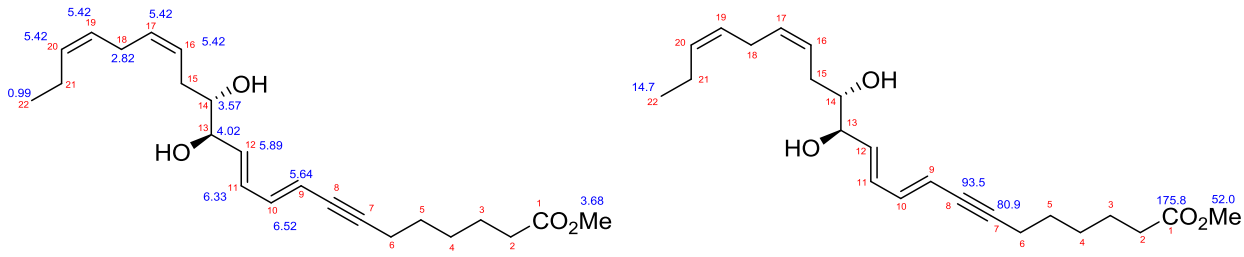

Figure 18. Assignment of ^{1}H and ^{13}C NMR signals for compound **89**.

Other characterization of compound 89

In the obtained MS spectrum, the molecular ion peak emerges at *m/z* 397.235 which is consistent to the calculated molecular mass of the sodium adduct for compound **89**. In the HRMS spectrum the measured *m/z* peak appears at 397.2349 which matches the calculated exact mass of the sodium adduct of compound **89** with an acceptable error of 0.1 ppm.

The calculated specific optical rotation for compound **89** is $[\alpha]_D^{20}$= 17.5 (c = 0.04, MeOH).

NMR and MS spectra confirm the formed structure is compound **89**.

2.5.5 Synthesis of methyl ester of MaR2$_{n\text{-}3\ DPA}$

For the *Z*-selective reduction of the triple bond, a Lindlar procedure was performed. The alkyne **89** was dissolved in a mixture of ethyl acetate, pyridine and 1-octene before the Lindlar catalyst was added. Using a balloon, the reaction was set under H_2-atmosphere. To spot the progress of the reaction, silver nitrate-TLC plates were used. Thereby, the starting material **89** and the formed product **90** had different R_f-values. After eight hours the solvents were removed, and the crude product was purified by column chromatography to afford the wanted product **90** in 72% yield. To achieve an acceptable purity of the product **90**, several eluent systems were tested. After the first attempt in purifying the compound **90** with the selected efficient eluent system, 94% purity was achieved. After another column chromatography, 95% purity was achieved (see HPLC spectrum in **Figure A-50** pp. 121).

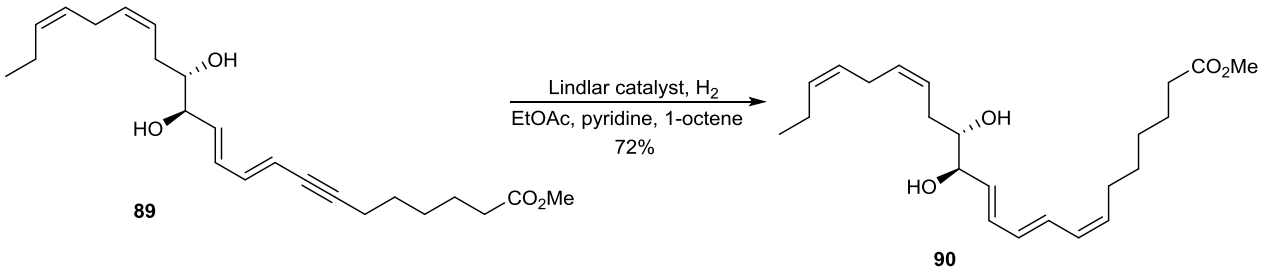

Scheme 30. Synthesis of methyl ester of MaR2$_{n\text{-}3\ DPA}$ **90**.

2.5.6 Characterization of methyl ester of MaR2$_{n\text{-}3\ DPA}$

NMR characterization of methyl ester of MaR2$_{n\text{-}3\ DPA}$

In the measured ^{1}H NMR spectrum, two additional hydrogens appear in the alkene region compared to the spectrum for compound **89**, which indicate a successful reduction. By using the

coupling constants and the (n+1) rule, each peak, in the alkene area, can be interpreted to the specific hydrogens. The doublet of doublets at 6.54 ppm (1H) gives two coupling constants (*J* = 14.9 and 11.2 Hz) indicating coupling with the hydrogens of the doublet of doublets at 6.24 ppm (1H) (*J* = 14.7 Hz) and the triplet at 6.04 ppm (1H) (*J* = 11.2 Hz). The doublet of doublets at 6.24 ppm (1H) also couples with the peak at 6.35 ppm (1H) (*J* = 10.6 Hz) which additionally couples with the doublet of doublets at 5.82 ppm (1H) (*J* = 15.2 Hz). Consequently, the hydrogen at C-9 matches the doublet of doublets at 6.54 ppm and the hydrogen of C-10 matches the doublet of doublets at 6.24 ppm. The peak at 6.35 ppm indicates the hydrogen of C-11 and the hydrogen of C-12 matches the doublet of doublets at 5.82 ppm. At last the triplet at 6.04 ppm matches the hydrogen at C-8. The hydrogen at C-7 appears together with the four hydrogens of the two non-conjugated *cis*-double bonds at C-16 and C-19 in a multiplet at 5.41 ppm (5H). Normally the hydrogens of a *cis*-double bond will be expected to appear as an assembled peak very close to the expected chemical shifts. However, since the *Z*-double bond between C-7 and C-8 are a part of a conjugated system, the hydrogen at C-8 appears as a part of the conjugated system, while the hydrogen at C-7 appearing together with the other hydrogens of *Z*-bonds. The multiplet at 4.02 ppm (1H) and the doublet of triplets at 3.57 ppm (1H) match the two hydrogens at C-13 and C-14. Based on the splitting pattern, the peak at 3.57 ppm matches the hydrogen at C-14. Consequently, the multiplet at 4.02 ppm indicates the hydrogen at C-13. The methyl group of the ester appears as the characteristic singlet at 3.66 ppm (3H). The three hydrogens at C-22 show up at 0.98 ppm (3H) as a multiplet. Comparison with the spectrum of compound **89**, the methylene group of C-18 matches the multiplet at 2.81 ppm (2H). The remaining peaks are multiplets at 2.35 (4H), 2.21 (2H), 2.08 (2H), 1.62 (2H) and 1.38 ppm (4H). These peaks match the remaining alkyl hydrogens at C-2, C-3, C-4, C-5, C-6, C-15 and C-21. The hydrogens of the hydroxyl groups do not appear in the spectrum.

In the obtained ^{13}C NMR spectrum, the absent of the alkyne peaks confirm the reduction reaction. Only 22 peaks appear in the spectrum, instead of the expected 23. However, the strong intensive peak at 133.4 ppm can indicate two carbons, which emerge at the same chemical shift. Therefore, the nine peaks, appearing at 133.7, 133.5, 133.4, 132.7, 131.0, 130.0, 129.4, 128.3 and 127.1 ppm, match the ten unsaturated carbons. The carbonyl carbon of the methyl ester appears at 176.0 ppm while the methyl carbon emerges at 52.0 ppm. The carbons of the two secondary alcohols

are indicated by the peaks at 76.3 and 75.9 ppm. The signal at 14.7 ppm matches the methyl C-22 concluded from previously spectra. The remaining peaks emerge at 34.8, 31.9, 30.4, 29.7, 28.6, 26.7, 25.9 and 21.5 ppm matching the eight remaining alkyl carbons C-2, C-3, C-4, C-5, C-6, C-15, C-18 and C-21. Thus, all of the carbons in the compound have been accounted for.

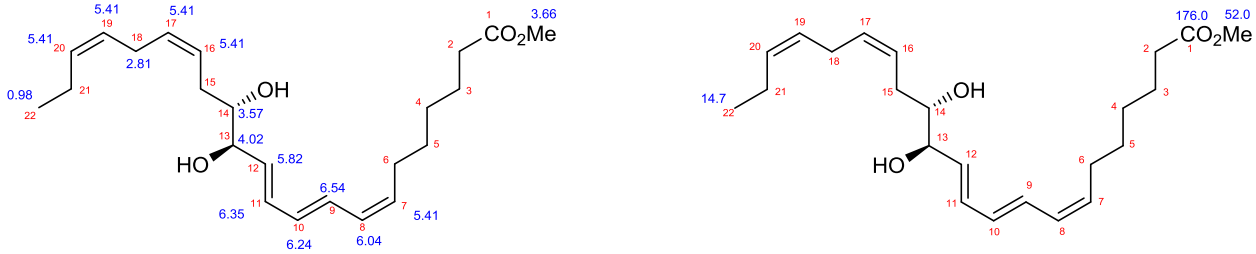

Figure 23. Assignment of ^{1}H and ^{13}C NMR signals for methyl ester of $MaR2_{n\text{-}3\ DPA}$ **90**.

Other characterizations of methyl ester $MaR2_{n\text{-}3\ DPA}$

In the obtained MS spectrum, a peak at *m/z* 425.287 appears as the base peak. The molecular ion peak (M^+) emerges at *m/z* 399.251 in agreement with the calculated molecular mass of the sodium adduct of compound **90**. In the reported HRMS spectrum the measured *m/z* peak appears at 399.2506 which matches the calculated exact mass of the sodium adduct of compound **90** with an acceptable error of 0.1 ppm.

The measured UV spectrum (**Fig. 24**) shows three at λ_{max} = 262, 272 and 283 nm thereby confirming the conjugated *Z*,*E*,*E*-triene of compound **90**.

Spectrum/Peak Report Date 3/26/2019 Time 09:38:21 Page 1 of 1

Method file : <method not saved>
Information : Default Method
Data File : <data not saved>

Overlaid Spectra:

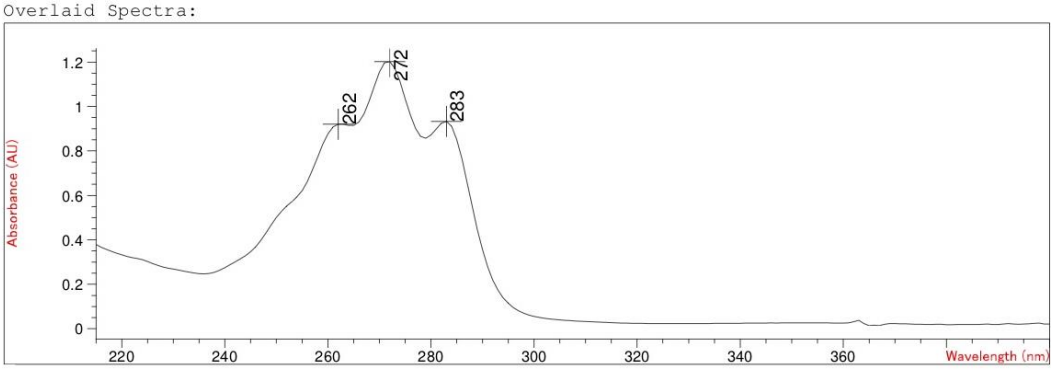

#	Name	Peaks(nm)	Abs(AU)
1		272.0	1.20180
1		283.0	0.93226

#	Name	Peaks(nm)	Abs(AU)
1		262.0	0.92076

Report generated by : Signature: .....

*** End Spectrum/Peak Report ***

Figure 24. Obtained UV spectrum of the methyl ester of MaR2$_{n\text{-}3\ DPA}$ (**90**).

In the obtained chromatogram for the HPLC analysis of **90**, four peaks appear. The major peak with retention time r_t =14.56 min indicates the wanted compound. The three minor peaks with the retention times r_t = 10.76, 13.58 and 15.91 min may indicate isomers. Integration of the peaks gives an estimated chemical purity of 95 %.

The specific optical rotation was calculated to be $[\alpha]_D^{20}$ = 16.0 (c = 0.05, MeOH) for compound **89**.

The above-mentioned analyses make a good basis for the verification of compound **90**.

2.5.7 Synthesis of MaR2$_{n\text{-}3\ DPA}$

To complete the total synthesis of MaR2$_{n\text{-}3\ DPA}$, a hydrolysis of methyl ester **90** was performed. Methyl ester **90** was dissolved in a solution of THF, methanol and water and cooled before LiOH was added. After stirring at 0 °C for six hours, the reaction mixture was warmed to room temperature and acidic work-up was done. Purification by column chromatography on silica was

performed resulting in the natural product **20** in 97% yield. Different eluent systems for column chromatography purification were tested. Unfortunately, an acceptable purity was not obtained due to time constraint.

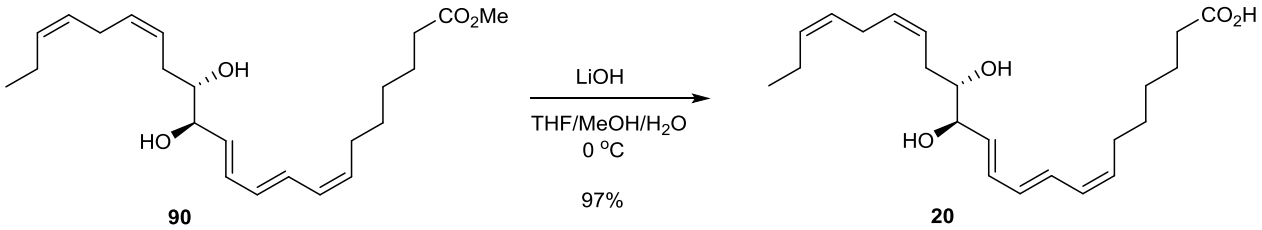

Scheme 31. Synthesis of $MaR2_{n\text{-}3\ DPA}$ (**20**).

2.5.8 Characterization of $MaR2_{n\text{-}3\ DPA}$

NMR characterization of $MaR2_{n\text{-}3\ DPA}$

In the recorded ^{1}H NMR spectrum the ten hydrogens of the unsaturated carbons appear as doublet of doublets at 6.55 (1H), 6.36 (1H), 6.24 (1H) and 5.82 ppm (1H), a triplet at 6.04 ppm (1H) as well as a multiplet at 5.41 ppm (5H). Based on the coupling patterns for the mentioned unsaturated hydrogens, it is indicated that; the doublet of doublets at 6.55 ppm matches the hydrogen at C-9, the doublet of doublets at 6.24 ppm matches the hydrogen at C-10, the doublet of doublets at 6.36 ppm matches the hydrogen at C-11, the peak at 5.82 ppm matches the hydrogen at C-12 and the triplet at 6.04 ppm matches the hydrogen at C-8. The hydrogen at C-7 appears together with the *Z*-bonded hydrogens at C-16, C-17, C-19 and C-20 due to the reason described in section 2.5.6. The two hydrogens at the carbinols emerge as a doublet of doublets at 4.03 ppm and a doublet of triplets at 3.57 ppm, respectively. Based on earlier analysis (see section 2.5.6) the hydrogen at C-13 matches the doublet of doublets at 4.03 ppm while the doublet of triplets at 3.57 ppm indicates the hydrogen at C-14. The triplet at 2.81 ppm (2H) matches the hydrogens of the allylic carbon C-18. The three methyl hydrogens at C-22 appear as a triplet at 0.97 ppm (3H). The multiplets at 2.21 (8H), 1.63 (2H) and 1.41 ppm (4H) match the remaining fourteen hydrogens of the compound at C-2, C-3, C-4, C-5, C-6, C-15 and C-21. Thus, all of the hydrogens in the compound have been accounted for beside the three hydrogens of the hydroxyl groups. They do not appear in the spectrum probably due to the chosen solvent (CD_3OD).

An effort of getting a ^{13}C NMR spectrum at 101 MHz was tried. However, due to the small amount of the compound, no peaks appeared in the spectrum. Higher purity is necessary before application of the NMR machine at 151 MHz.

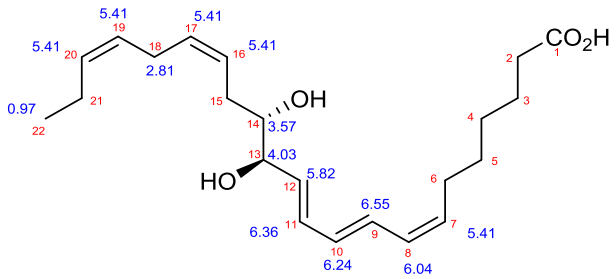

Figure 25. Assignment of ^{1}H NMR signals for $MaR2_{n\text{-}3\ DPA}$.

Other characterizations of $MaR2_{n\text{-}3\ DPA}$

In the obtained MS spectrum, the molecular ion peak appears as the base peak at *m/z* 385.235 which agree with the calculated molecular mass of the sodium adduct of compound **20**. In the HRMS spectrum the measured *m/z* peak appears at 385.2350 which corresponds with the calculated exact mass of the sodium adduct of compound **20** with an acceptable error of -0.1 ppm.

The chromophore emerges as three peaks in the registered UV spectrum (**Fig. 26**). The program recorded only the absorbance of the last two peaks even though it apparently is three peaks in the spectrum. Therefore, the first peak is determined manually to λ_{max} = 262 nm while the other peaks determined by the program to absorption at λ_{max} = 272 and 282 nm. The spectrum confirms the conjugated *Z*,*E*,*E*-triene of compound **20**.

Spectrum/Peak Report Date 3/27/2019 Time 10:29:46 Page 1 of 1

Method file : <method not saved>
Information : Default Method
Data File : <data not saved>

Overlaid Spectra:

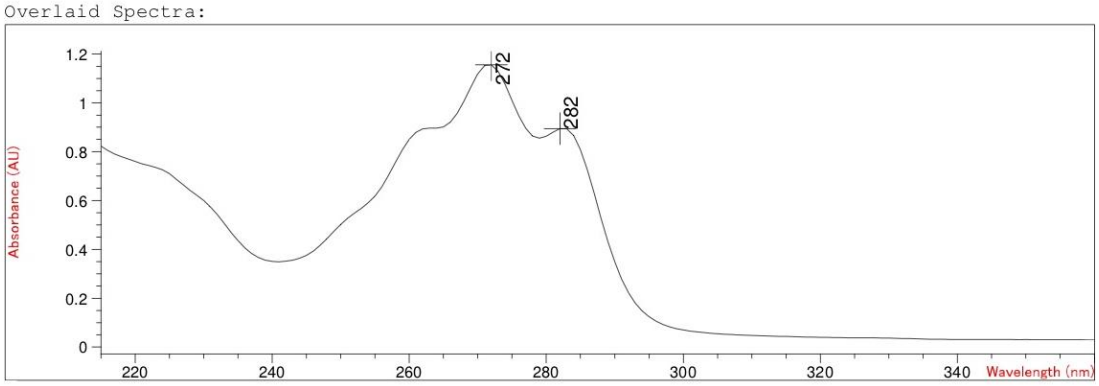

#	Name	Peaks(nm)	Abs(AU)	#	Name	Peaks(nm)	Abs(AU)
1		272.0	1.15580	1		***	***
1		282.0	0.89456	1		***	***
1		***	***	1		***	***
1		***	***	1		***	***
1		***	***	1		***	***

Report generated by : Signature: .....

*** End Spectrum/Peak Report ***

Figure 26. Obtained UV spectrum of MaR2$_{n\text{-}3\ DPA}$ (**20**).

The specific optical rotation was calculated to be $[\alpha]_D^{20}$ = 2.0 (c = 0.10, MeOH) for compound **20**.

It emerges from the obtained proton spectrum of compound **20** that the achieved purity is not satisfying, even though several attempts have been done by column chromatography. The amount of the compound in the NMR sample is only a few milligrams, which resulting in extreme visibility of the impurities. The methyl group of the precursor ester **90** appeared at 3.66 ppm as a relative intensive singlet in comparison to the other peaks in the spectrum for this compound. In the obtained spectrum for MaR2$_{n\text{-}3\ DPA}$ (**20**), a minor singlet at 3.65 ppm is observed. The integral for the peak is only 0.25 hydrogens which may indicate not completely conversion of the methyl ester **90** to the free acid of **20**. The obtained MS and UV spectra of compound **20** confirm in cooperation with the recorded ^{1}H NMR spectrum, that the formed compound is MaR2$_{n\text{-}3\ DPA}$.

3 Conclusions and Future Studies

The synthetic efforts reported herein resulted in a synthesis of the methyl ester of $MaR2_{n\text{-}3\ DPA}$ (**90**) from the commercially available starting materials 2-deoxy-D-ribose (**32**), *Z*-hex-3-en-1-ol (**41**) and cycloheptanone (**36**). The synthesis of the methyl ester $MaR2_{n\text{-}3\ DPA}$ (**90**) was achieved over 12 steps (LLS) in 0.07% overall yield and in 95% purity.

The free acid of $MaR2_{n\text{-}3\ DPA}$ (**20**) was achieved in mg scale but was, after several attempts to purify by column chromatography on silica, difficult to obtain in high enough purity. Because of time constraint, further purification by preparatory or high-pressure chromatography of the final product **20** is postponed. Hopefully, this will result in an acceptable purity of $MaR2_{n\text{-}3\ DPA}$.

One of the most difficult step in the presented synthesis of the methyl ester of $MaR2_{n\text{-}3\ DPA}$ was the *Z*-selective reduction of the alkyne **89**. After the Lindlar reduction, the product **89** required several efforts of purification. In **Figure 27** an alternative synthetic pathway is suggested, where the difficult *Z*-selective reduction is avoided. Therefore, instead of a Sonogashira coupling reaction between the alkyne **34** and the vinyl-iodide **33**, a *Z*-selective Wittig reaction is proposed between the α,β-unsaturated aldehyde **91** and the Wittig salt **92**. Thereby, the *Z*-double bond is directly obtained and only a deprotection of the TBS-groups followed by hydrolysis are needed to give $MaR2_{n\text{-}3\ DPA}$ (**20**). The Wittig salt **92** has already been prepared by the LIPCHEM group in the synthesis of $PD1_{n\text{-}3\ DPA}$.[59] The aldehyde **91** may be prepared in a double Wittig reaction with (triphenyl-phosphoranylidene)acetaldehyde and compound **37**, which is prepared from 2-deoxy-D-ribose (**32**) and *Z*-hex-3-en-1-ol (**41**) in the same way as the performed synthesis in this thesis. There may be some challenges with formation of unwanted isomers in the double Wittig reaction, but this has to be tested to know.

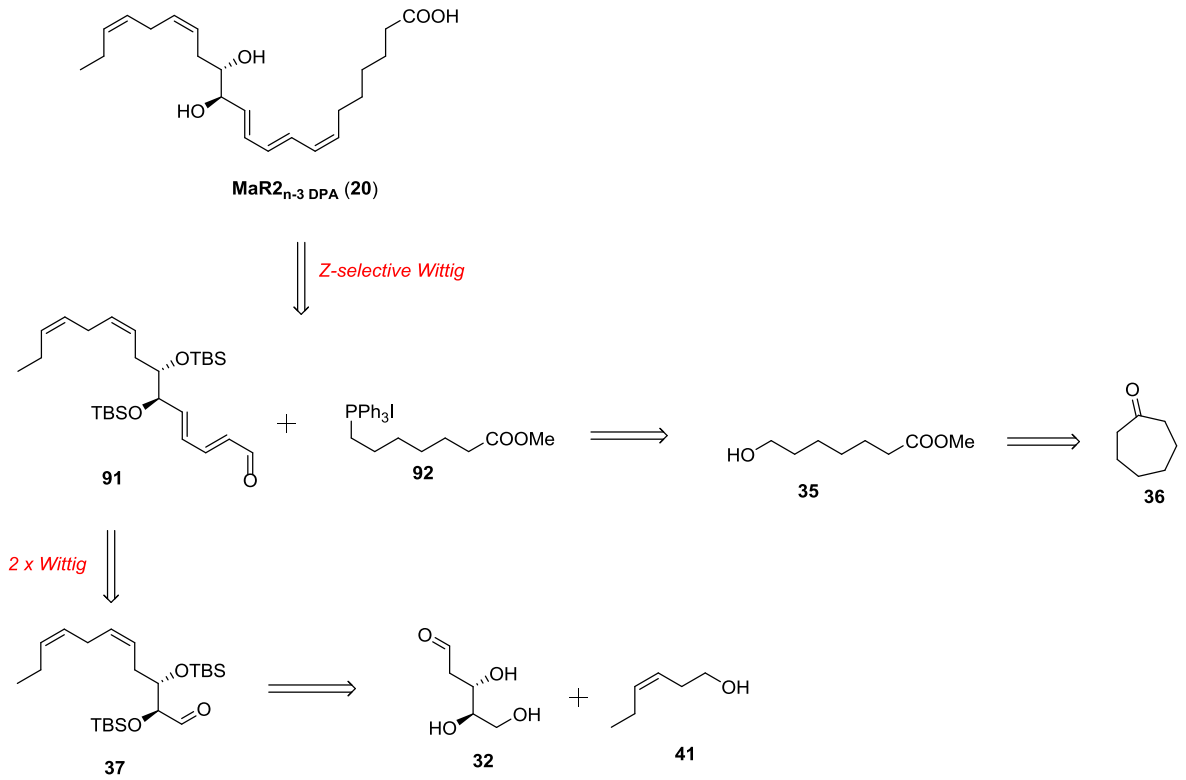

Scheme 32. A proposed alternative retrosynthesis of MaR2$_{n\text{-}3\ DPA}$ (**20**).

The prepared methyl ester of MaR2$_{n\text{-}3\ DPA}$ will be submitted to matching experiments with biological material after hydrolysis of the said ester. The Dalli group at John Vane Science Centre in London will perform these studies. If the structure is confirmed as the assumed structure of MaR2$_{n\text{-}3\ DPA}$ (**20**), exact structural assignment will be made of MaR2$_{n\text{-}3\ DPA}$. Then *in vitro* and *in vivo* experiments can be performed to investigate the pro-resolving activities of the compound. The knowledge obtained from such investigations is of interest towards potential lead compounds as a further step in the effort of making new pro-resolving drugs.

4 Experimental

4.1 Materials and apparatus

All commercially available reagents and solvents were used without further purification unless stated otherwise. The stated yields are based on isolated material. Analytical thin layer chromatography (TLC) was performed on Merck 250 μm silica gel 60 F_{254} aluminum-backed plates unless stated otherwise. For flash column chromatography silica gel 60 (40-63 μm) by Merck was used. The NMR spectra were recorded on a Bruker AVII 400 instrument or on a Bruker AVII600 instrument. For ^{1}H NMR spectra 400 or 600 MHz was used, and 101 or 151 MHz was used for ^{13}C NMR. All reported coupling constants (*J*) are stated in Hertz and the chemical shifts (δ) are reported in parts per million relative to the central residual protium solvent resonance in ^{1}H NMR ($CDCl_3$ = δ 7.26 and CD_3OD = δ 4.87) and the central carbon solvent resonance in ^{13}C NMR ($CDCl_3$ = δ 77.00 and CD_3OD = δ 49.00). Mass spectra and high-resolution mass spectra were recorded at the Department of Chemistry at UIO on Waters Prospec Q with ESI as method. Optical rotations were measured on an Anton Paar MCP 100 polarimeter using a 1.0 mL cell with 1.0 dm path length. For UV spectra a Cary 8454 UV-Vis instrument from Agilent Technologies was used with an ultra-micro rect cell. High pressure liquid chromatography was performed on an Agilent Technologies 1200 series with a UV detector using an Agilent Eclipse XDB-C18 column.

4.2 Experimental procedures

4.2.1 Synthesis of (2*R*,3*S*)-5,5-bis(ethylthio)pentane-1,2,3-triol

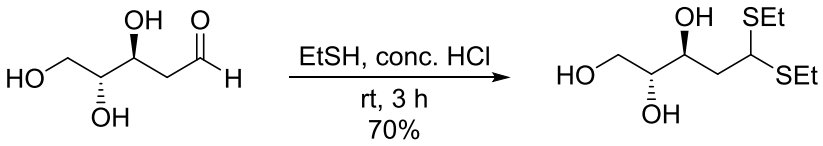

32 **42**

Commercial 2-deoxy-D-ribose (**32**) (5.01 g, 37.4 mmol, 1.00 eq.) was dissolved in conc. HCl (6.50 mL) and ethanethiol (6.50 mL, 89.5 mmol, 2.40 eq.) was added slowly. After stirring for 3 h and 10 minutes at room temperature the solution was neutralized with saturated aqueous solution of K_2CO_3 (30 mL). The layers were separated, and the aqueous layer was extracted with CH_2Cl_2 (3 x 50 mL). The combined organic layers were dried ($MgSO_4$), filtered and concentrated *in vacuo*. After column chromatography on silica (3.8% MeOH in CH_2Cl_2) the thioacetal **42** (6.26 g, 26.0 mmol, 70%) was obtained as a yellow oil. The spectroscopic and physical data were in accordance with the literature.[41] **Yield:** 6.26 g (70%). **^{1}H NMR** (400 MHz, $CDCl_3$) δ 4.10 – 4.03 (m, 2H), 3.81 – 3.76 (m, 2H), 3.63 – 3.58 (m, 1H), 2.79 – 2.56 (m, 4H), 2.26 (s, 3H), 2.06 – 1.98 (m, 2H), 1.30 – 1.24 (m, 6H). **^{13}C NMR** (101 MHz, $CDCl_3$) δ 73.8, 72.2, 63.6, 48.7, 39.0, 24.5, 24.2, 14.6, 14.6. **TLC** (10% MeOH in CH_2Cl_2, $KMnO_4$ stain): R_f = 0.6; $[\alpha]_D^{20}$= -14.5 (c = 2.9, MeOH).

4.2.2 Synthesis of (5*S*,6*R*)-5-(2,2-bis(ethylthio)ethyl)-6-((*tert*-butyldimethylsilyl)oxy)-2,2,3,3,9,9,10,10-octamethyl-4,8-dioxa-3,9-disilaundecane

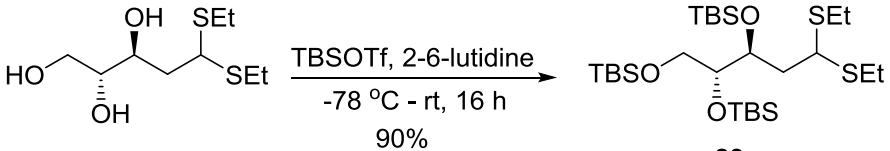

42 **83**

To thioacetal **42** (6.05 g, 25.1 mmol, 1.00 eq.) in dry CH_2Cl_2 (80 mL) cooled down to -78 °C, 2,6-lutidine (23.4 mL, 100.5 mmol, 8.00 eq.) and TBSOTf (23.1 mL, 100.5mmol, 8.00 eq.) were added. The reaction mixture was under stirring slowly warmed up to room temperature over night.

Saturated aqueous solution of NH_4Cl (76 mL) was added, the phases were separated and the aqueous phase was extracted with CH_2Cl_2 (3 x 80 mL). The organic phases were combined and washed with brine (40 mL), dried ($MgSO_4$), filtered and concentrated *in vacuo*. After purification by column chromatography (2.5% EtOAc in hexane) TBS-triol **83** (13.2 g, 22.6 mmol, 90%) was obtained as a colourless oil. All the spectroscopic and physical data were in accordance with the literature.[41] **Yield:** 13.2 g (90%). **^{1}H NMR** (400 MHz, $CDCl_3$) δ 4.17 (ddd, *J* = 9.4, 2.6, 1.4 Hz, 1H), 3.93 (dd, *J* = 11.0, 3.8 Hz, 1H), 3.72 – 3.66 (m, 1H), 3.51 (dd, *J* = 10.7, 7.1 Hz, 1H), 3.44 (dd, *J* = 10.2, 5.7 Hz, 1H), 2.73 – 2.51 (m, 4H), 2.07 (ddd, *J* = 14.2, 9.8, 3.7 Hz, 1H), 1.78 (ddd, *J* = 14.6, 11.0, 2.6 Hz, 1H), 1.27 – 1.22 (m, 6H), 0.93 – 0.85 (m, 27H), 0.13 – -0.00 (m, 18H).**^{13}C NMR** (101 MHz, $CDCl_3$) δ 77.8, 72.2, 64.5, 48.2, 39.0, 26.2, 26.1, 26.1, 25.9, 24.6, 23.2, 18.4, 18.4, 18.3, 14.8, 14.5, -2.8, -3.5, -4.3, -4.4, -4.6, -5.3, -5.3. **TLC** (5% EtOAc in hexane, $KMnO_4$ stain): R_f = 0.9; $[\alpha]_D^{20}$= -4.3 (c = 0.31, MeOH).

4.2.3 Synthesis of (3*S*,4*R*)-3,4,5-tris((*tert*-butyldimethylsilyl)oxy)pentanal

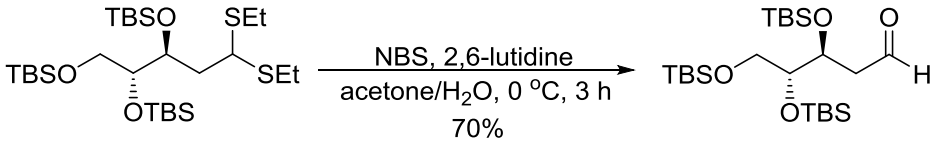

83 **39**

TBS-triol **83** (7.77 g, 13.3 mmol, 1.00 eq.) was dissolved in a solution of acetone/water (75 mL/25 mL) and the mixture was cooled down to 0 °C. Then 2,6-lutidine (12.5 mL, 107 mmol, 8.03 eq.) and NBS (19.0 g, 107 mmol, 8.01 eq.) were added. The reaction mixture was stirred on ice bath for 3 h before the solution was neutralized with sat. aq. $Na_2S_2O_3$ (65 mL). EtO_2 (65 mL) was added, the layers were separated, and the aqueous layer was extracted with Et_2O (3 x 65 mL). The organic layers were combined and washed with HCl (1.00 M, 26 mL), sat. aq. $NaHCO_3$ (26 mL) and at last brine (26 mL). The organic layer was dried ($MgSO_4$), filtered and concentrated *in vacuo*. The TBS-aldehyde **39** (4.45 g, 9.33 mmol, 70%) appeared as a clear oil after column chromatography (1% EtOAc in hexane). All the spectroscopic and physical data were in accordance with the literature.[41] **Yield:** 4.45 g (70%). **^{1}H NMR** (400 MHz, $CDCl_3$) δ 9.85 (dd, *J* = 3.4, 1.7 Hz, 1H), 4.35 (dt, *J* = 5.2, 2.3 Hz, 1H), 3.80 – 3.74 (m, 1H), 3.49 (dd, *J* = 10.3, 5.2 Hz, 1H), 3.41 (dd, *J* = 10.3, 8.0 Hz, 1H), 2.59 (ddd, *J* = 16.3, 5.5, 3.4 Hz, 1H), 2.46 (ddd, *J* = 16.3, 4.8, 1.7 Hz, 1H), 1.00 – 0.77 (m, 27H), 0.18 – -

0.03 (m, 18H). **^{13}C NMR** (101 MHz, $CDCl_3$) δ 202.7, 77.3, 69.7, 64.5, 45.8, 26.0, 26.0, 18.4, 18.3, 18.2, -4.2, -4.4, -4.5, -4.8, -5.3, -5.4. **TLC** (2% EtOAc in hexane, $KMnO_4$ stain): R_f = 0,28. $[\alpha]_D^{20}$= -11.8 (c = 0.42, MeOH).

4.2.4 Synthesis of (*Z*)-hex-3-en-1-yliodotriphenyl-λ^5-phosphane

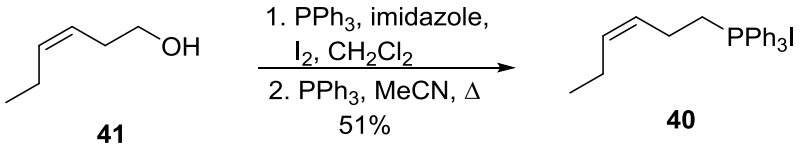

41 **40**

Z-hex-3-en-1-ol (**41**) (6.00 mL, 49.9 mmol, 1.00 eq.) was dissolved in dry CH_2Cl_2 (300 mL) and triphenylphosphine (20.1 g, 76.7 mmol, 1.54 eq.) and imidazole (5.26 g, 77.2 mmol, 1.55) were added. The mixture was stirred at 0 °C in 20 minutes before iodine (19.6 g, 77.3 mmol, 1.55 eq.) was added. After 15 minutes the ice bath was removed, and the solution was stirred at room temperature in 3h. A saturated aq. solution of $MgSO_4$ (114 mL) was added and the layers were separated. The aqueous layer was extracted with CH_2Cl_2 (3 x 300 mL) and the combined organic layers were dried ($MgSO_4$), filtered and concentrated *in vacuo*. The dark red crude product was purified by a silica gel column chromatography (hexane) to yield a dark purple oil (5.05 g, 24.0 mmol, 48%). The oil was then dissolved in dry MeCN (140 mL) and triphenylphosphine (10.8 g, 41.1 mmol, 0.82 eq.) was added. The solution was refluxed for 19 h, cooled down and concentrated *in vacuo*. After flash chromatography on silica (CH_2Cl_2 until all the PPh_3 was out then 10 % MeOH in CH_2Cl_2) the Wittig salt **40** (12.0 g, 25.3 mmol, quant.) was yielded as a clear oil. The oil crystallized after a little while to yield white crystals. All the spectroscopic and physical data were in accordance with the literature.[61] **Yield:** 12.0 g (51% over two steps). **^{1}H NMR** (400 MHz, $CDCl_3$) δ 7.85 – 7.74 (m, 9H), 7.75 – 7.65 (m, 6H), 5.52 – 5.42 (m, 1H), 5.40 – 5.30 (m, 1H), 3.74 – 3.59 (m, 2H), 2.48 – 2.35 (m, 2H), 1.82 – 1.74 (m, 2H), 0.82 (t, *J* = 7.5 Hz, 3H). **^{13}C NMR** (101 MHz, $CDCl_3$) δ 135.3 (d, 4'J_{CP} = 3.0 Hz, 3C), 134.4 (d, 4J_{CP} = 1.1 Hz, 1C), 133.7 (d, 3'J_{CP} = 10.2 Hz, 6C), 130.7 (d, 2'J_{CP} = 12.6 Hz, 6C), 125.2 (d, 3J_{CP} = 14.3 Hz, 1C), 118.0 (d, 1'J_{CP} = 86.2 Hz, 3C), 23.6 (d, 1J_{CP} = 48.7 Hz, 1C), 20.7, 20.3 (d, 2J_{CP} = 3.7 Hz, 1C), 14.0. **TLC** (10% MeOH in CH_2Cl_2, $KMnO_4$ stain): R_f = 0.79;

4.2.5 Synthesis of (5*S*,6*R*)-6-((*tert*-butyldimethylsilyl)oxy)-2,2,3,3,9,9,10,10-octamethyl-5-((2*Z*,5*Z*)-octa-2,5-dien-1-yl)-4,8-dioxa-3,9-disilaundecane

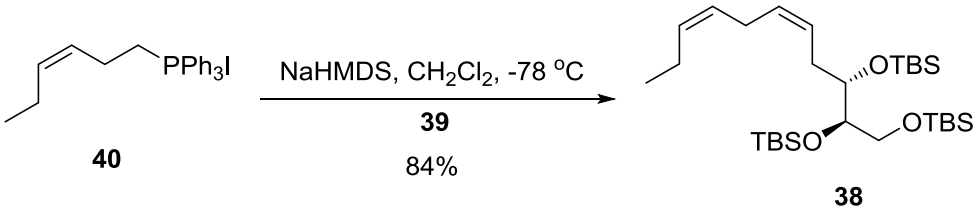

40 **39** 84% **38**

The Wittig salt **40** (2.22 g, 4.70 mmol, 1.25 eq.) was dissolved in dry DCM (20 mL) and the solution was cooled down to -78 °C before NaHMDS (7.80 mL, 4.70 mmol, 1.25 eq.) was added. The aldehyde **39** (1.80 g, 3.77 mmol, 1.00 eq.) in dry DCM (7 mL) was added and the reaction mixture was stirred and slowly warmed up to room temperature. After 16 h the mixture was neutralized with phosphate buffer (30 mL, pH = 7.0). Et_2O (45 mL) was added, the layers were separated, and the aqueous layer was extracted with Et_2O (2 x 45 mL). The combined organic layers were dried ($MgSO_4$), filtered and concentrated *in vacuo*. Flash column chromatography on silica (hexane) was performed which gave the target molecule **38** (1.71 g, 3.16 mmol, 84%) as a clear oil. **Yield:** 1.71 g (84%). **^{1}H NMR** (400 MHz, $CDCl_3$) δ 5.51 – 5.26 (m, 4H), 3.80 (dt, *J* = 7.1, 2.3 Hz, 1H), 3.70 (dt, *J* = 6.2, 2.3 Hz, 1H), 3.62 (dd, *J* = 10.1, 6.2 Hz, 1H), 3.47 (dd, *J* = 10.0, 5.9 Hz, 1H), 2.85 – 2.70 (m, 2H), 2.33 – 2.22 (m, 2H), 2.10 – 2.03 (m, 2H), 0.97 (t, *J* = 7.5 Hz, 3H), 0.92 – 0.85 (m, 27H), 0.13 – -0.03 (m, 18H).**^{13}C NMR** (101 MHz, $CDCl_3$) δ 131.8, 129.4, 127.3, 127.1, 77.2, 74.2, 64.8, 30.6, 26.0, 26.0, 25.7, 20.6, 18.3, 18.2, 18.2, 14.3, -4.2, -4.4, -4.5, -4.6, -5.3, -5.4. **TLC** (hexane, CAM stain): R_f = 0.20. $[\alpha]_D^{20}$= 2.46 (c = 0.41, MeOH). **HRMS (ESI):** calculated $C_{29}H_{62}NaO_3Si_3$: 565.3899, found: 565.3899.

4.2.6 Synthesis of (2*R*,3*S*,5*Z*,8*Z*)-2,3-bis((*tert*-butyldimethylsilyl)oxy)undeca-5,8-dien-1-ol

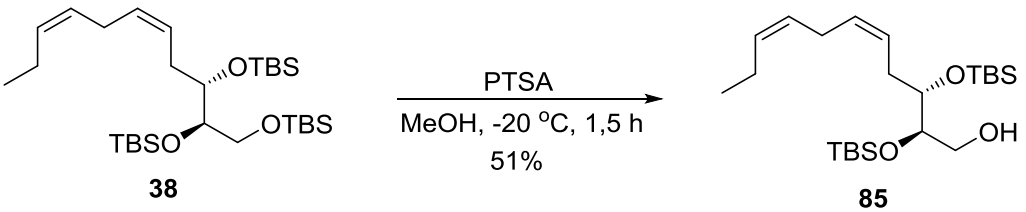

38 **85**

The TBS-diene **38** (1.49 g, 2.75 mmol, 1.00 eq.) was dissolved in MeOH (34 mL) and cooled down to -20 °C. PTSA (0.523 g, 2.75 mmol, 1.00 eq.) was added and the mixture was stirred at -20 °C.

After 1.5 h the reaction was neutralized with a saturated aqueous solution of $NaHCO_3$ (64 mL) and diluted with EtOAc (32 mL). The phases were separated, and the aqueous layer was extracted with EtOAc (3 x 32 mL). The combined organic phases were washed with brine (34 mL), dried with $MgSO_4$, filtered and concentrated *in vacuo*. The primary alcohol **85** (0.796 g, 1.86 mmol, 61%) appeared after column chromatography (3% EtOAc in hexane) as a clear oil, and the unreacted starting material was reisolated. **Yield:** 0.796 g (61%). **^{1}H NMR** (400MHz, $CDCl_3$) δ 5.49 – 5.24 (m, 4H), 3.83 – 3.70 (m, 2H), 3.68 – 3.57 (m, 2H), 2.84 – 2.70 (m, 2H), 2.39 – 2.23 (m, 2H), 2.17 (s, 1H), 2.10 – 2.03 (m, 1H), 0.97 (t, *J* = 7.6 Hz, 3H), 0.93 – 0.86 (m, 18H), 0.12 – 0.03 (m, 12H). **^{13}C NMR** (101 MHz, $CDCl_3$) δ 132.3, 130.3, 127.0, 125.6, 75.0, 74.9, 63.9, 32.1, 26.1, 26.0, 26.0, 20.7, 18.3, 18.2, 14.4, -4.3, -4.3, -4.4, -4.4. **TLC** (3% EtOAc in hexane, $KMnO_4$ stain): R_f = 0.16. $[\alpha]_D^{20}$ = 5.17 (c = 0.10, MeOH). **HRMS (ESI):** calculated $C_{23}H_{48}NaO_3Si_2$: 451.3034, found: 451.3034.

4.2.7 Synthesis of (2*S*,3*S*,5*Z*,8*Z*)-2,3-bis((*tert*-butyldimethylsilyl)oxy)undeca-5,8-dienal

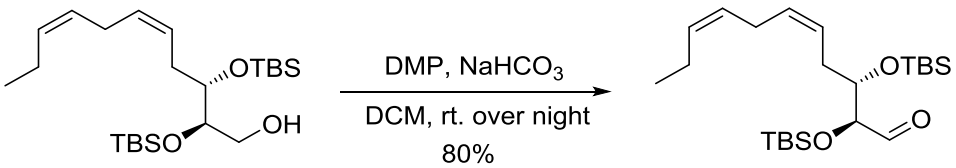

85 **37**

The alcohol **85** (0.467 g, 1.09 mmol, 1.00 eq.) was dissolved in CH_2Cl_2 (25 mL) and $NaHCO_3$ (0.522 g, 6.21 mmol, 5.70 eq.) and DMP (1.02 g, 2.40 mmol, 2.00 eq.) were added. The reaction mixture was stirred over night at room temperature. Further DMP (3 x 0.20 eq.) was added over the next 5 h for full conversion of the starting material **85** to product **37**. The reaction was stopped by adding saturated aqueous solution of $Na_2S_2O_3$ (11 mL) and CH_2Cl_2 (11 mL). The phases were separated, and the aqueous phase was extracted with CH_2Cl_2 (2 x 11 mL). The combined organic phases were washed with brine (20 mL), dried ($MgSO_4$), filtered and concentrated *in vacuo*. The crude product was purified by column chromatography (3% EtOAc in hexane) to yield the wanted product **37** (0.370 g, 0.867 mmol, 80%) as a clear oil. **Yield:** 0.370 g (80%). **^{1}H NMR** (400 MHz, $CDCl_3$) δ 9.56 (d, *J* = 1.6 Hz, 1H), 5.48 – 5.36 (m, 2H), 5.35 – 5.26 (m, 2H), 3.99 – 3.89 (m, 2H), 2.82 – 2.78 (m, 2H), 2.52 – 2.40 (m, 1H), 2.30 – 2.20 (m, 1H), 2.10 – 2.03 (m, 2H), 0.97 (t, *J* = 7.6 Hz, 3H), 0.94 – 0.86 (m,

18H), 0.10 – 0.05 (m, 12H). **^{13}C NMR** (101 MHz, $CDCl_3$) δ 203.9, 132.4, 131.6, 126.9, 124.8, 81.1, 76.1, 31.8, 26.0, 25.9, 20.7, 18.4, 18.2, 14.4, -4.4, -4.5, -4.6, -4.6. **TLC** (3% EtOAc in hexane, $KMnO_4$ stain): R_f = 0.50. $[\alpha]_D^{20}$= 9.26 (c = 0.37, MeOH). **HRMS (ESI):** Calculated $C_{23}H_{46}NaO_3Si_2$: 449.2878, found: 449.2878.

4.2.8 Synthesis of (2*E*,4*R*,5*S*,7*Z*,10*Z*)-4,5-bis((*tert*-butyldimethylsilyl)oxy)trideca-2,7,10-trienal

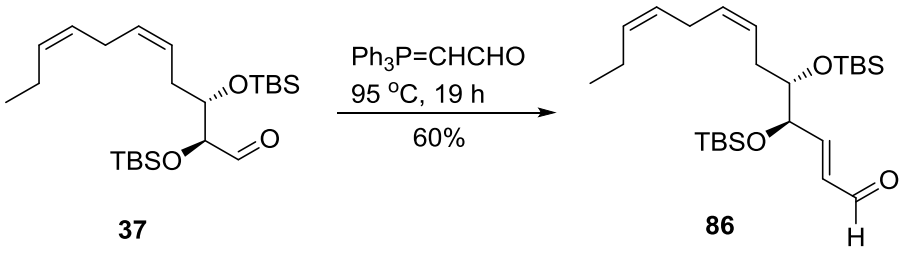

37 **86**

The TBS-aldehyde **37** (0.597 g, 1.40 mmol, 1.00 eq.) was dissolved in toluene (27 mL) and (triphenyl-phosphoranylidene)acetaldehyde (0.402 g, 1.32 mmol, 0.94 eq.) was added. The mixture was stirred at 95 °C for 6 h before another equivalent of (triphenyl-phosphoranylidene) acetaldehyde (0.403 g, 1.32 mmol, 0.94 eq.) was added. Stirring for 13 h at 95 °C, the reaction mixture was cooled down to room temperature and concentrated *in vacuo*. The α,β-unsaturated aldehyde **86** (0.382 g, 0.844 mmol, 60%) was obtained after flash chromatography (3% EtOAc in hexane) as a light-yellow oil and unreacted starting material was reisolated. **Yield:** 0.382 g (60%). **^{1}H NMR** (400MHz, $CDCl_3$) δ 9.58 (d, *J* = 8.0 Hz, 1H), 6.88 (dd, *J* = 15.6, 5.2 Hz, 1H), 6.25 (ddd, *J* = 15.7, 8.0, 1.4 Hz, 1H), 5.51 – 5.24 (m, 4H), 4.35 – 4.27 (m, 1H), 3.75 (td, *J* = 6.1, 3.7 Hz, 1H), 2.84 – 2.70 (m, 2H), 2.34 – 2.25 (m, 2H), 2.09 – 2.02 (m, 2H), 0.97 (t, *J* = 7.6 Hz, 3H), 0.93 – 0.85 (m, 18H), 0.08 – 0.02 (m, 12H). **^{13}C NMR** (101 MHz, $CDCl_3$) δ 193.5, 157.5, 132.3, 132.2, 130.6, 126.7, 125.2, 76.5, 75.5, 31.9, 25.9, 25.8, 20.6, 18.2, 18.1, 14.2, -4.2, -4.4, -4.5, -4.7. **TLC** (3% EtOAc in hexane, $KMnO_4$ stain): R_f = 0.28. $[\alpha]_D^{20}$= 37.8 (c = 0.087, MeOH). **HRMS (ESI):** calculated $C_{25}H_{48}NaO_3Si_2$: 475.3034, found: 475.3034.

4.2.9 Synthesis of (5*R*,6*S*)-5-((1*E*,3*E*)-4-iodobuta-1,3-dien-1-yl)-2,2,3,3,8,8,9,9-octamethyl-6-((2*Z*,5*Z*)-octa-2,5-dien-1-yl)-4,7-dioxa-3,8-disiladecane

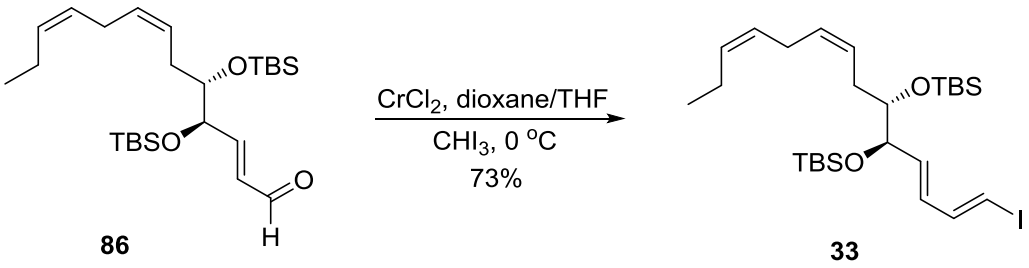

$CrCl_2$ (438 mg, 3.56 mmol, 29.5 eq.) was dissolved in a mixture of dioxane/THF (6 mL, 6/1), cooled down to 0 °C and a solution of aldehyde **86** (55.0 mg, 0.121 mmol, 1.00 eq.) and CHI_3 (381 mg, 0.968 mmol, 8.00 eq.) in dioxane/THF (2.0 mL, 6/1) were added. The reaction mixture was stirred for 30 minutes at 0 °C. After 1,5 h at room temperature EtOAc (10 mL) was added followed by saturated aqueous solution of $Na_2S_2O_3$ (6.7 mL) and saturated aqueous solution of NH_4Cl (4.5 mL). The layers were separated, and the aqueous layer was extracted with EtOAc (3 x 9 mL). The combined organic layers were washed with brine (10 mL), dried ($MgSO_4$), filtered and concentrated *in vacuo*. After purification by flash chromatography (hexane) the vinyl iodide **33** (46.0 mg, 0.080 mmol, 73%) was obtained as a yellow oil. **Yield:** 46.0 g (73%). **^{1}H NMR** (400MHz, $CDCl_3$) δ 7.03 (dd, *J* = 14.4, 10.7 Hz, 1H), 6.28 (d, *J* = 14.4 Hz, 1H), 6.06 (dd, *J* = 15.4, 10.7 Hz, 1H), 5.72 (dd, *J* = 15.3, 7.0 Hz, 1H), 5.45 – 5.25 (m, 4H), 3.98 (dd, *J* = 7.0, 4.1 Hz, 1H), 3.63 (dt, *J* = 6.1, 4.0 Hz, 1H), 2.79 – 2.72 (m, 2H), 2.27 – 2.19 (m, 2H), 2.09 – 2.02 (m, 1H), 0.97 (t, *J* = 7.5 Hz, 3H), 0.91 – 0.85 (m, 18H), 0.06 – -0.01 (m, 12H). **^{13}C NMR** (101 MHz, $CDCl_3$) δ 145.0, 135.4, 132.1, 131.2, 130.0, 127.2, 126.2, 78.8, 76.5, 76.5, 31.8, 26.1, 26.0, 20.7, 18.4, 18.3, 14.4, -4.0, -4.0, -4.2, -4.3, -4.5. **TLC** (hexane, $KMnO_4$ stain): R_f = 0.20. $[\alpha]_D^{20}$= 1.46 (c = 0.14, MeOH). **HRMS (ESI):** calculated $C_{26}H_{49}INaO_2Si_2$: 599.2208, found 599.2207.

4.2.10 Synthesis of methyl 7-hydroxyheptanoate

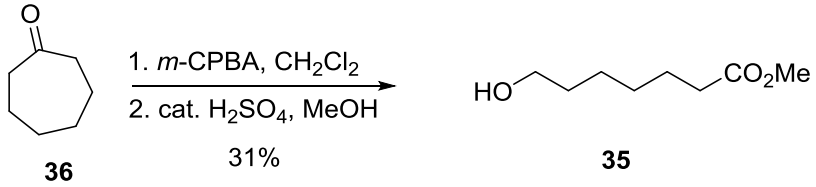

The alcohol ester **35** was prepared from the commercial cycloheptanone (**36**) via a Baeyer-Villiger reaction followed by a Fisher esterification.[59,63] First *m*-CPBA (16.2 g, 77%, 55.8 mmol, 1.50 eq.) was dissolved in CH_2Cl_2 (100 mL) and the solution was cooled down to 0 °C under stirring. Cycloheptanone (**36**) (4.40 mL, 37.2 mmol, 1.00 eq.) was added and the mixture was stirred at room temperature for 7 days. The mixture was cooled to 0 °C and stirred for 20 min. The reaction mixture was filtered over in a separatory funnel and the organic phase was washed with sat. aq. $NaHCO_3$ (25 mL), dried ($MgSO_4$), filtered and concentrated *in vacuo*. The crude product was taken up in dry MeOH (75 mL), a few drops of conc. H_2SO_4 was added, and the mixture was refluxed overnight. The mixture was cooled down to room temperature, added sat. aq. $NaHCO_3$ (7.5 mL) and concentrated *in vacuo*. Thereafter further sat. aq. $NaHCO_3$ (25 mL) was added, the phases were separated, and the water phase was extracted with Et_2O (4 x 50 mL). The combined organic phases were dried ($MgSO_4$), filtered and concentrated *in vacuo*. The alcohol ester **35** (1.83 g, 11.4 mmol, 31%) appeared as a clear oil after purification by column chromatography on silica (20% EtOAc in hexane) and unreacted starting material was re-isolated. All the spectroscopic and physical data were in accordance with the literature.[63,59] **Yield:** 1.83 g (31%). **^{1}H NMR** (400 MHz, $CDCl_3$) δ 3.64 (s, 3H), 3.60 (t, *J* = 6.6 Hz, 2H), 2.29 (t, *J* = 7.5 Hz, 2H), 1.82 (s, 1H), 1.66 – 1.49 (m, 4H), 1.40 – 1.28 (m, 4H). **^{13}C NMR** (101 MHz, $CDCl_3$) δ 174.4, 62.8, 51.6, 34.1, 32.6, 28.9, 25.5, 24.9. **TLC** (20% EtOAc in hexane, $KMnO_4$ stain): R_f = 0.19.

4.2.11 Synthesis of methyl 7-oxoheptanoate

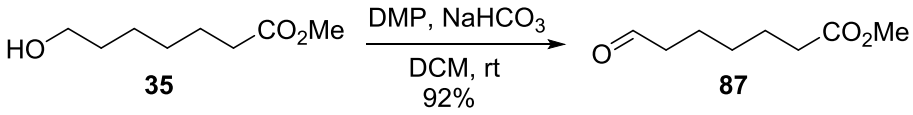

To a solution of alcohol **35** (1.61 g, 10.0 mmol, 1.00 eq.) in CH_2Cl_2 (100 mL) $NaHCO_3$ (4.80 g, 57.1 mmol, 5.70 eq.) and DMP (9.77 g, 23.1 mmol, 2.30 eq.) were added and the reaction mixture was stirred at room temperature in 2 h. The mixture was then quenched with sat. aq. $Na_2S_2O_3$ (104 mL), the layers were separated, and the aqueous layer was extracted with CH_2Cl_2 (3 x 100 mL). The combined organic phases were washed with brine (100 mL), dried ($MgSO_4$), filtered and concentrated *in vacuo*. The yellow crude product was purified by column chromatography on silica (20% EtOAc in hexane) and the aldehyde **87** (1.46 g, 9.22 mmol, 92%) was obtained as a clear oil.

Yield: 1.46 g (92%). **^{1}H NMR** (400 MHz, $CDCl_3$) δ 9.72 (s, 1H), 3.62 (s, 3H), 2.41 (t, *J* = 7.3 Hz, 2H), 2.28 (t, *J* = 7.4 Hz, 2H), 1.65 – 1.57 (m, 4H), 1.40 – 1.27 (m, 2H); **^{13}C NMR** (101 MHz, $CDCl_3$ δ 202.5, 174.0, 51.6, 43.7, 33.9, 28.6, 24.7, 21.7. **TLC** (20% EtOAc in hexane, $KMnO_4$ stain): R_f = 0.31.

4.2.12 Synthesis of methyl oct-7-ynoate

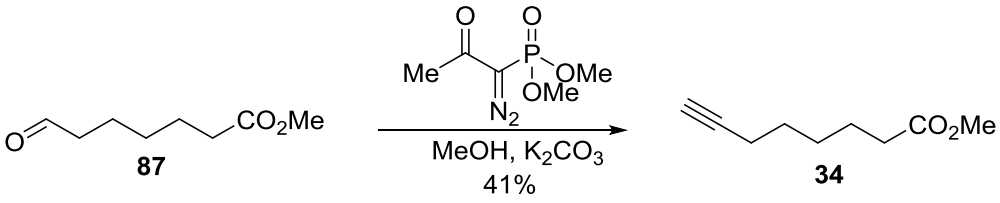

Utilizing an Ohira-Bestmann reaction the aldehyde **87** was transformed to the terminal alkyne **34**. The aldehyde **87** (1.38 g, 8.71 mmol, 1.00 eq.) in a solution of dry MeOH (80.0 mL) was added K_2CO_3 (2.41 g, 17.4 mmol, 2.00 eq.). The reaction flask was flushed with N_2(g) before the Ohira-Bestmann reagent dimethyl(1-diazo-2-oxopropyl) phosphonate (1.70 mL, 11.3 mmol, 1.30 eq.) was added through the septum. The reaction mixture was stirred at room temperature and after 4 h the mixture was diluted with Et_2O (218 mL) and transferred to a separatory funnel. A solution of 5% aq. $NaHCO_3$ (108 mL) was added and the layers were separated. The aqueous layer was extracted with Et_2O (1 x 65 mL), followed by combined organic layers washed with a 5% aq. solution of $NaHCO_3$ (3 x 65 mL) and brine (65 mL). The solution was dried (Na_2SO_4), filtered and concentrated *in vacuo*. After purification with flash chromatography on silica gel (5% EtOAc in hexane) the desired product **34** (0.547 g, 3.55 mmol, 41%) was obtained as a clear oil. **Yield:** 0.547 g, 3.55 mmol (41%). **^{1}H NMR** (400 MHz, $CDCl_3$ δ 3.62 (s, 3H), 2.28 (t, *J* = 7.5 Hz, 2H), 2.15 (dt, *J* = 7.1, 2.6 Hz, 2H), 1.90 (t, *J* = 2.7 Hz, 1H), 1.64 – 1.56 (m, 2H), 1.54 – 1.44 (m, 2H), 1.45 – 1.34 (m, 2H); **^{13}C NMR** (101 MHz, $CDCl_3$) δ 174.0, 84.3, 68.4, 51.5, 33.9, 28.2, 28.1, 24.5, 18.3. **TLC** (20% EtOAc in hexane, $KMnO_4$ stain): R_f = 0.64.

4.2.13 Synthesis of methyl (9*E*,11*E*,13*R*,14*S*,16*Z*,19*Z*)-13,14-bis((*tert*-butyldimethylsilyl)oxy)docosa-9,11,16,19-tetraen-7-ynoate

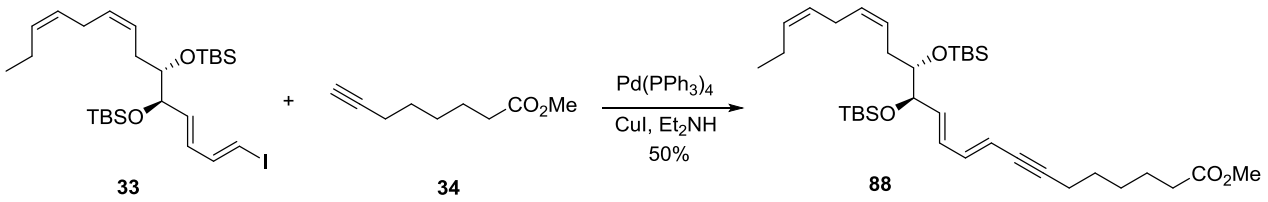

Vinyl-iodide **33** (26.5 mg, 0.046 mmol, 1.00 eq.) was dissolved in Et_2NH (0.2 mL) and benzene (0.04 mL), then $Pd(PPh_3)_4$ (3.00 mg, 5 mol%) was added and the mixture was stirred in the dark at room temperature. After 35 minutes a solution of alkyne **34** (9.00 mg, 0.058 mmol, 1.30 eq.) and CuI (0.440 mg, 5 mol%) in Et_2NH (0.09 mL) was added. After stirring 21 h at room temperature the reaction was quenched by addition of saturated aqueous solution of NH_4Cl (1.2 mL) followed by addition of Et_2O (0.9 mL). The phases were separated, and aqueous phase was extracted with Et_2O (2 x 1.2 mL). The organic phases were combined, dried (Na_2SO_4), filtered and concentrated *in vacuo*. After purification by column chromatography on silica (2% EtOAc in hexane) the title compound **88** (14.0 mg, 0.023 mmol, 50%) was obtained as a white oil and unreacted starting material was reisolated. **Yield:** 14.0 mg (50%). **^{1}H NMR** (400 MHz, CD_3OD) δ 6.47 (dd, *J* = 15.5, 10.8 Hz, 1H), 6.21 (dd, *J* = 15.3, 10.9 Hz, 1H), 5.76 (dd, *J* = 15.3, 7.2 Hz, 1H), 5.60 (d, *J* = 15.5 Hz, 1H), 5.49 – 5.27 (m, 4H), 4.11 (dd, *J* = 7.2, 4.0 Hz, 1H), 3.73 – 3.69 (m, 1H), 3.67 (s, 3H), 2.89 – 2.71 (m, 2H), 2.36 (t, *J* = 7.4 Hz, 4H), 2.34 – 2.20 (m, 2H), 2.13 – 2.05 (m, 2H), 1.69 – 1.62 (m, 2H), 1.62 – 1.50 (m, 2H), 1.51 – 1.42 (m, 2H), 0.99 (t, *J* = 7.6 Hz, 3H), 0.95 – 0.88 (m, 18H), 0.10 – 0.03 (m, 12H). **^{13}C NMR** (101 MHz, CD_3OD) δ 175.8, 140.9, 136.5, 132.8, 132.5, 130.9, 128.2, 127.3, 113.1, 93.6, 80.9, 78.2, 78.0, 52.0, 49.6, 49.4, 49.2, 49.0, 49.0, 48.8, 48.6, 48.4, 34.7, 32.6, 29.5, 29.4, 26.8, 26.6, 26.6, 25.6, 21.6, 20.1, 19.2, 19.1, 14.7, -3.7, -3.8, -4.1, -4.3. **TLC** (6% EtOAc in Hexane, $KMnO_4$ stain): R_f = 0.26. $[\boldsymbol{\alpha}]_{\boldsymbol{D}}^{\mathbf{20}}$= -12.8 (c = 0.05, MeOH). **HRMS (ESI):** calculated $C_{35}H_{62}NaO_4Si_2$: 625.4079, found: 625.4077.

4.2.14 Synthesis of methyl (9*E*,11*E*,13*R*,14*S*,16*Z*,19*Z*)-13,14-dihydroxydocosa-9,11,16,19-tetraen-7-ynoate

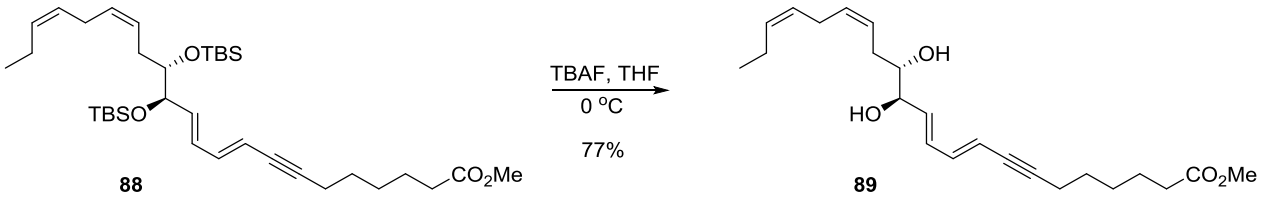

TBS-protected alkyne **88** (0.090 g, 0.149 mmol, 1.00 eq.) was dissolved in THF (3.9 mL) and cooled down to 0 °C. TBAF (0.745 mL 1.0 M in THF, 0.745 mmol, 5.00 eq.) was added and the reaction was stirred over night before phosphate buffer (pH = 7.0, 2.4 mL), brine (3.9 mL) and CH_2Cl_2 (8 mL) were added. The phases were separated, and the aqueous phase was extracted with CH_2Cl_2 (2 x 8 mL). The combined organic phases were dried ($MgSO_4$), filtered and concentrated *in vacuo.* After column chromatography on silica (hexane/EtOAc/CH_2Cl_2/MeOH 57.5:30:10:2.5) the deprotected alcohol **89** (43.0 mg, 0.115 mmol, 77%) was afforded as a viscous pale yellow oil. **Yield:** 43 mg (77%) **^{1}H NMR** (400 MHz, CD_3OD) δ 6.52 (dd, *J* = 15.4, 10.8 Hz, 1H), 6.33 (dd, *J* = 15.2, 10.8 Hz, 1H), 5.89 (dd, *J* = 15.2, 6.8 Hz, 1H), 5.64 (d, *J* = 15.4 Hz, 1H), 5.57 – 5.26 (m, 4H), 4.02 (t, *J* = 5.3 Hz, 1H), 3.68 (s, 3H), 3.61 – 3.52 (m, 1H), 2.84 – 2.81 (m, 2H), 2.42 – 2.31 (m, 4H), 2.26 – 2.01 (m, 4H), 1.69 – 1.62 (m, 2H), 1.60 – 1.51 (m, 2H), 1.51 – 1.41 (m, 2H), 0.99 (t, *J* = 7.6 Hz, 3H). **^{13}C NMR** (101 MHz, CD_3OD) δ 175.3, 141.2, 135.4, 132.7, 132.5, 131.0, 128.3, 127.1, 113.1, 93.5, 80.9, 76.0, 75.8, 52.0, 34.7, 31.8, 29.5, 29.3, 26.6, 25.5, 21.5, 20.0, 14.7. **TLC** (hexane/EtOAc/CH_2Cl_2/MeOH 57.5:30:10:2.5, CAM stain): R_f = 0.26. $[\alpha]_D^{20}$= 17.5 (c = 0.04, MeOH). **HRMS (ESI):** calculated $C_{23}H_{34}NaO_4$: 397.2349, found: 397.2349.

4.2.15 Synthesis of methyl (7*Z*,9*E*,11*E*,13*R*,14*S*,16*Z*,19*Z*)-13,14-dihydroxydocosa-7,9,11,16,19-pentaenoate

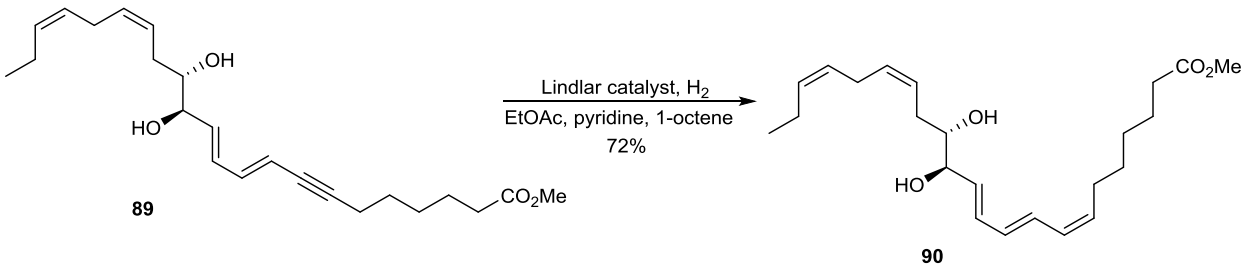

The alkyne **89** (14.5 mg, 0.039 mmol, 1.00 eq.) was dissolved in a solution of EtOAc/pyridine/1-octene (0.45 mL). Lindlar's catalyst (18.8 mg) was added and the reaction mixture was stirred at room temperature under H_2 atmosphere for 8 h. The solvent was removed, and the crude product was purified by column chromatography on silica (hexane/EtOAc/DCM/MeOH 77.5/10/10/2.5) to afford the wanted triene **90** (10.5 mg, 0.028 mmol, 72%) as a clear viscous oil. **Yield:** 10.5 mg (72%), HPLC analysis (Eclipse XDB-C18, MeOH/H_2O 80:20, 1.0 mL/min, t_r = 14.559 min (95%). **^{1}H NMR** (600 MHz, CD_3OD) δ 6.54 (dd, *J* = 14.9, 11.2 Hz, 1H), 6.35 (dd, *J* = 15.2, 10.7 Hz, 1H), 6.24 (dd, *J* = 14.8, 10.6 Hz, 1H), 6.04 (t, *J* = 11.2 Hz, 1H), 5.82 (dd, *J* = 15.2, 7.1 Hz, 1H), 5.54 – 5.28 (m, 5H), 4.05 – 3.99 (m, 1H), 3.66 (s, 3H), 3.57 (dt, *J* = 8.1, 4.9 Hz, 1H), 2.87 – 2.74 (m, 2H), 2.40 – 2.29 (m, 4H), 2.26 – 2.15 (m, 2H), 2.11 – 2.06 (m, 2H), 1.67 – 1.57 (m, 2H), 1.46 – 1.29 (m, 4H), 1.01 – 0.94 (m, 3H).**^{13}C NMR** (151 MHz, CD_3OD) δ 176.0, 133.7, 133.5, 133.4, 132.7, 131.0, 130.0, 129.4, 128.3, 127.1, 76.3, 75.9, 52.0, 34.8, 31.9, 30.4, 29.7, 28.6, 26.7, 25.9, 21.5, 14.7. **TLC** (hexane/EtOAc/CH_2Cl_2/MeOH, 62.5:25.0:10.0:2.50, CAM stain): R_f = 0.13. $[\boldsymbol{\alpha}]_{\boldsymbol{D}}^{\boldsymbol{20}}$= 16.0 (c = 0.05, MeOH). **UV** (MeOH): λ_{max} 262, 272, 283 nm. **HRMS (ESI):** calculated $C_{23}H_{36}NaO_4$: 399.2506, found: 399.2506.

4.2.16 Synthesis of (7*Z*,9*E*,11*E*,13*R*,14*S*,16*Z*,19*Z*)-13,14-dihydroxydocosa-7,9,11,16,19-pentaenoic acid

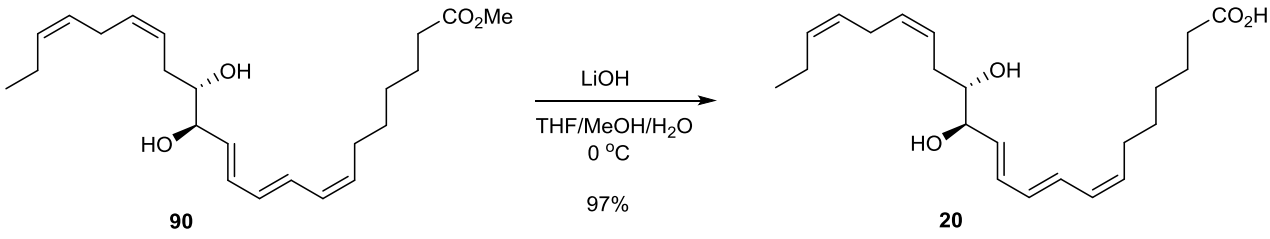

90 **20**

The methyl ester **90** (4.70 mg, 0.013 mmol, 1.00 eq.) was dissolved in a solution of THF/MeOH/H_2O (2/2/1, 1.5 mL) and the solution was cooled down to 0 °C. LiOH (11.0 mg, 0.459 mmol, 35.0 eq.) was added and the reaction mixture was stirred at 0 °C for 6.25 h, before warmed to room temperature and addition of saturated aqueous solution of NaH_2PO_4 (1.66 mL) and EtOAc (1.66 mL). The phases were separated, the aqueous phase was extracted with EtOAc (3 x 1.66 mL) before the combined organic phases were dried ($MgSO_4$) and concentrated *in vacuo*. The crude was purified by column chromatography on silica (5% MeOH in CH_2Cl_2) to afford the wanted

product **20** (4.40 mg, 0.012 mmol, 97%) as a colorless oil. **Yield:** 4.4 mg (97%) **^{1}H NMR** (400 MHz, CD_3OD) δ 6.55 (dd, *J* = 14.8, 11.3 Hz, 1H), 6.36 (dd, *J* = 15.3, 10.7 Hz, 1H), 6.24 (dd, *J* = 14.6, 10.6 Hz, 1H), 6.04 (t, *J* = 11.0 Hz, 1H), 5.82 (dd, *J* = 15.2, 7.2 Hz, 1H), 5.56 – 5.26 (m, 5H), 4.03 (dd, *J* = 10.5, 4.8 Hz, 1H), 3.57 (dt, *J* = 8.0, 4.8 Hz, 1H), 2.81 (t, *J* = 7.0 Hz, 2H), 2.41 – 2.01 (m, 8H), 1.70 – 1.55 (m, 2H), 1.47 – 1.35 (m, 4H), 0.97 (t, *J* = 7.6 Hz, 3H). **TLC** (10% MeOH in CH_2Cl_2, CAM stain): R_f = 0.39. $[\boldsymbol{\alpha}]_{\boldsymbol{D}}^{\boldsymbol{20}}$= 2.0 (c = 0.10, MeOH). **UV** (MeOH): λ_{max} 262, 272, 282 nm. **HRMS (ESI):** calculated $C_{22}H_{34}NaO_4$: 385.2349, found: 385.2350.

5 Reference

(1) Serhan, C. N.; Ward, P. A.; Gilroy, D. W. *Fundamentals of Inflammation*; Cambridge University Press, 2010; pp 1–27.
(2) Tabas, I.; Glass, C. K. *Science* **2013**, *339*, 166.
(3) Serhan, C. N.; Petasis, N. A. *Chemical Reviews* **2011**, *111*, 5922.
(4) Samuelsson, B.; Dahlén, S. E.; Lindgren, J. A.; Rouzer, C. A.; Serhan, C. N. *Science* **1987**, *237*, 1171.
(5) Serhan, C. N. *Prostaglandins Leukotrienes & Essential Fatty Acids* **2005**, *73*, 141.
(6) Serhan, C. N.; Hamberg, M.; Samuelsson, B. *Proceedings of the National Academy of Sciences of the United States of America* **1984**, *81*, 5335.
(7) Hansen, T. V.; Vik, A.; Serhan, C. N. *Frontiers Pharmacology* **2019**, *9*, 12390.
(8) Samuelsson, B. *The Journal of Biological Chemistry* **2012**, *287*, 10070.
(9) Serhan, C. N. *Annual Review of Immunology* **2007**, *25*, 101.
(10) Serhan, C. N.; Savill, J. *Nature Immunology* **2005**, *6*, 1191.
(11) Levy, B. D.; Clish, C. B.; Schmidt, B.; Gronert, K.; Serhan, C. N. *Nature Immunology* **2001**, *2*, 612.
(12) Serhan, C. N. *Nature* **2014**, *510*, 92.
(13) Serhan, C. N.; Clish, C. B.; Brannon, J.; Colgan, S. P.; Chiang, N.; Gronert, K. *Journal of Experimental Medicine* **2000**, *192*, 1197.
(14) Serhan, C. N.; Hong, S.; Gronert, K.; Colgan, S. P.; Devchand, P. R.; Mirick, G.; Moussignac, R.-L. *Journal of Experimental Medicine* **2002**, *196*, 1025.
(15) Hong, S.; Gronert, K.; Devchand, P. R.; Moussignac, R.-L.; Serhan, C. N. *Journal of Biological Chemistry* **2003**, *278*, 14677.
(16) Mukherjee, P. K.; Marcheselli, V. L.; Serhan, C. N.; Bazan, N. G. *Proceedings of the National Academy of Sciences of the United States of America* **2004**, *101*, 8491.
(17) Serhan, C. N.; Dalli, J.; Karamnov, S.; Choi, A.; Park, C.-K.; Xu, Z.-Z.; Ji, R.-R.; Zhu, M.; Petasis, N. A. *FASEB Journal* **2012**, *26*, 1755.
(18) Deng, B.; Wang, C.-W.; Arnardottir, H. H.; Li, Y.; Cheng, C.-Y. C.; Dalli, J.; Serhan, C. N. *PLOS ONE* **2014**, *9*, e102362.
(19) Serhan, C. N.; Yang, R.; Martinod, K.; Kasuga, K.; Pillai, P. S.; Porter, T. F.; Oh, S. F.; Spite, M. *The Journal of Experimental Medicine* **2009**, *206*, 15.
(20) Rodriguez, A. R.; Spur, B. W. *Tetrahedron Letters* **2015**, *56* (42), 5811–5815.
(21) Dalli, J.; Colas, R. A.; Arnardottir, H.; Serhan, C. N. *Immunity* **2017**, *46*, 92.
(22) Dalli, J.; Ramon, S.; Norris, P. C.; Colas, R. A.; Serhan, C. N. *FASEB Journal* **2015**, *29*, 2120.
(23) Dalli, J.; Chiang, N.; Serhan, C. N. *Proceedings of the National Academy of Sciences of the United States of America* **2014**, *111*, E4753.
(24) Dalli, J.; Colas, R. A.; Serhan, C. N. *Scientific Reports* **2013**, *3*, 1940.
(25) Fullerton, J. N.; Gilroy, D. W. *Nature Reviews Drug Discovery* **2016**, *15*, 551.
(26) Serhan, C. N.; Chiang, N. *British Journal of Pharmacology* **2008**, *153*, S200–S215.
(27) Ariel, A.; Li, P.-L.; Wang, W.; Tang, W.-X.; Fredman, G.; Hong, S.; Gotlinger, K. H.; Serhan, C. N. *Journal of Biological Chemistry* **2005**, *280*, 43079.
(28) Chiang, N.; Fredman, G.; Bäckhed, F.; Oh, S. F.; Vickery, T.; Schmidt, B. A.; Serhan, C. N. *Nature* **2012**, *484*, 524.

(29) Serhan, C. N.; Dalli, J.; Colas, R. A.; Winkler, J. W.; Chiang, N. *Biochimica et Biophysica Acta* **2015**, *1851*, 397.
(30) Dalli, J.; Zhu, M.; Vlasenko, N. A.; Deng, B.; Haeggström, J. Z.; Petasis, N. A.; Serhan, C. N. *FASEB Journal* **2013**, *27*, 2573.
(31) Sasaki, K.; Urabe, D.; Arai, H.; Arita, M.; Inoue, M. *Chemistry a Asian Journal* **2011**, *6*, 534.
(32) Rodriguez, A. R.; Spur, B. W. *Tetrahedron Letters* **2012**, *53*, 4169.
(33) Ogawa, N.; Tojo, T.; Kobayashi, Y. *Tetrahedron Letters* **2014**, *55*, 2738.
(34) Tungen, J. E.; Aursnes, M.; Hansen, T. V. *Tetrahedron Letters* **2015**, *56*, 1843.
(35) Gong, J.; Wu, Z.-Y.; Qi, H.; Chen, L.; Li, H.-B.; Li, B.; Yao, C.-Y.; Wang, Y.-X.; Wu, J.; Yuan, S.-Y.; Yao, S.-L.; Shang, Y. *British Journal of Pharmacology* **2014**, *171*, 3539.
(36) Ferdinandusse, S.; Denis, S.; Mooijer, P. A.; Zhang, Z.; Reddy, J. K.; Spector, A. A.; Wanders, R. J. *The Journal of Lipid Research* **2001**, *42*, 1987.
(37) Tungen, J. E.; Aursnes, M.; Dalli, J.; Arnardottir, H.; Serhan, C. N.; Hansen, T. V. *Chemistry – A European Journal* **2014**, *20*, 14537.
(38) Dalli, J.; Sanger, J. M.; Rodriguez, A. R.; Chiang, N.; Spur, B. W.; Serhan, C. N. *PLOS ONE* **2016**, *11*, e0149319.
(39) Rodriguez, A. R.; Spur, B. W. *Tetrahedron Letters* **2015**, *56*, 3936.
(40) Bannenberg, G. L.; Chiang, N.; Ariel, A.; Arita, M.; Tjonahen, E.; Gotlinger, K. H.; Hong, S.; Serhan, C. N. *Journal of Immunology* **2005**, *174*, 4345.
(41) Tungen, J. E.; Gerstmann, L.; Vik, A.; De Matteis, R.; Colas, R. A.; Dalli, J.; Chiang, N.; Serhan, C. N.; Kalesse, M.; Hansen, T. V. *Chemistry – A European Journal* **2019**, *25*, 1476.
(42) Wittig, G.; Geissler, G. *Justus Liebigs Annalen der Chemie* **1953**, *580*, 44.
(43) Maryanoff, B. E.; Reitz, A. B. *Chemical Reviews* **1989**, *89*, 863.
(44) Vedejs, E. *Journal of Organic Chemistry* **2004**, *69*, 5159.
(45) Robiette, R.; Richardson, J.; Aggarwal, V. K.; Harvey, J. N. *Journal of the American Chemical Society* **2006**, *128*, 2394.
(46) Warren, S.; Wyatt, P. *Organic Synthesis*, 2nd ed.; John Wiley & Sons, 2008; pp 108–118.
(47) Müller, S.; Liepold, B.; Roth, G. J.; Bestmann, H. J. *Synlett* **1996**, *1996*, 521.
(48) Ohira, S. *Synthetic Communications* **1989**, *19*, 561.
(49) Gilbert, J. C.; Weerasooriya, U. *Journal of Organic Chemistry* **1982**, *47*, 1837.
(50) Seyferth, D.; Marmor, R. S.; Hilbert, P. *Journal of Organic Chemistry* **1971**, *36*, 1379.
(51) Takai, K.; Nitta, K.; Utimoto, K. *Journal of Organic Chemistry* **1986**, *108*, 7408.
(52) Werner, D.; Anwander, R. *Journal of American Chemical Society* **2018**, *140*, 14334.
(53) Aursnes, M.; Tungen, J. E.; Vik, A.; Dalli, J.; Hansen, T. V. *Organic & Biomolecular Chemistry* **2014**, *12*, 432.
(54) Sonogashira, K.; Tohda, Y.; Hagihara, N. *Tetrahedron Letters* **1975**, *50*, 4467.
(55) Chinchilla, R.; Nájera, C. *Chemical Reviews* **2007**, *107*, 874.
(56) Dieck, H. A.; Heck, F. R. *Journal of Organometallic Chemistry* **1975**, *93*, 259.
(57) Cassar, L. *Journal of Organometallic Chemistry* **1975**, *93*, 253.
(58) Lindlar, H. *Helvetica Chimica Acta* **1952**, *35*, 446.
(59) Aursnes, M.; Tungen, J. E.; Vik, A.; Colas, R.; Cheng, C.-Y. C.; Dalli, J.; Serhan, C. N.; Hansen, T. V. *Journal of Natural Products* **2014**, *77*, 910.
(60) Lindlar, H. *Organic Syntheses* **1966**, *5*, 880.
(61) Primdahl, K. G. *Stereoselective Syntheses of Oxygenated Polyunsaturated Fatty Acid Mediators and Investigations of Biosynthetic Pathways*; 2017; Vol. ISSN 1501-7710, pp 95.

(62) Primdahl, K. G.; Tungen, J. E.; De Souza, P. R. S.; Colas, R. A.; Dalli, J.; Hansen, T. V.; Vik, A. *Organic & Biomolecular Chemistry* **2017**, *15*, 8606.
(63) Kai, K.; Takeuchi, J.; Kataoka, T.; Yokoyama, M.; Watanabe, N. *Tetrahedron Letters* **2008**, *64*, 6760.

6 Appendix

6.1 NMR spectra of the synthesized compounds

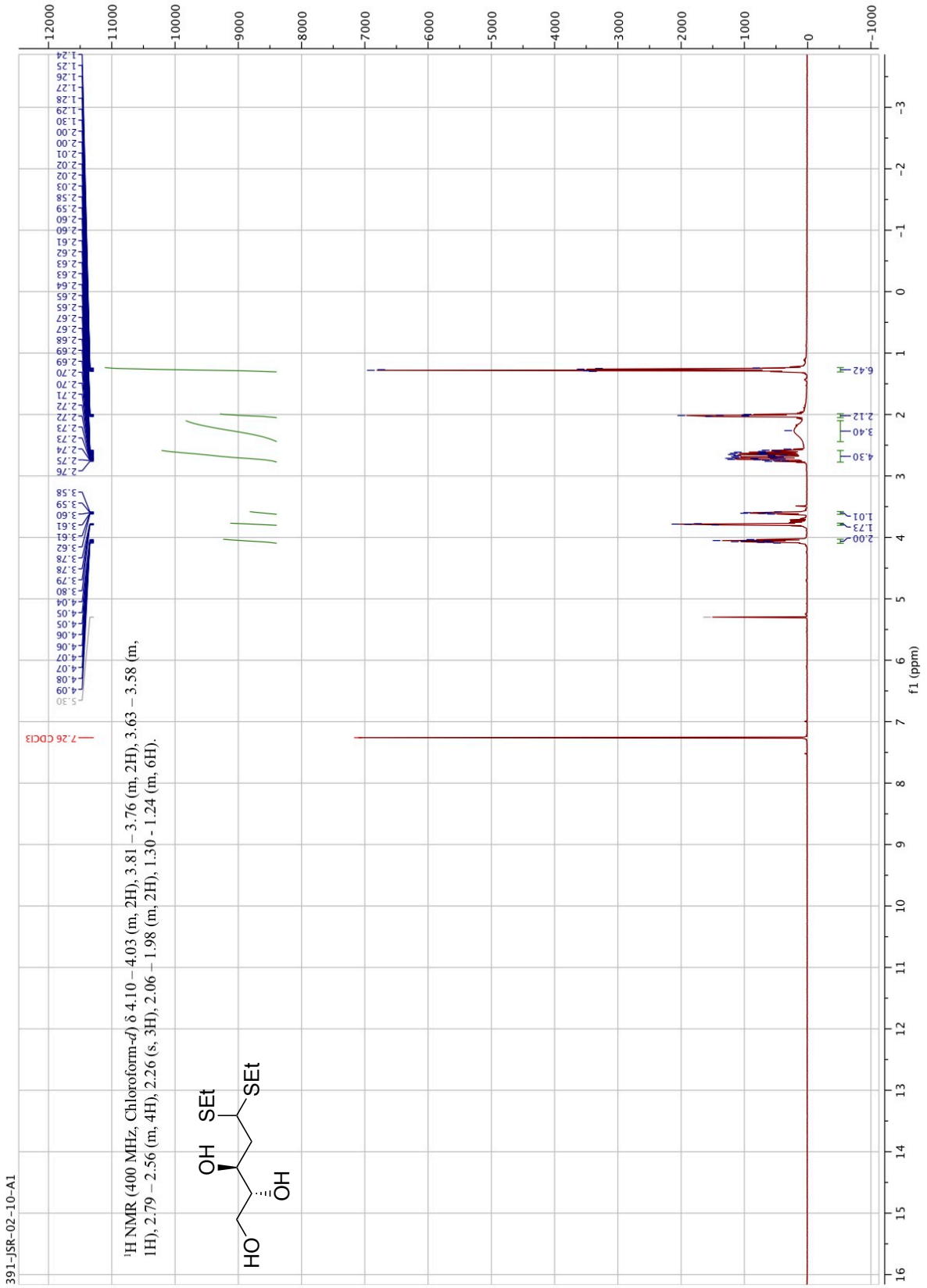

Figure A-1. ^{1}H NMR spectrum of compound **42**.

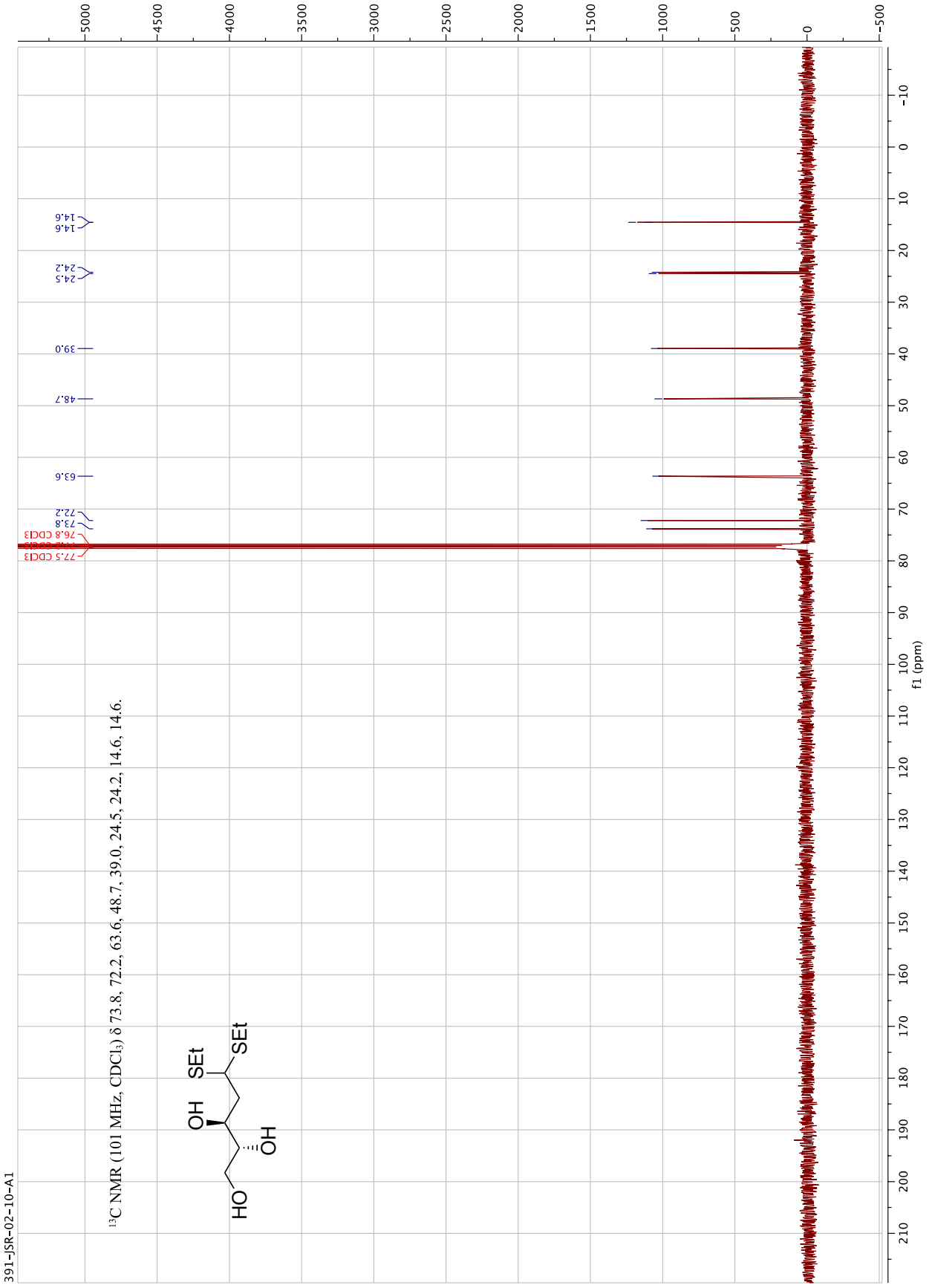

Figure A-2. ^{13}C NMR spectrum of compound **42**.

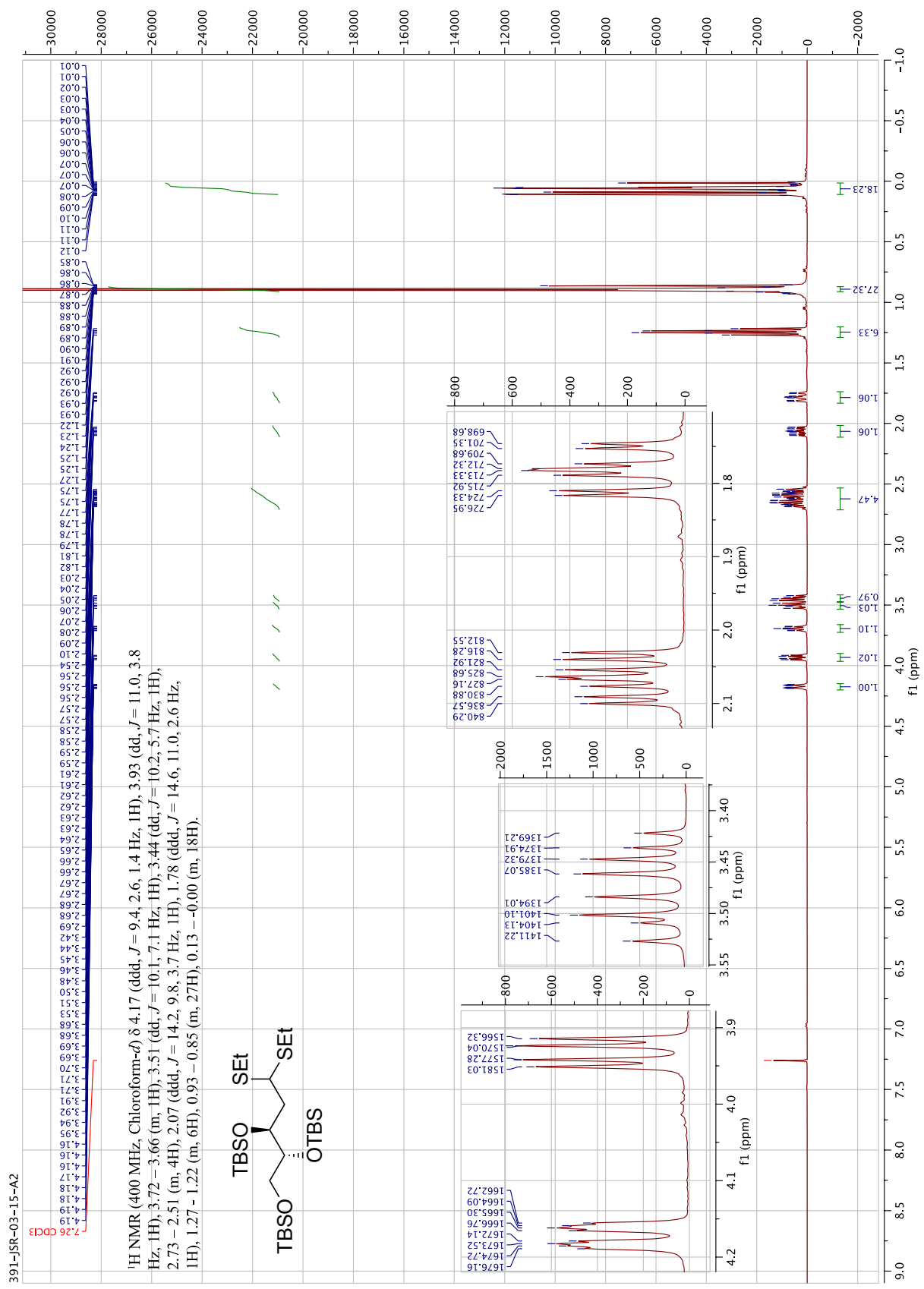

Figure A-3. ^{1}H NMR spectrum of compound **83**.

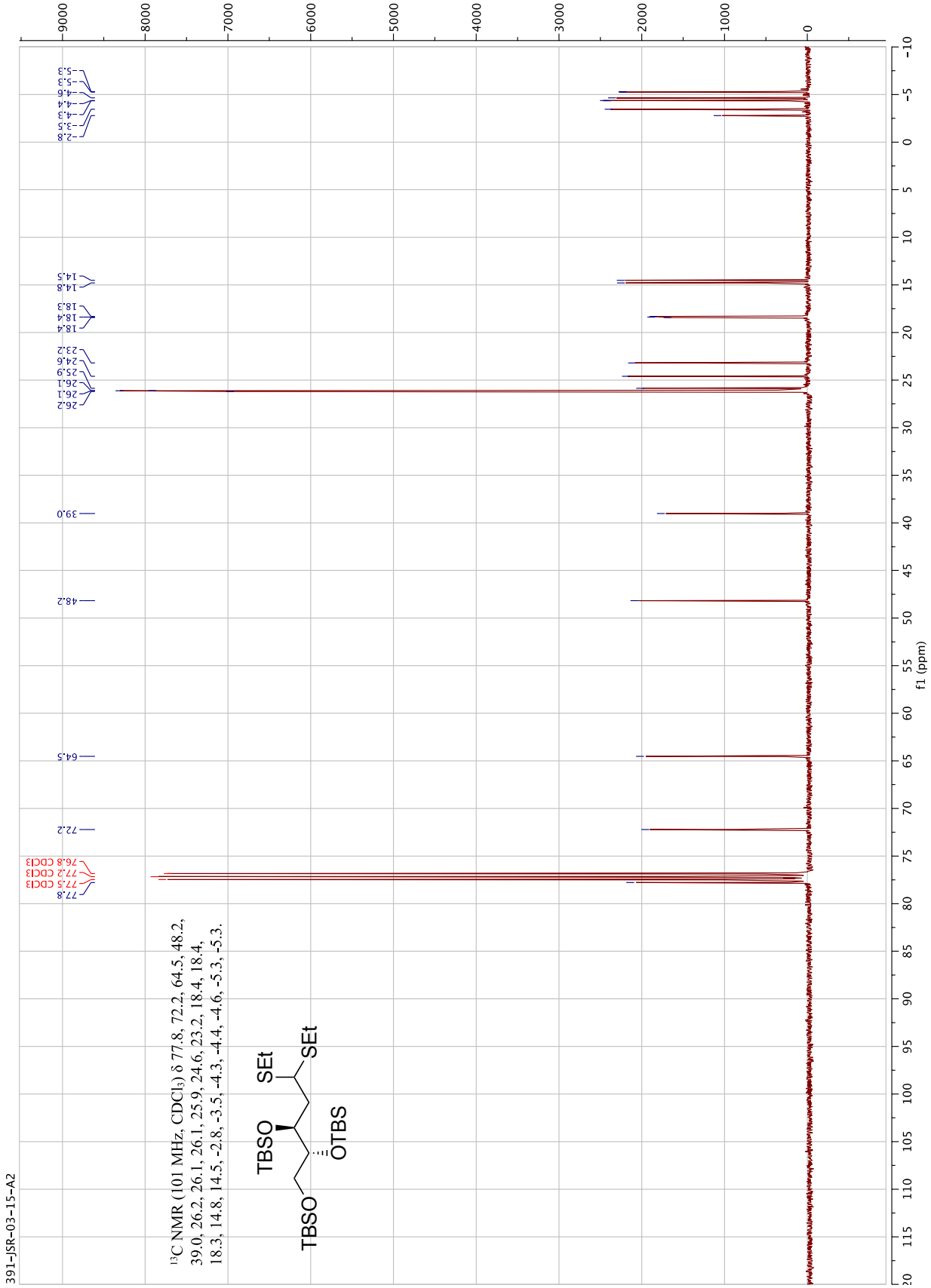

Figure A-4. ^{13}C NMR spectrum of compound **83**.

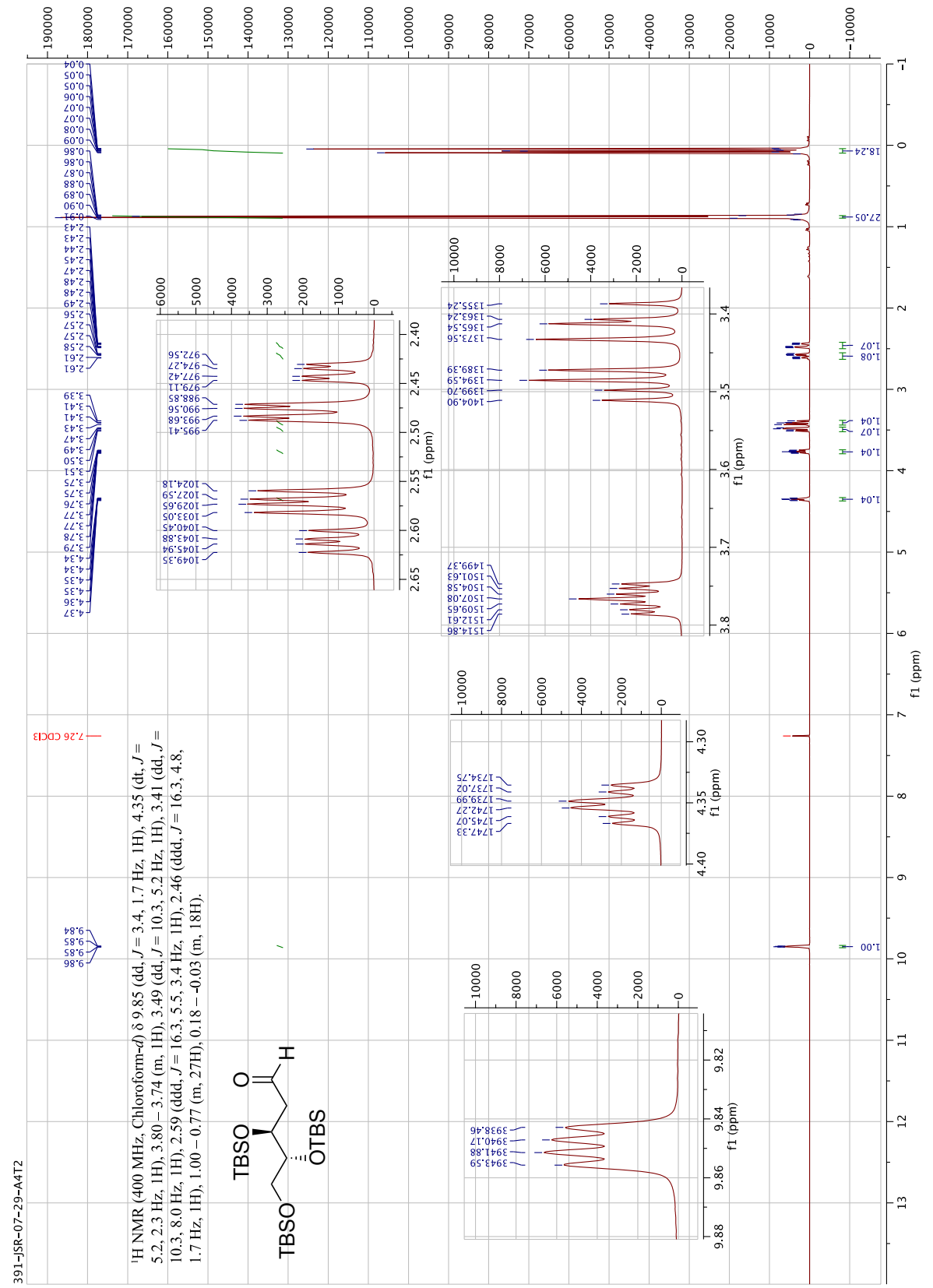

Figure A-5. ^{1}H NMR spectrum of compound **39**.

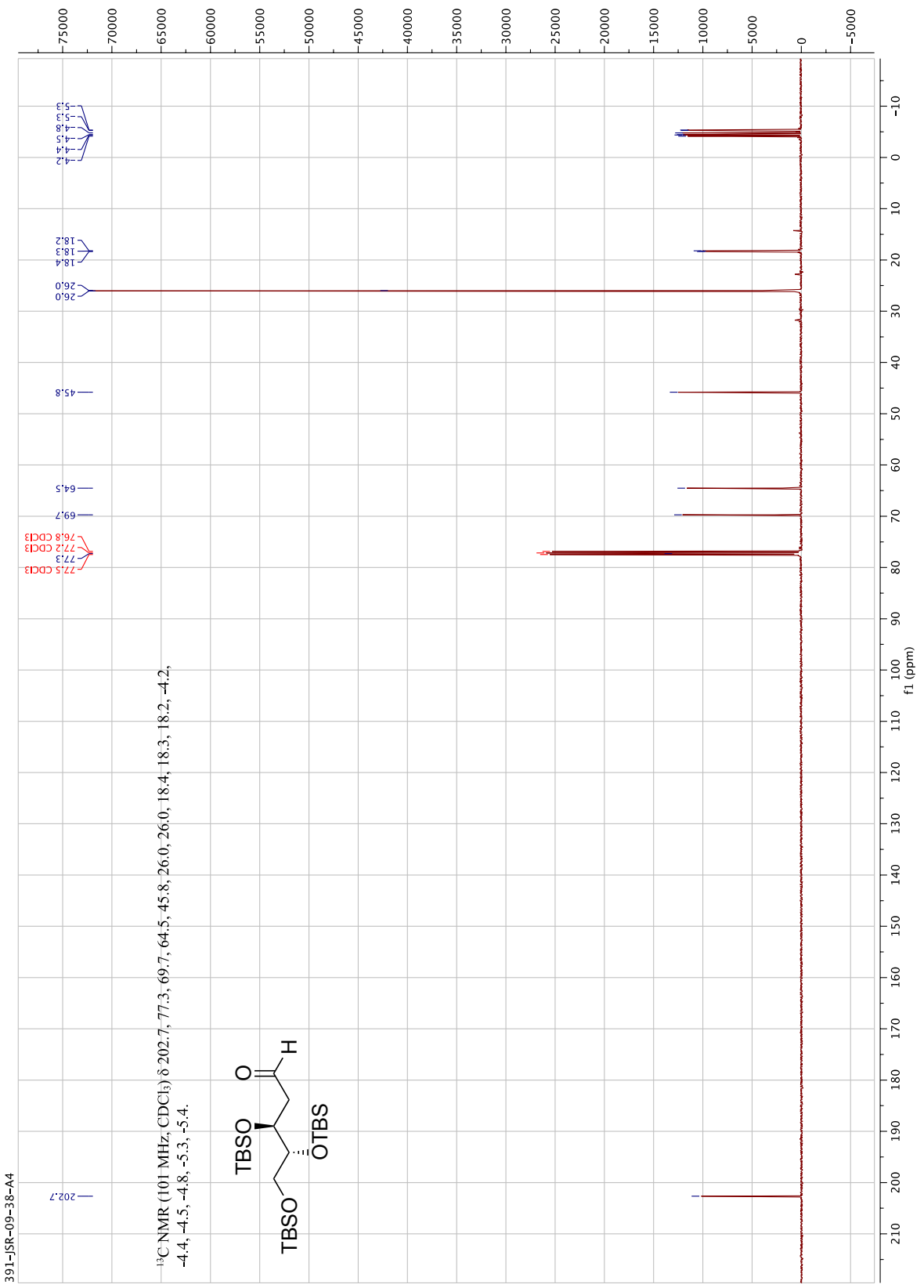

Figure A-6. ^{13}C NMR spectrum of compound **39**.

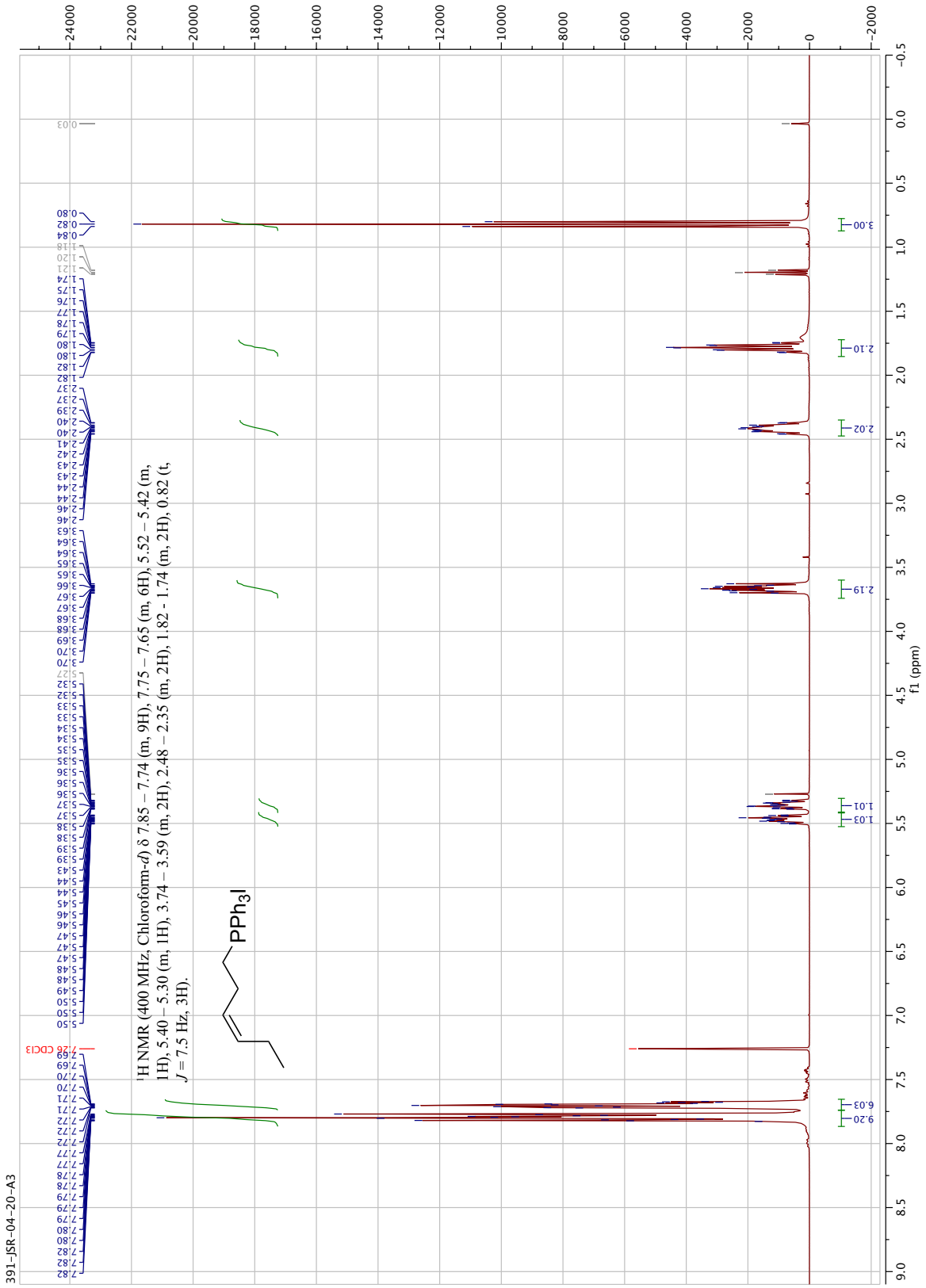

Figure A-7. ^{1}H NMR spectrum of compound **40**.

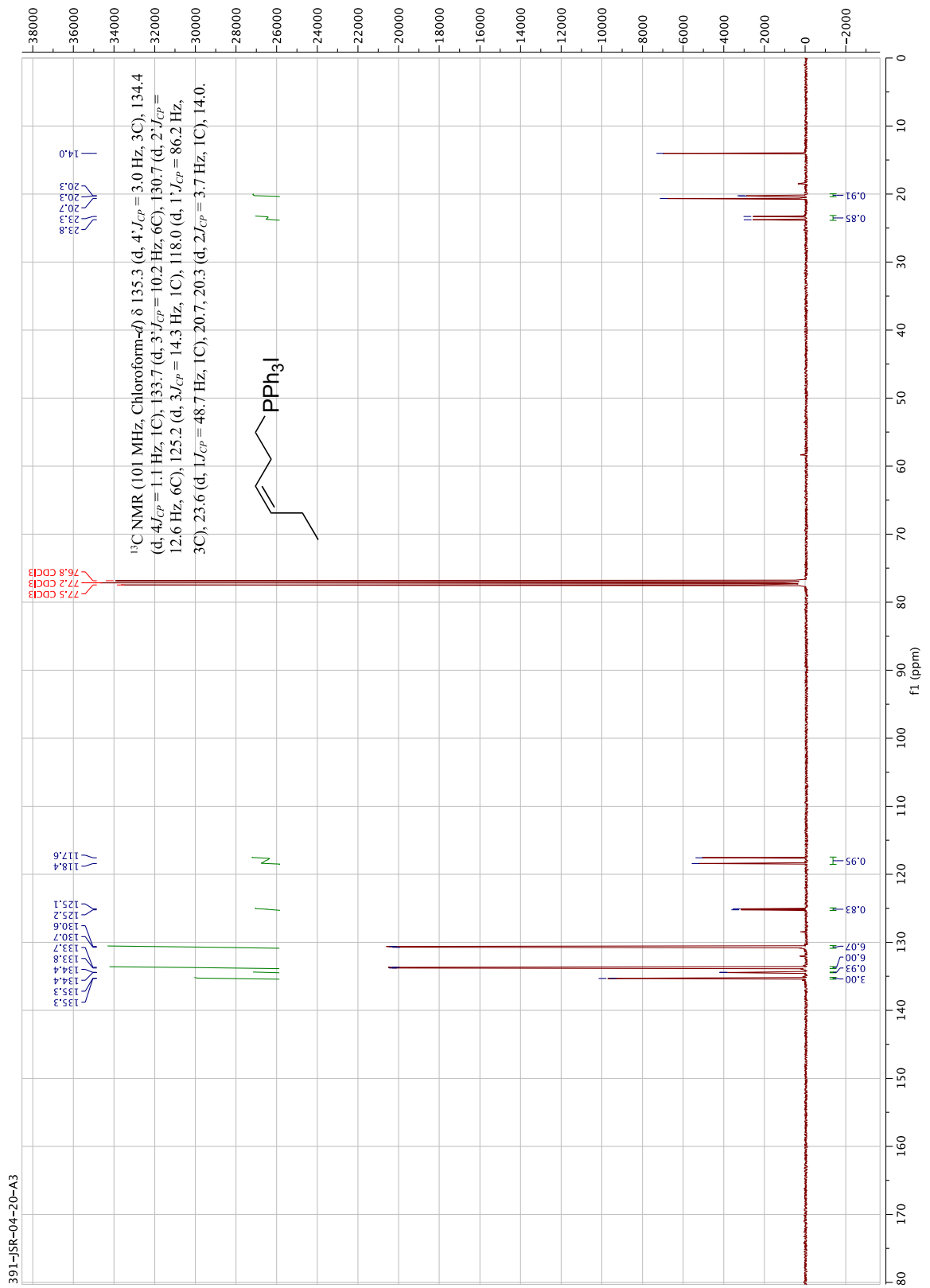

Figure A-8. ^{13}C NMR spectrum of compound **40**.

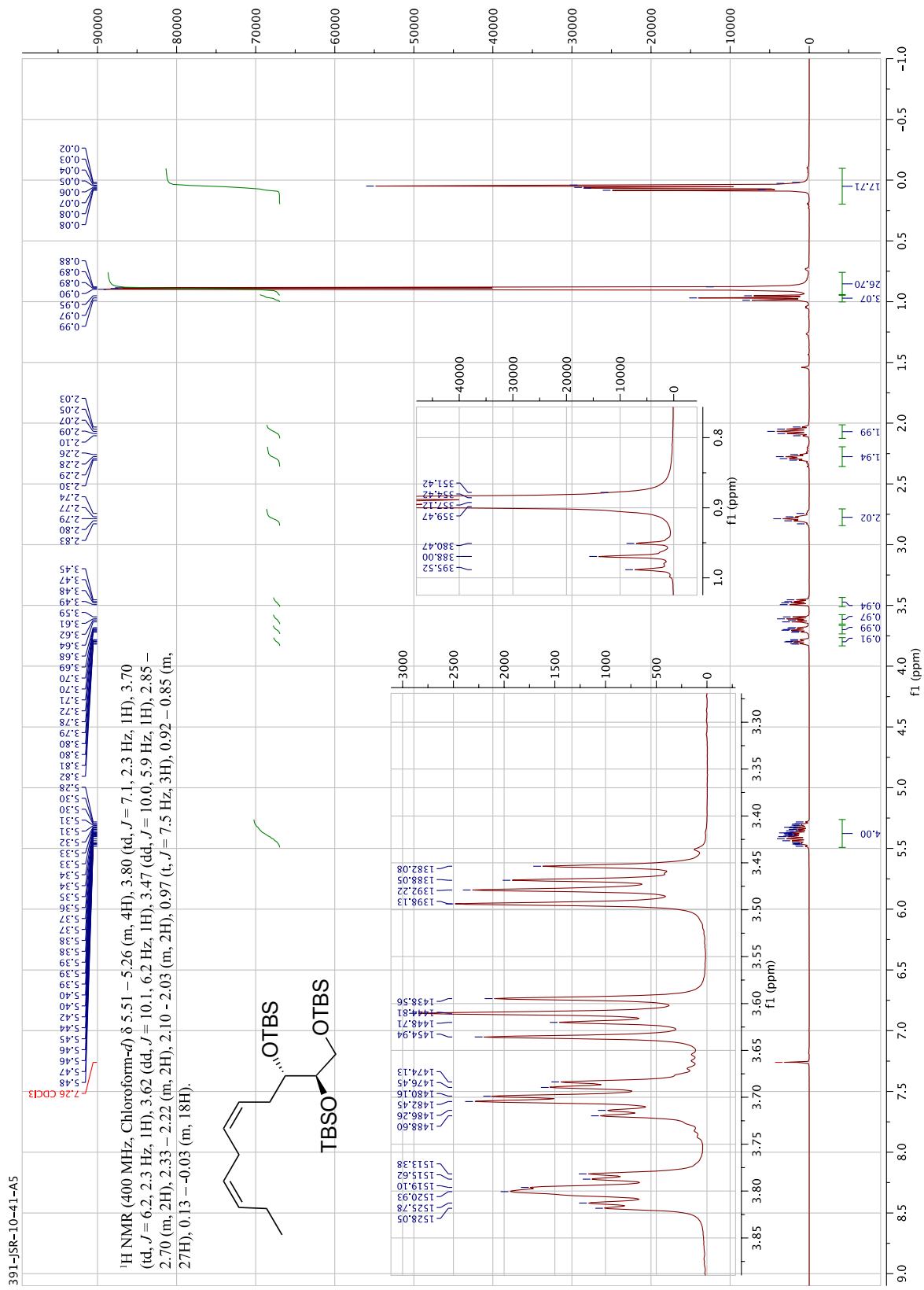

Figure A-9. ^{1}H NMR spectrum of compound **38**.

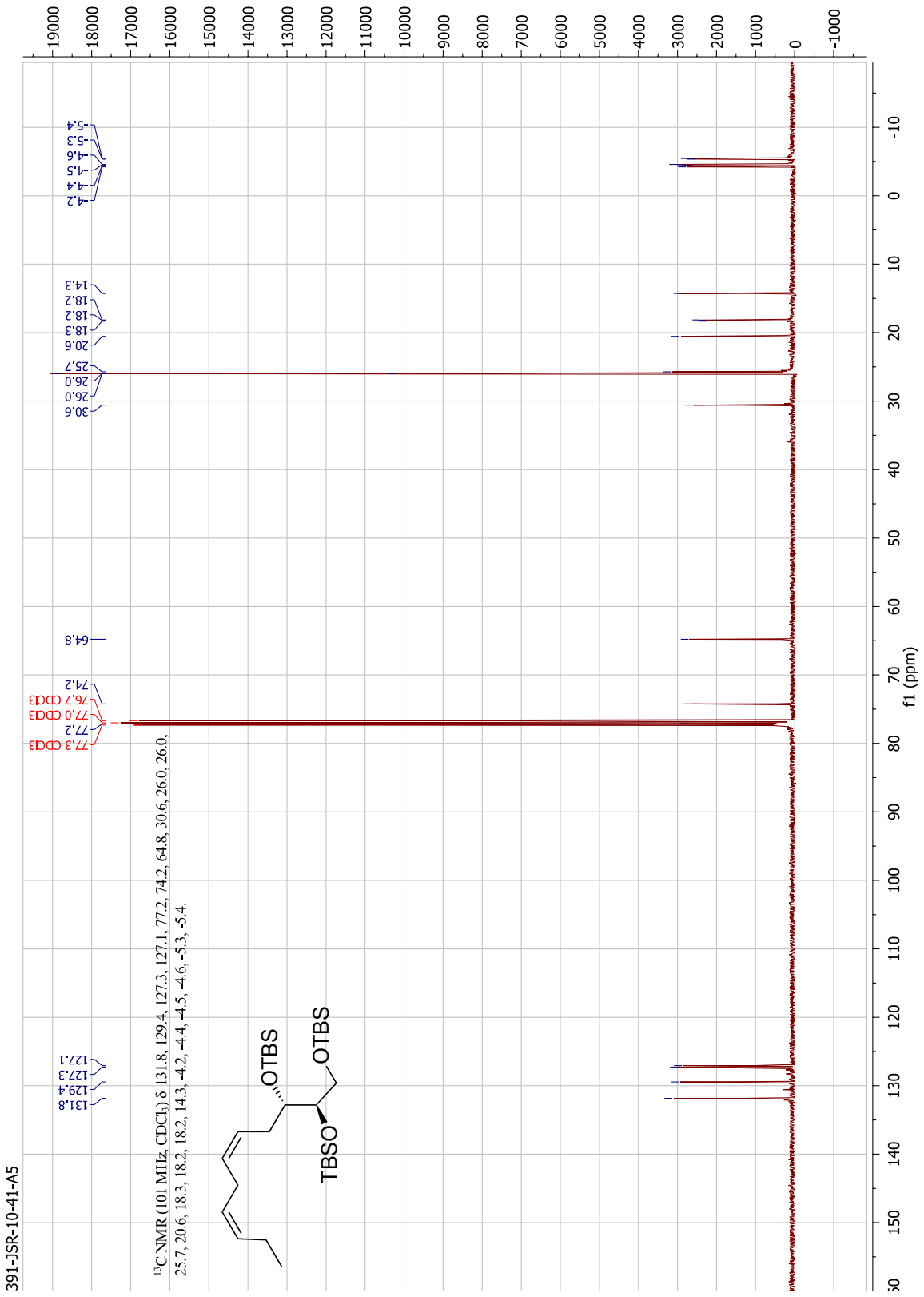

Figure A-10. ^{13}C NMR spectrum of compound **38**.

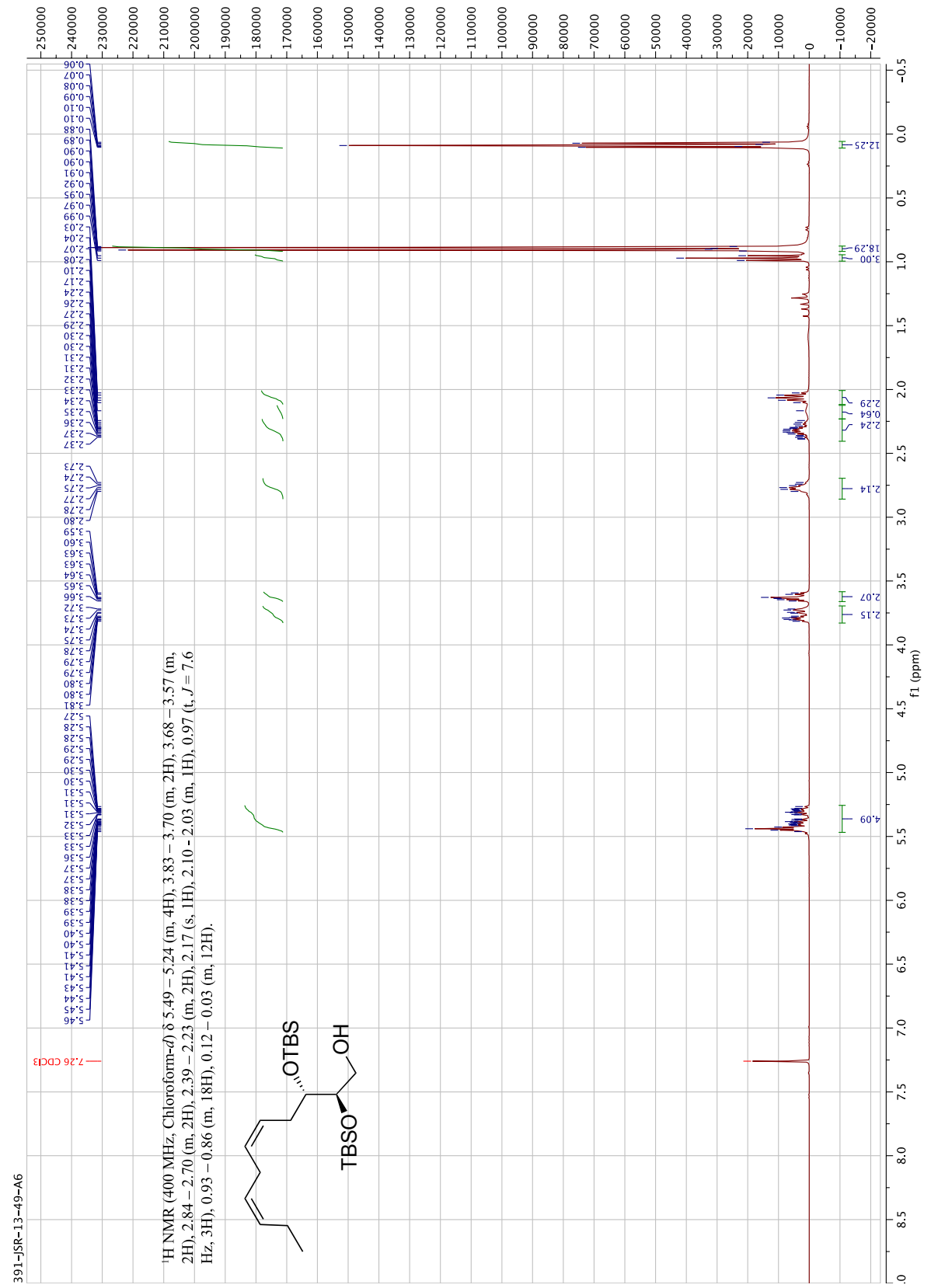

Figure A-11. ^{1}H NMR spectrum of compound **85**.

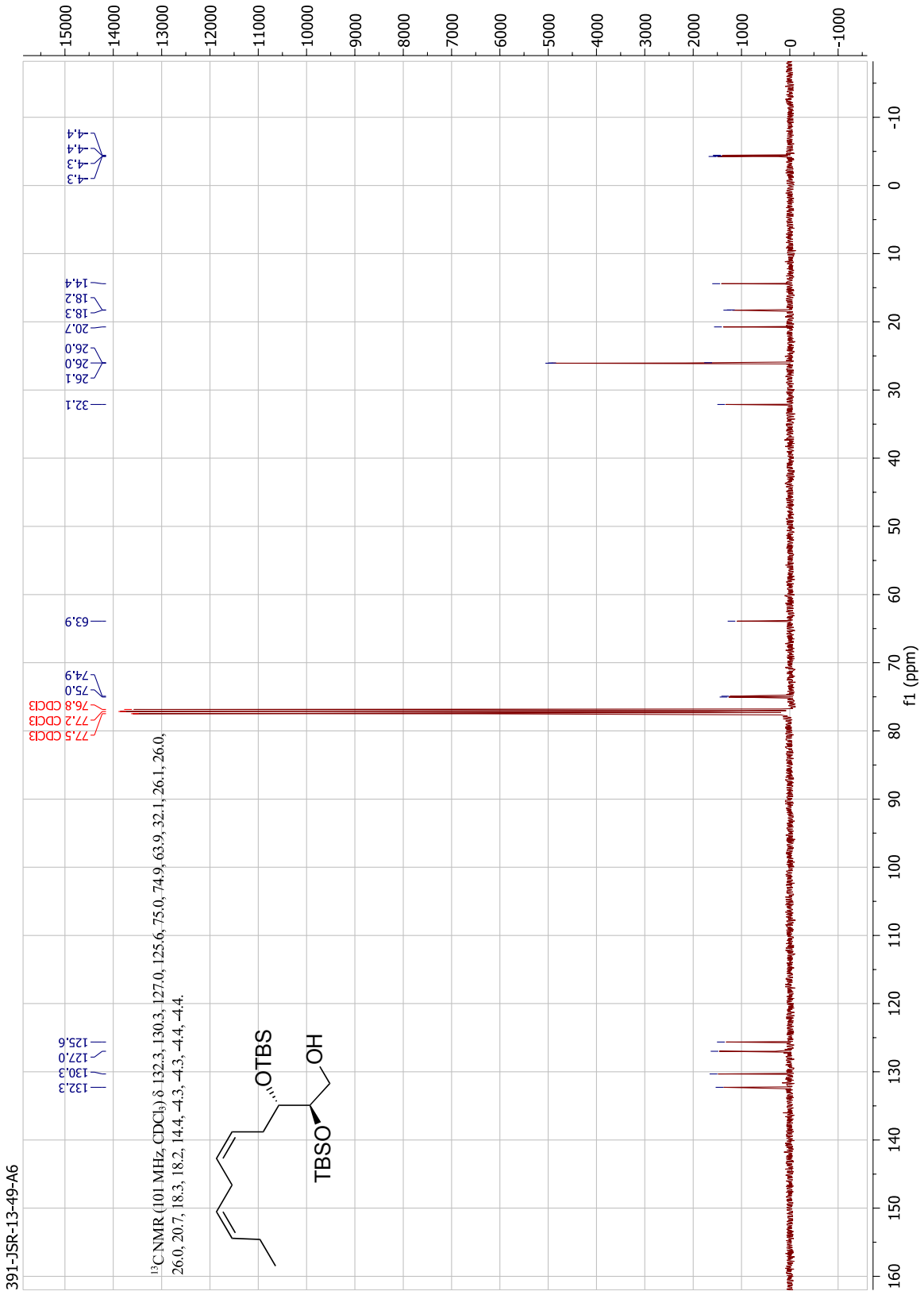

Figure A-12. ^{13}C NMR spectrum of compound **85**.

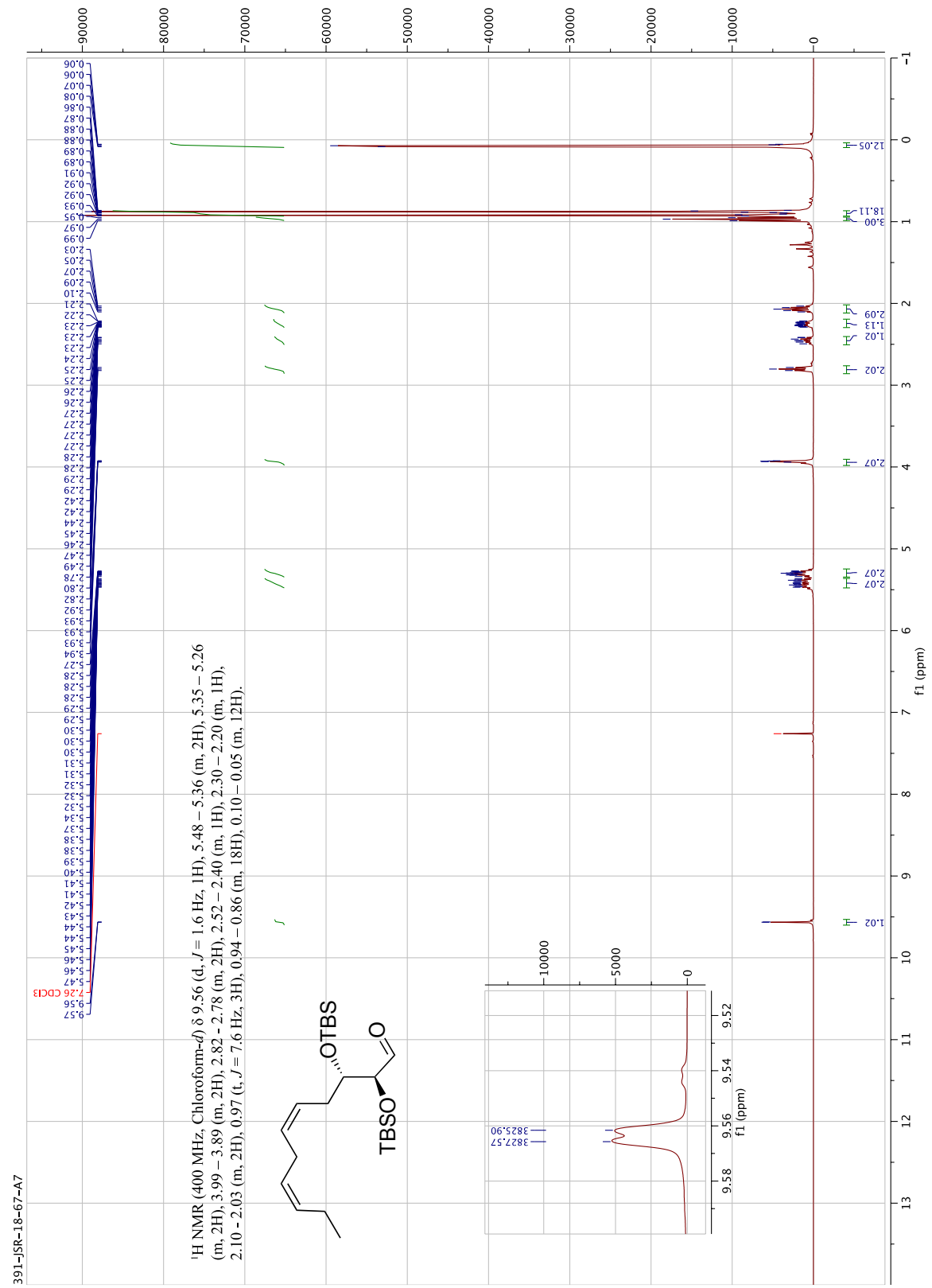

Figure A-13. ^{1}H NMR spectrum of compound **37**.

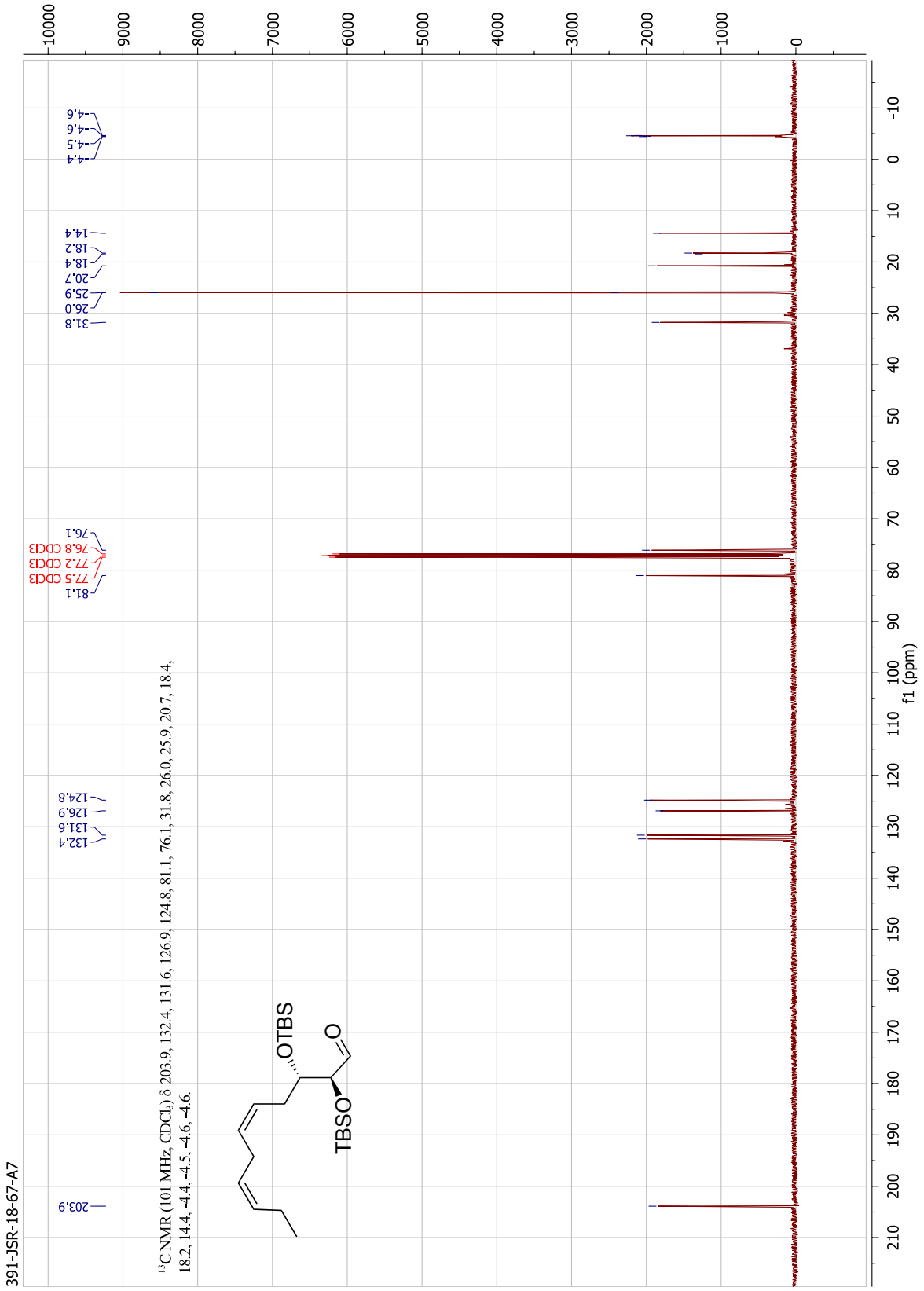

Figure A-14. ^{13}C NMR spectrum of compound **37**.

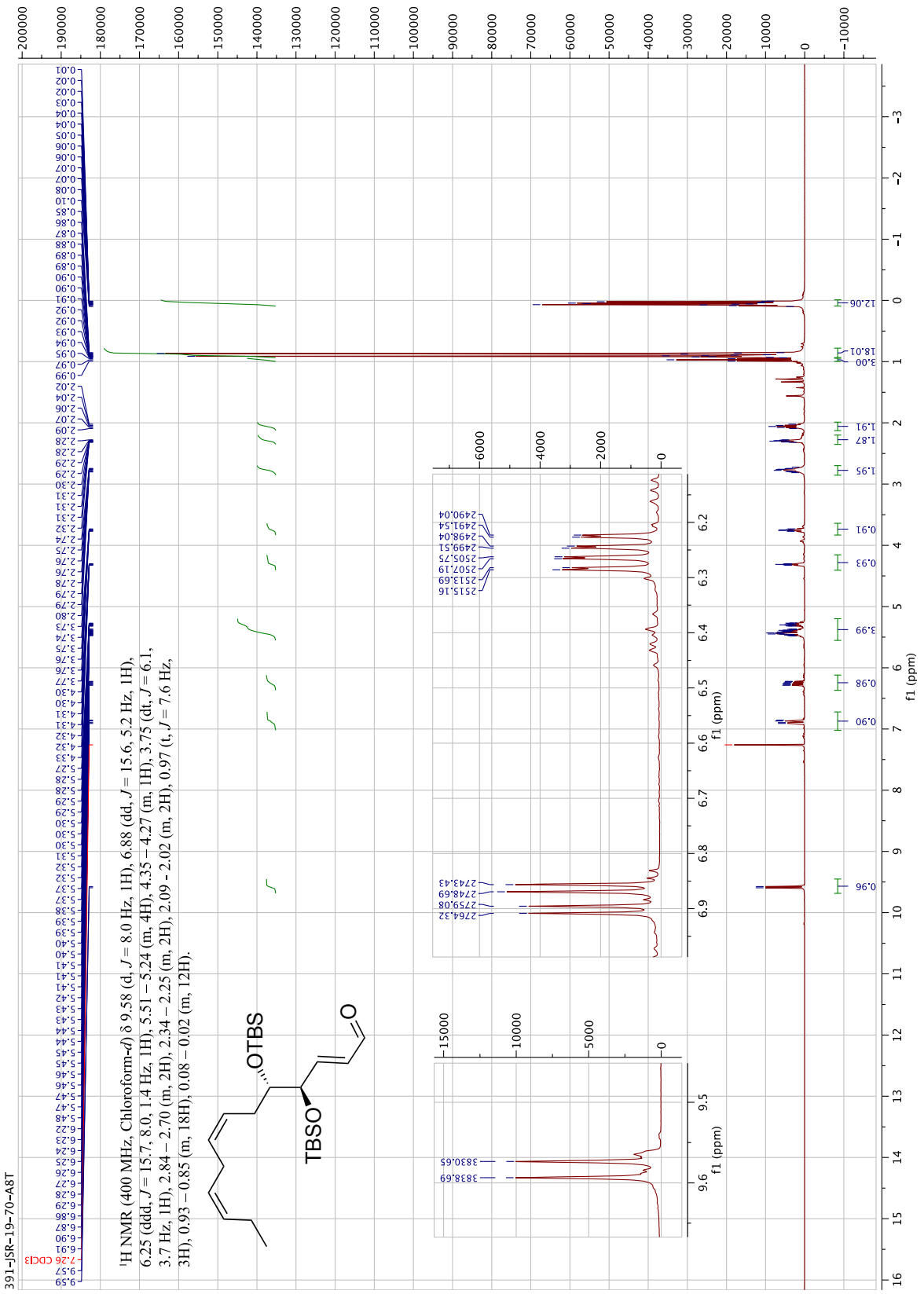

Figure A-15. ^{1}H NMR spectrum of compound **86**.

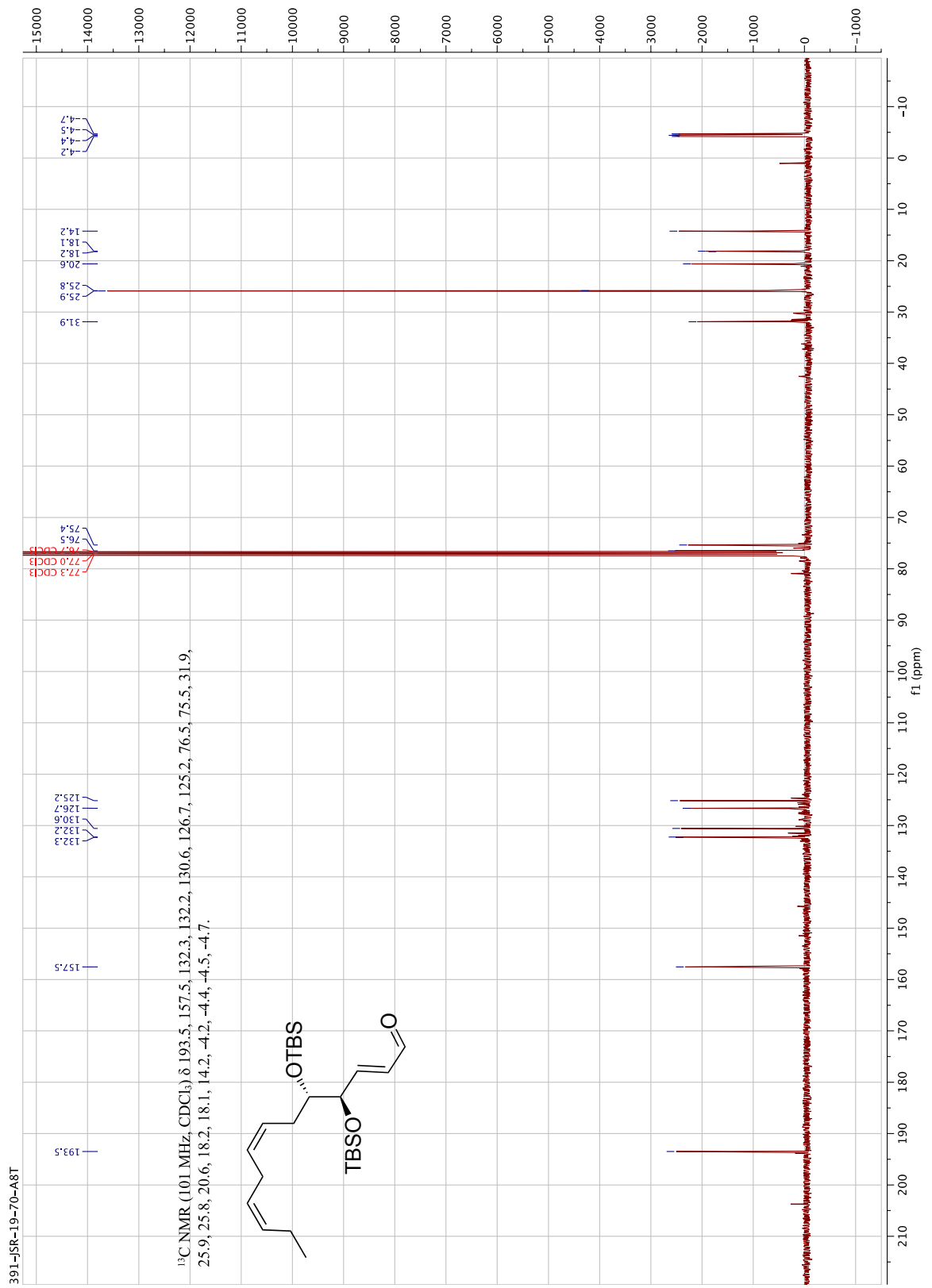

Figure A-16. ^{13}C NMR spectrum of compound **86**.

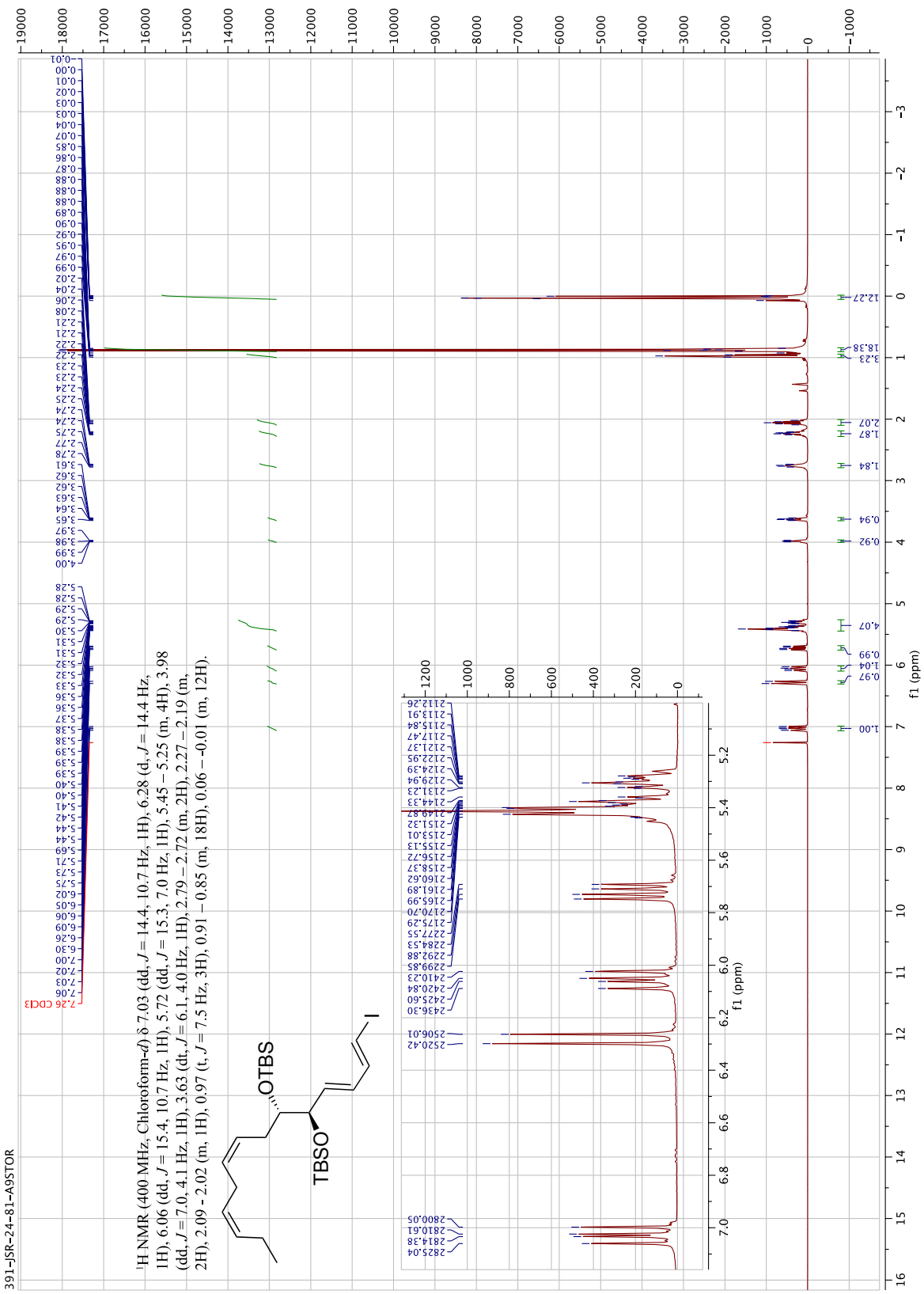

Figure A-17. ^{1}H NMR spectrum of compound **33**.

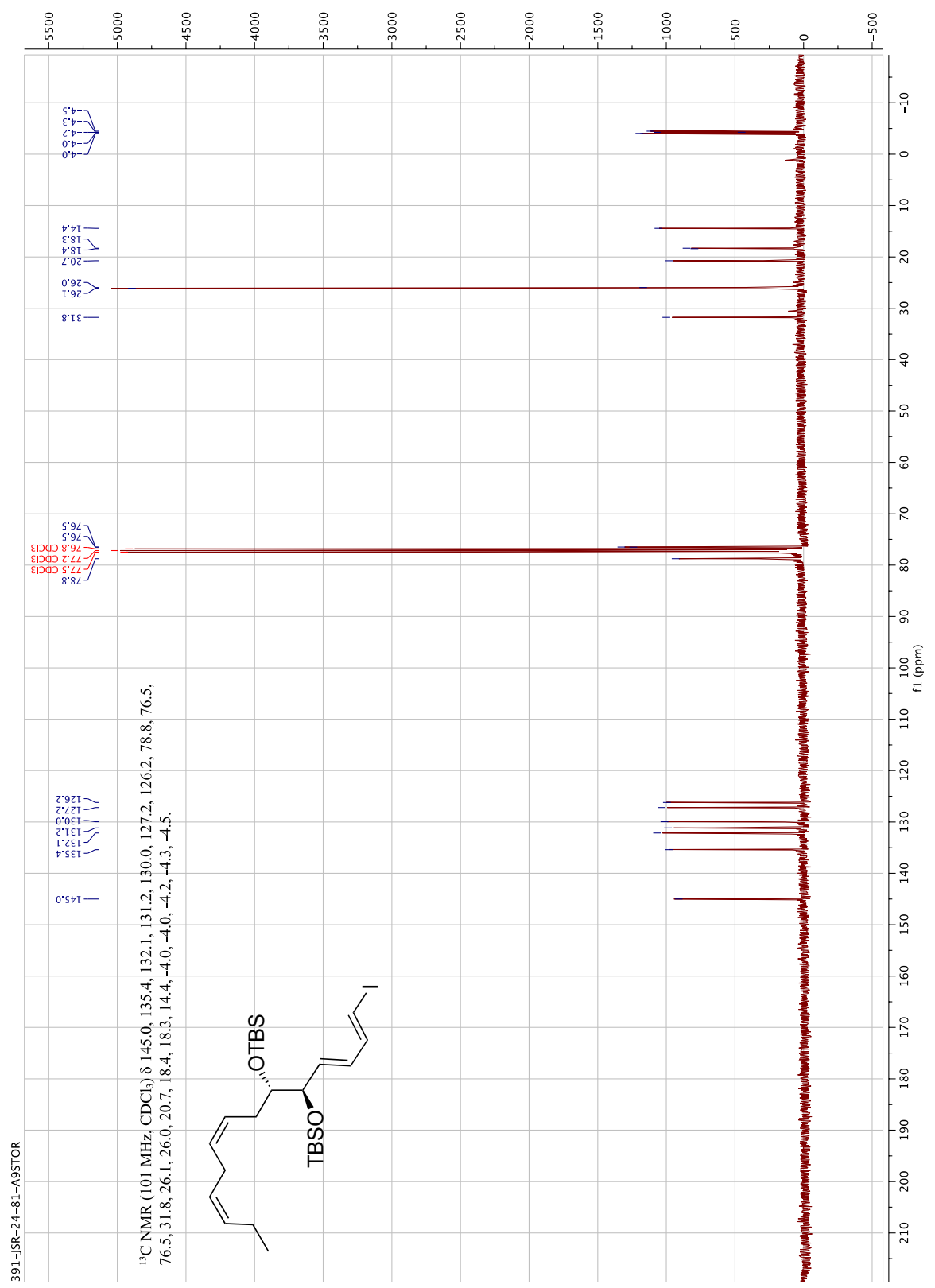

Figure A-18. ^{13}C NMR spectrum of compound **33**.

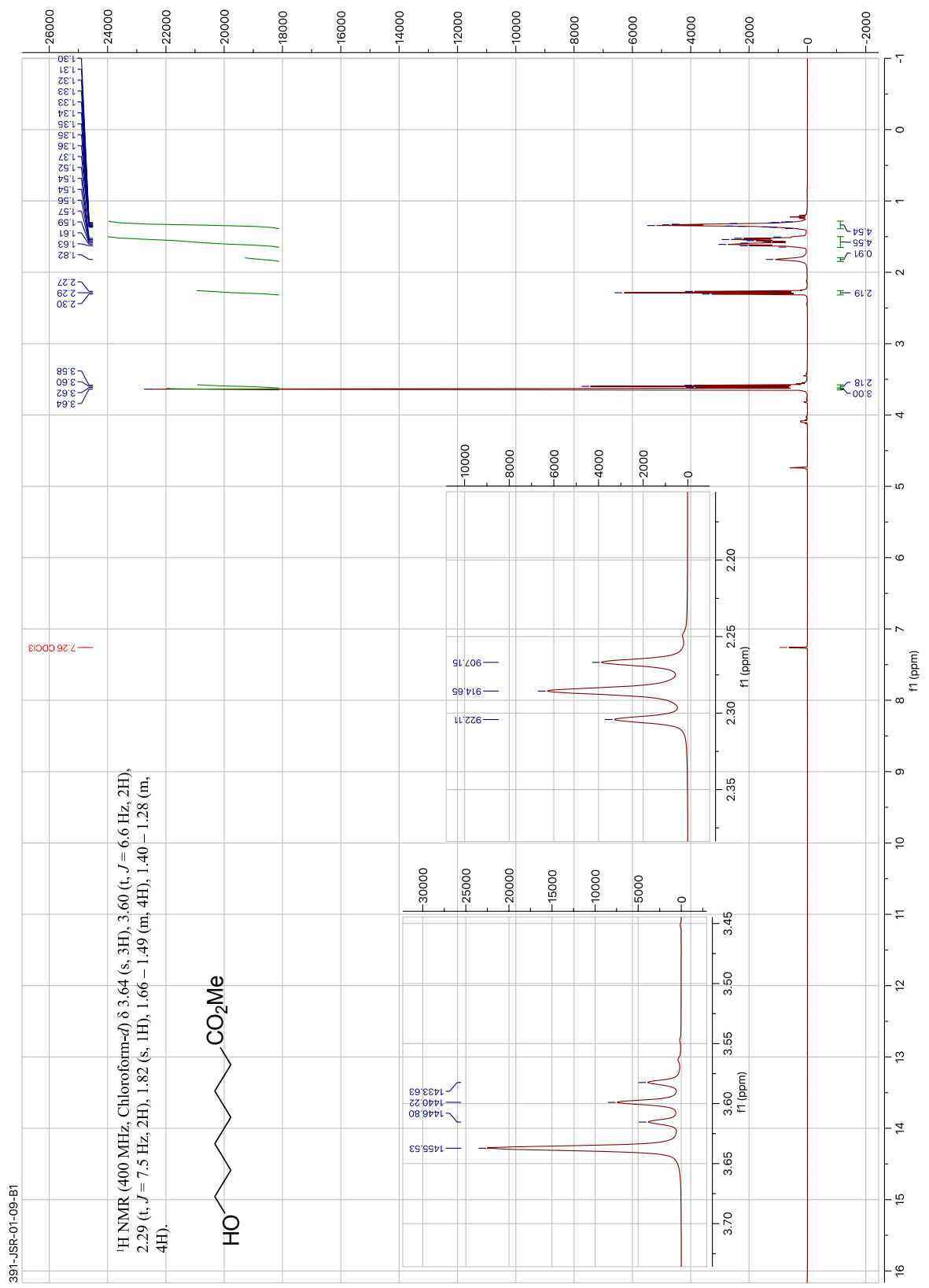

Figure A-19. ^{1}H NMR spectrum of compound **35**.

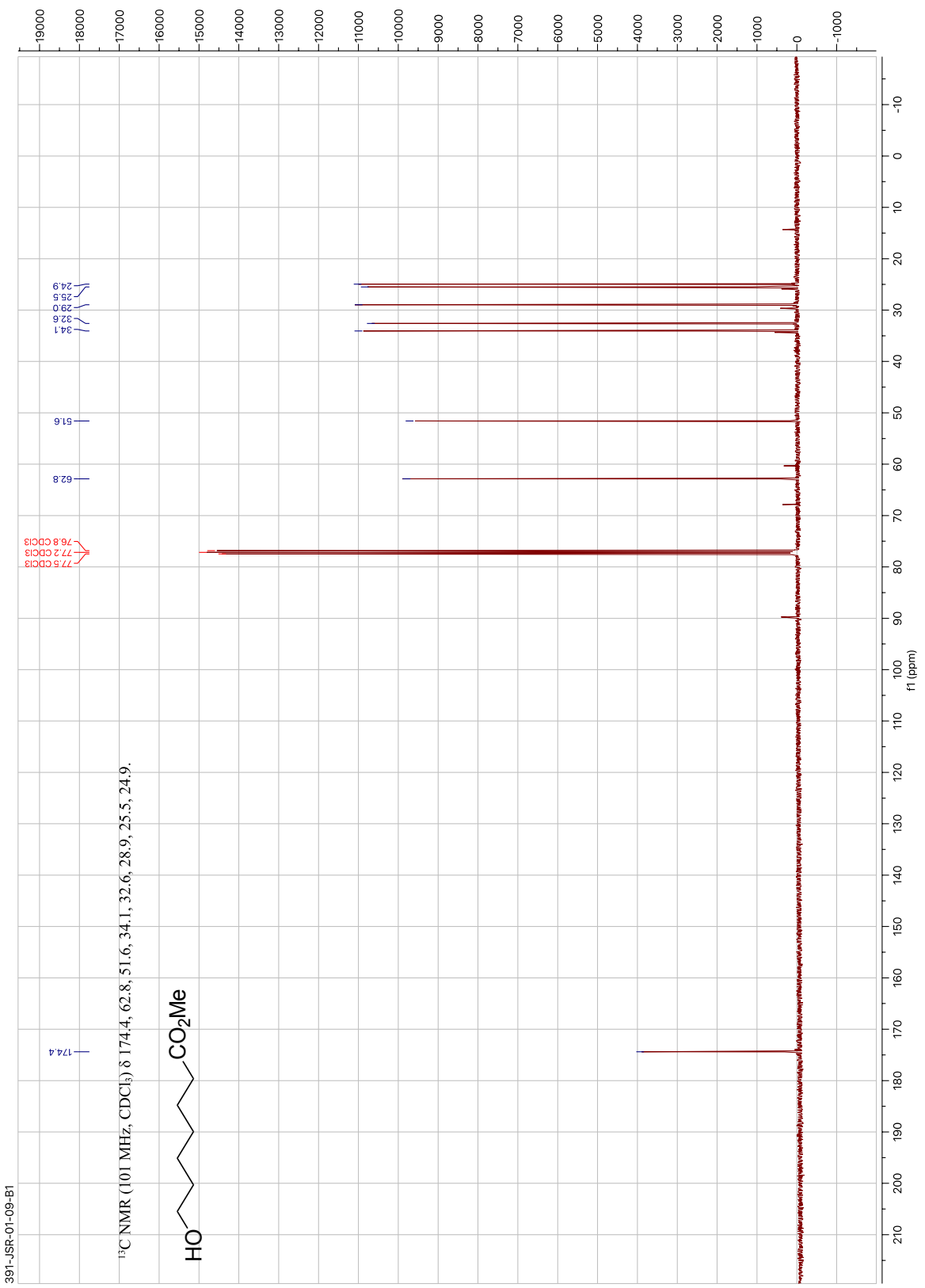

Figure A-20. ^{13}C NMR spectrum of compound **35**.

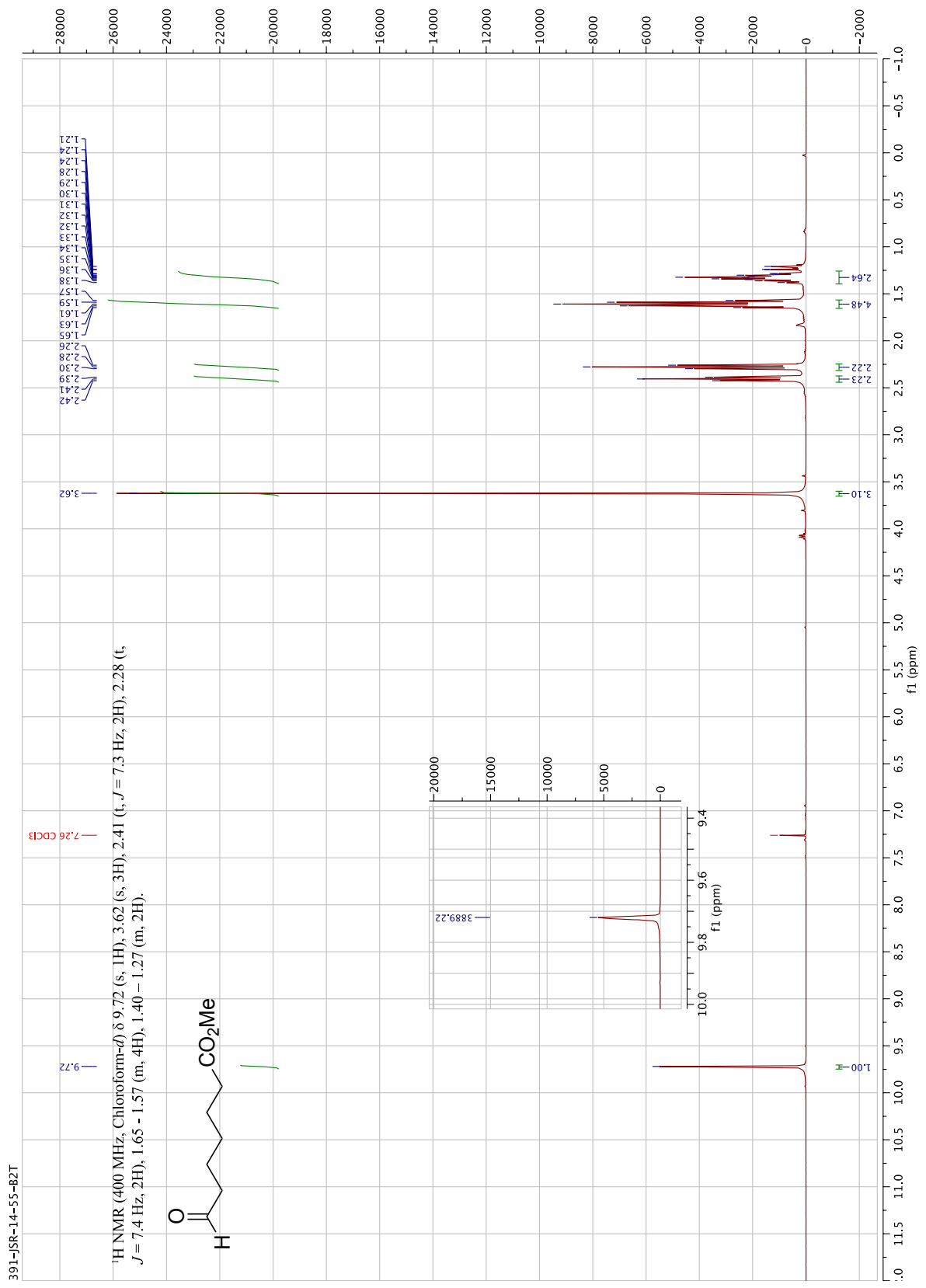

Figure A-21. ^{1}H NMR spectrum of compound **87**.

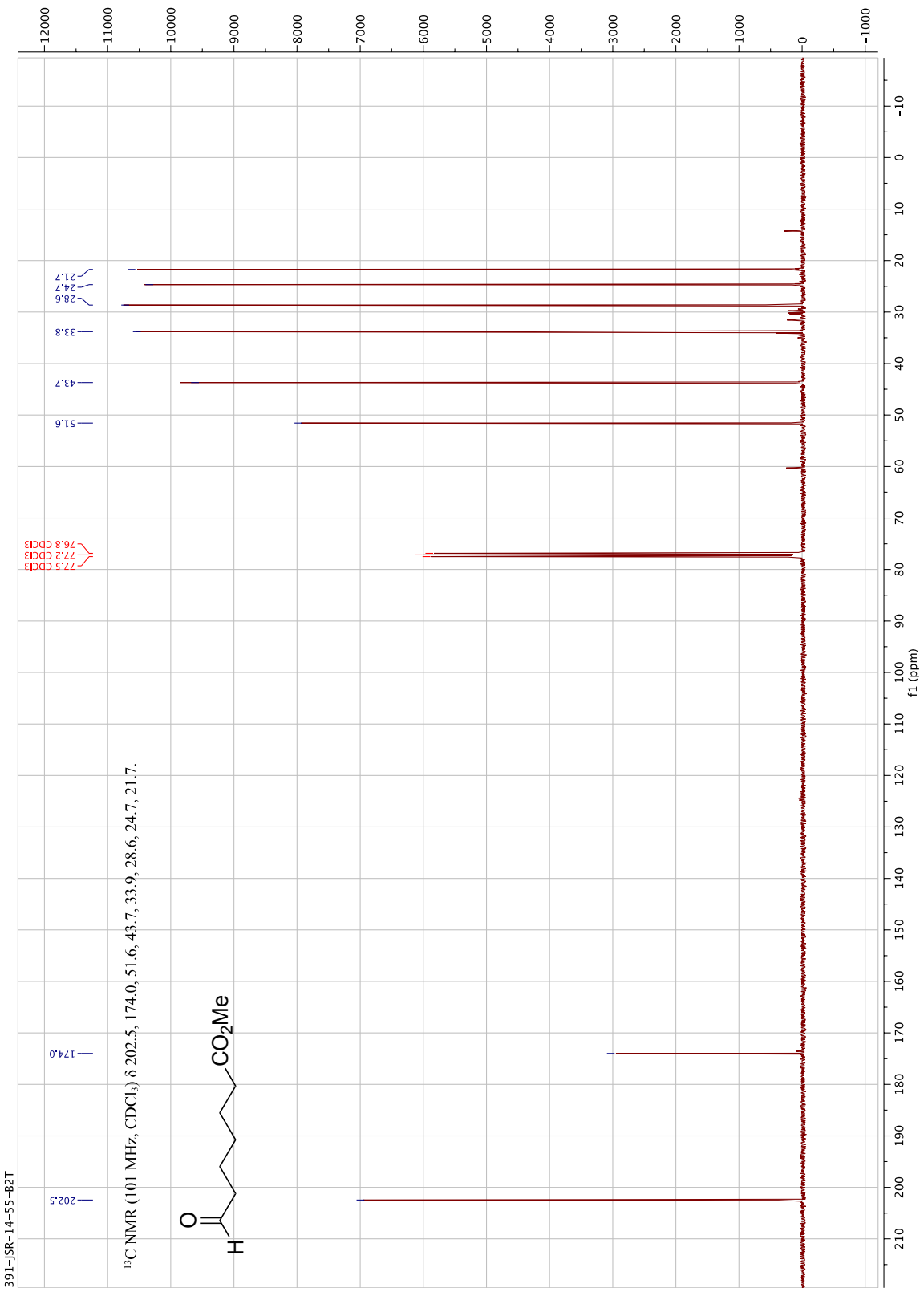

Figure A-22. ^{13}C NMR spectrum of compound **87**.

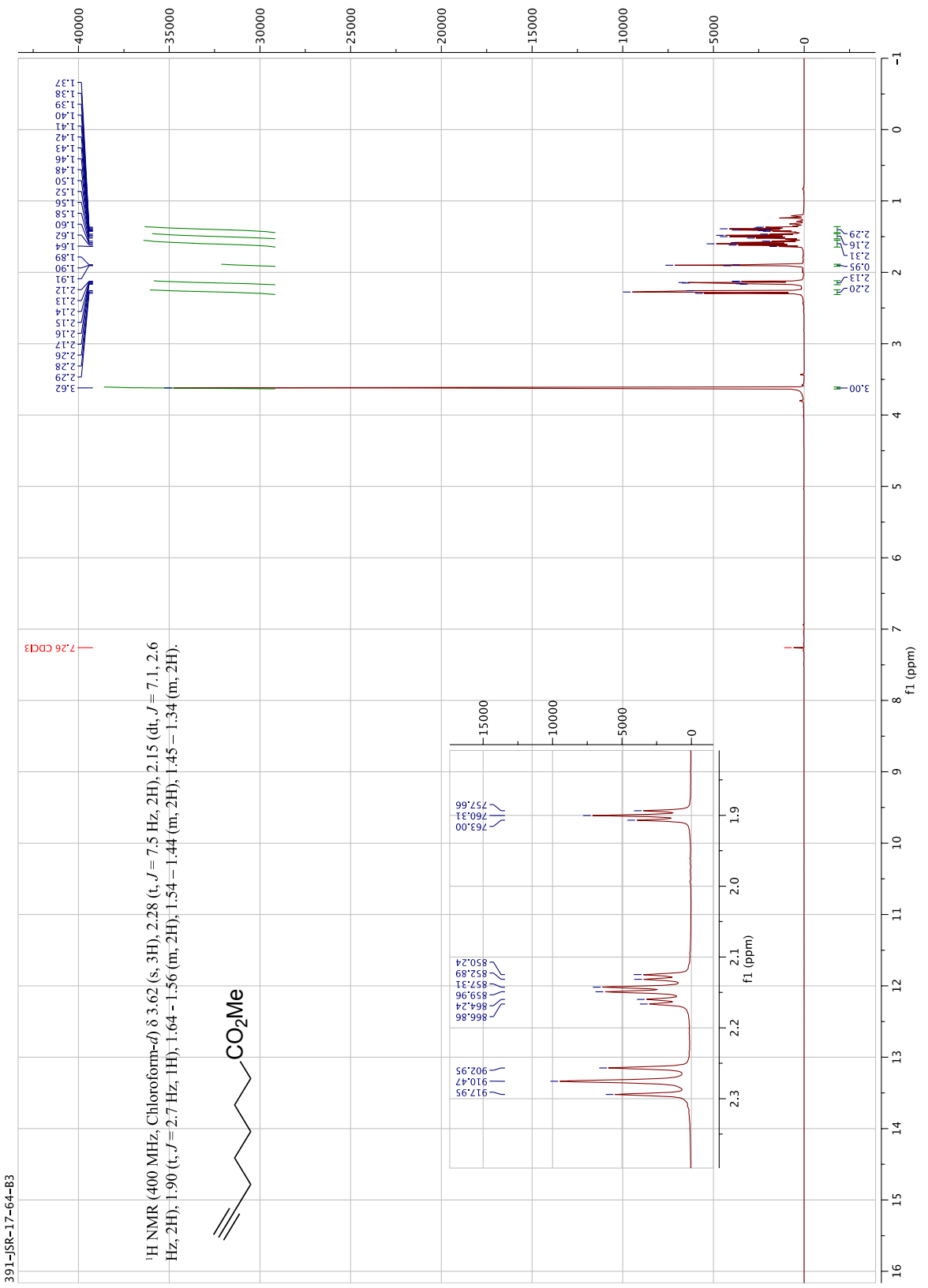

Figure A-23. ^{1}H NMR spectrum of compound **34**.

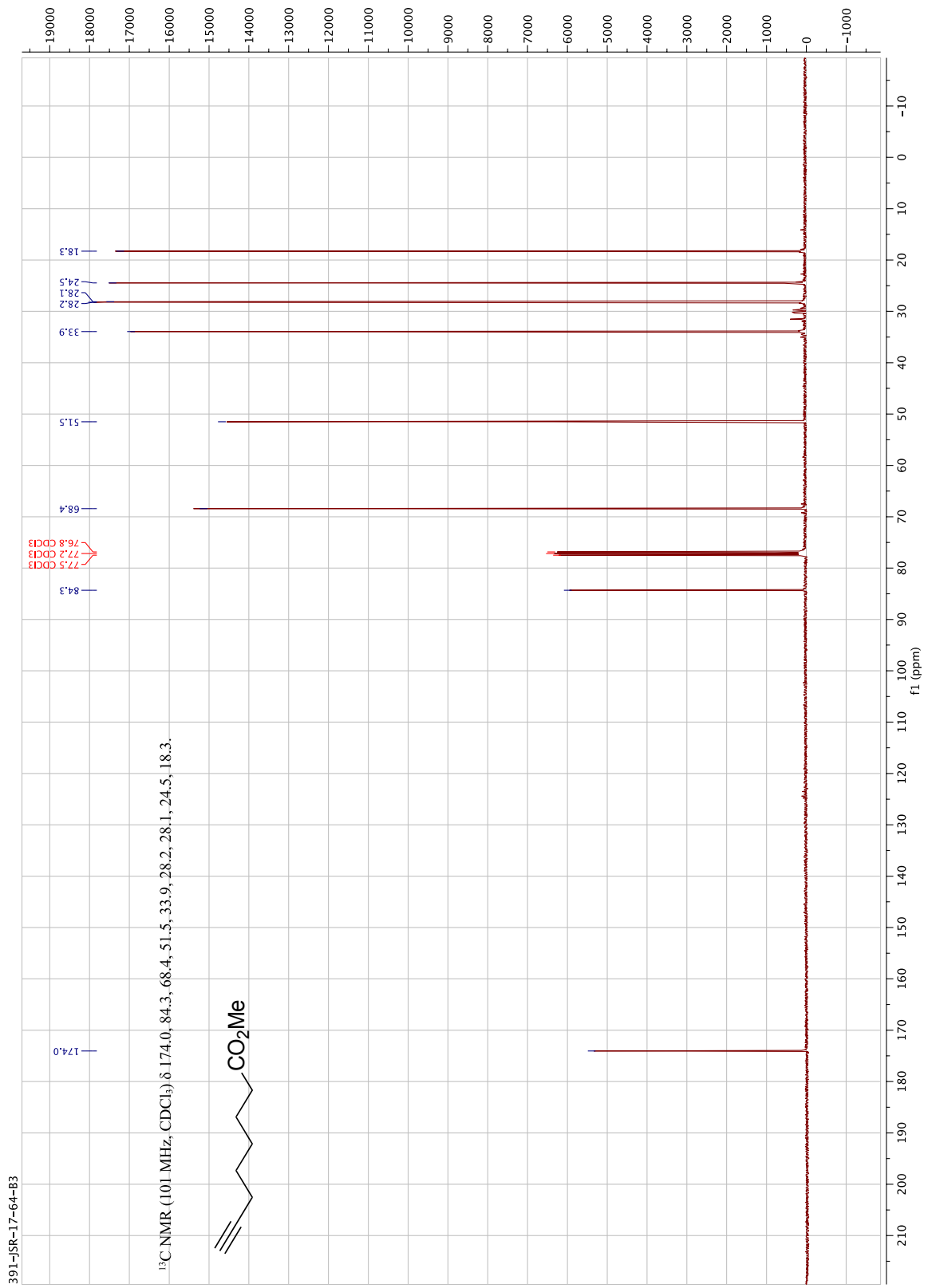

Figure A-24. ^{13}C NMR spectrum of compound **34**.

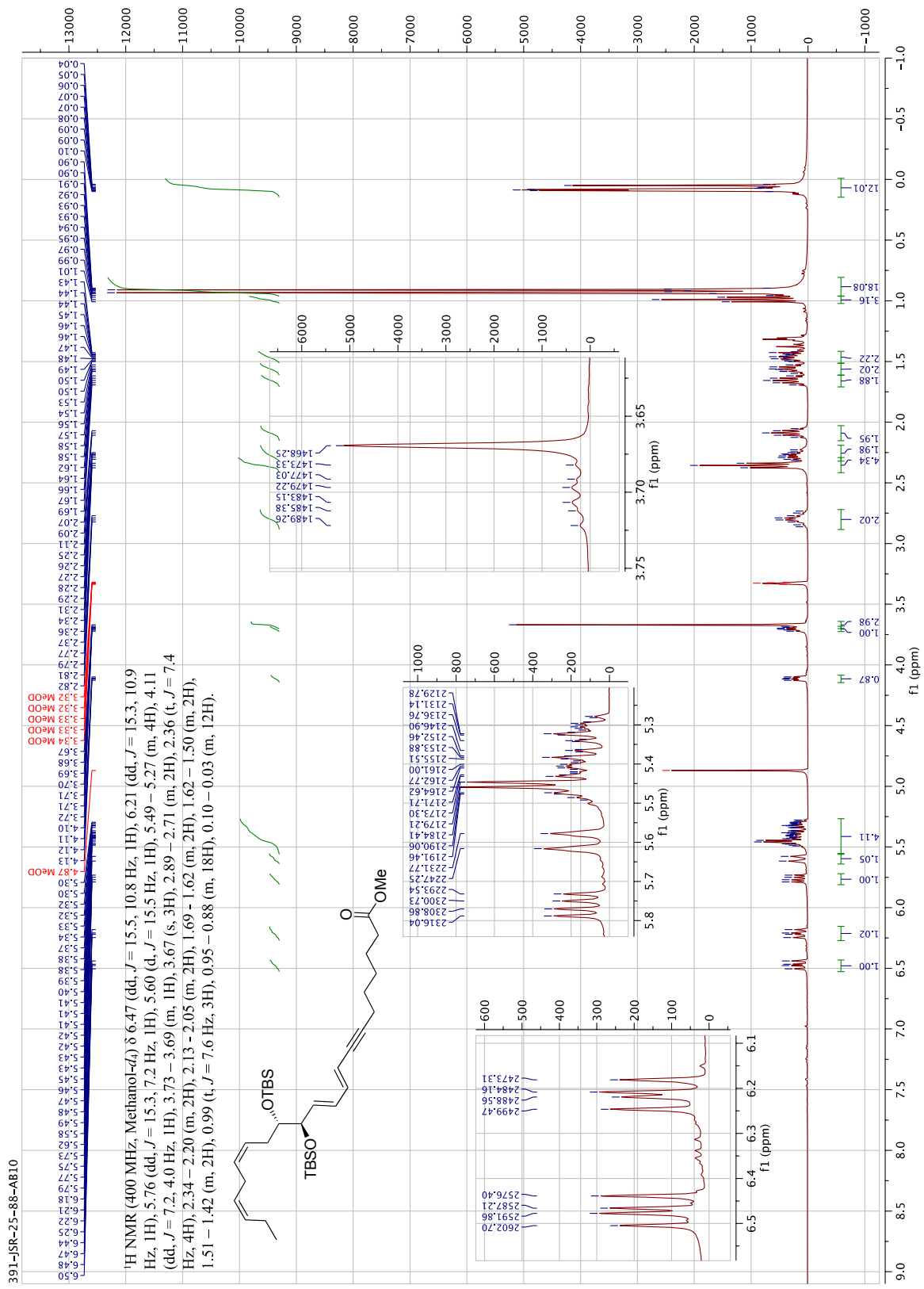

Figure A-25. ^{1}H NMR spectrum of compound **88**.

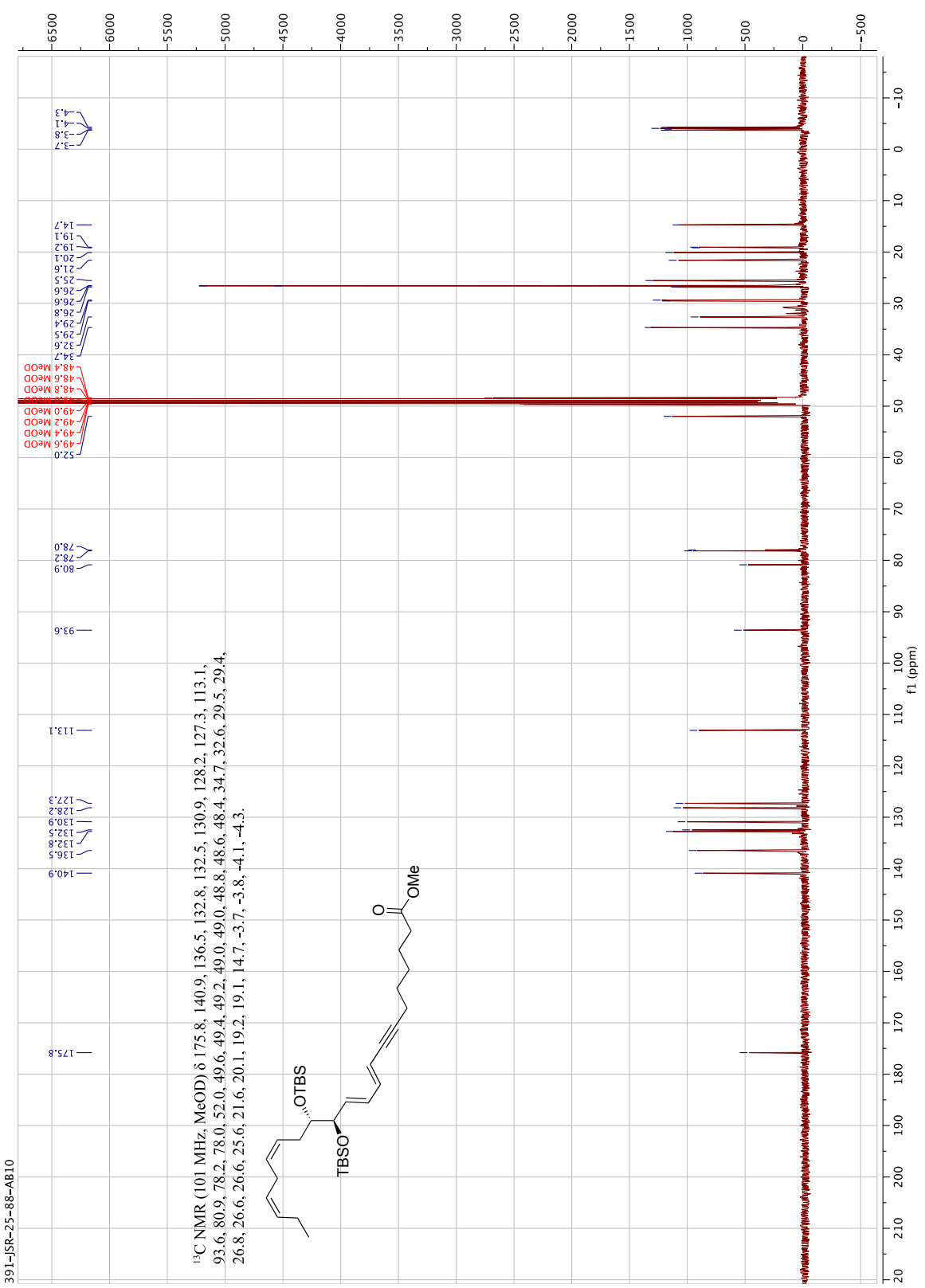

Figure A-26. ^{13}C NMR spectrum of compound **88**.

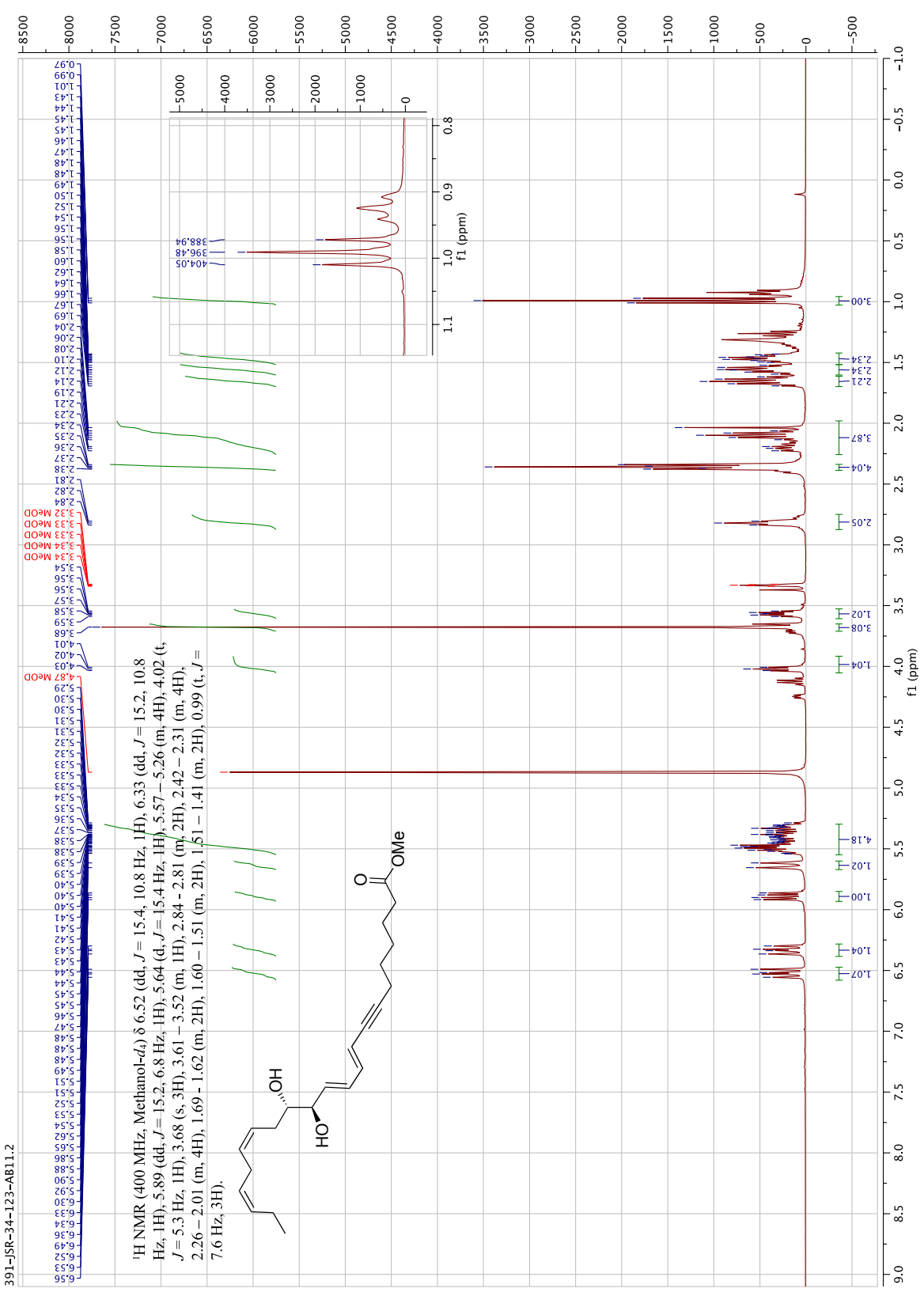

Figure A-27. ^{1}H NMR spectrum of compound **89**.

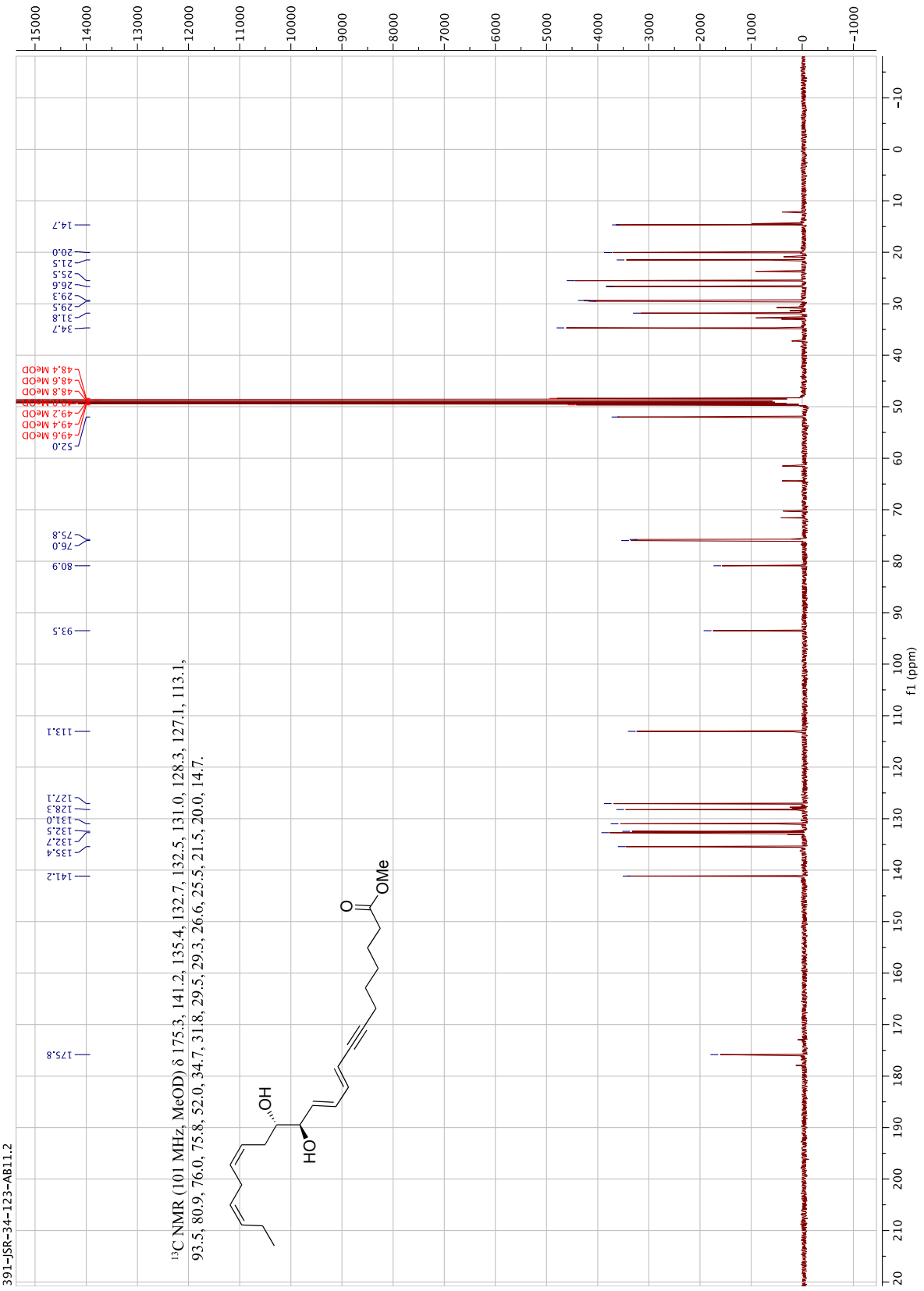

Figure A-28. ^{13}C NMR spectrum of compound **89**.

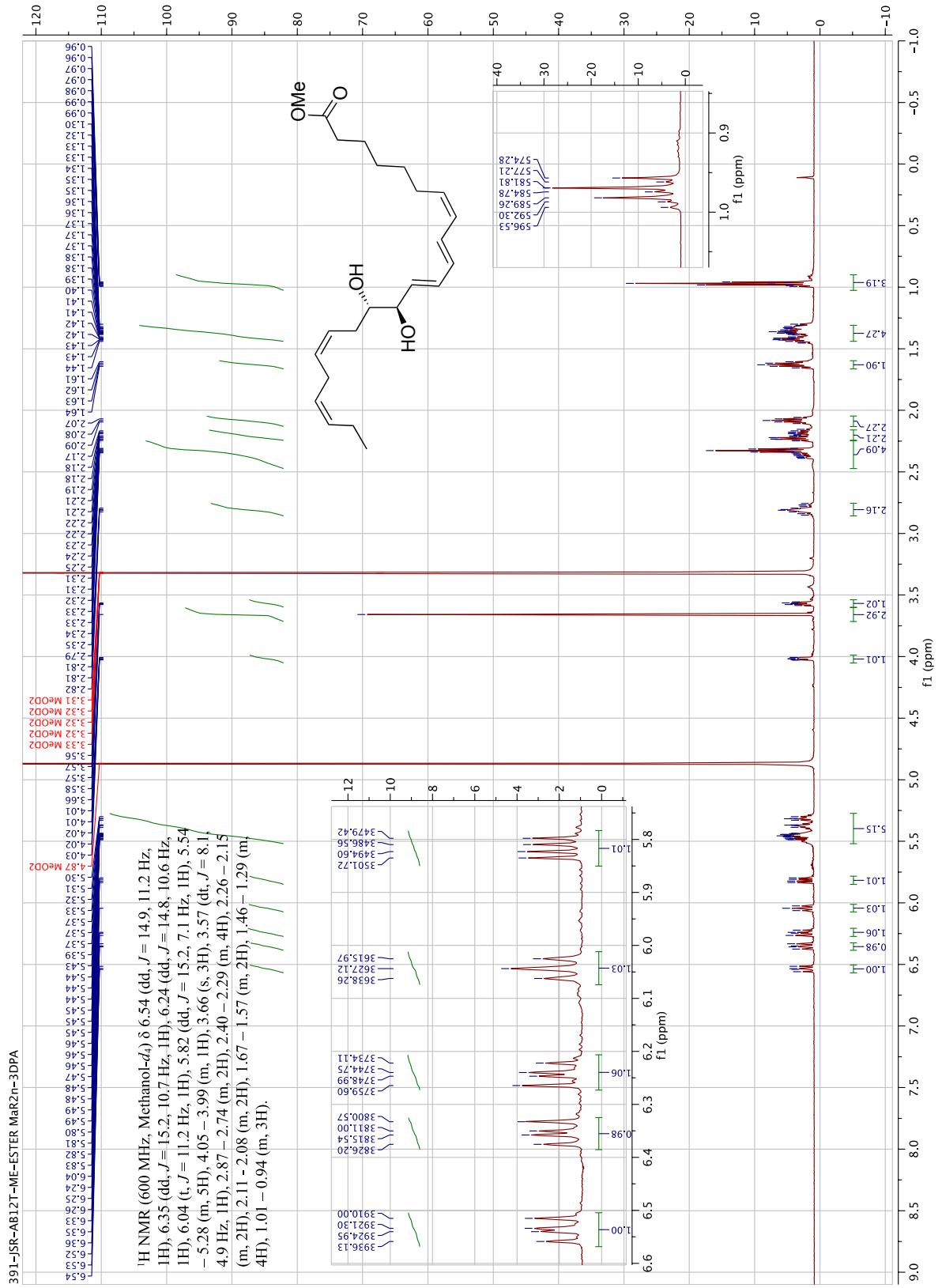

Figure A-29. ^{1}H NMR spectrum of compound **90**.

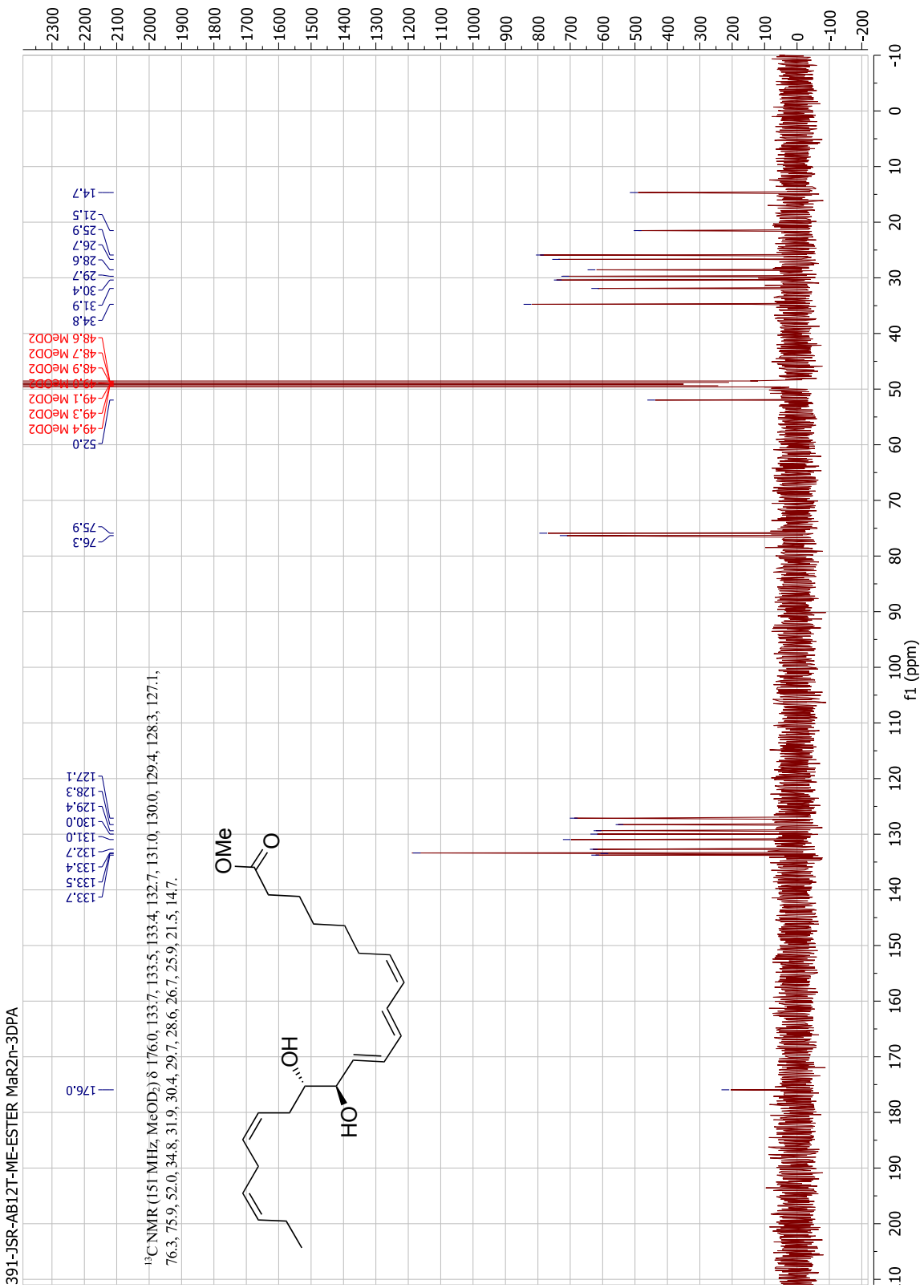

Figure A-30. ^{13}C NMR spectrum of compound **90**.

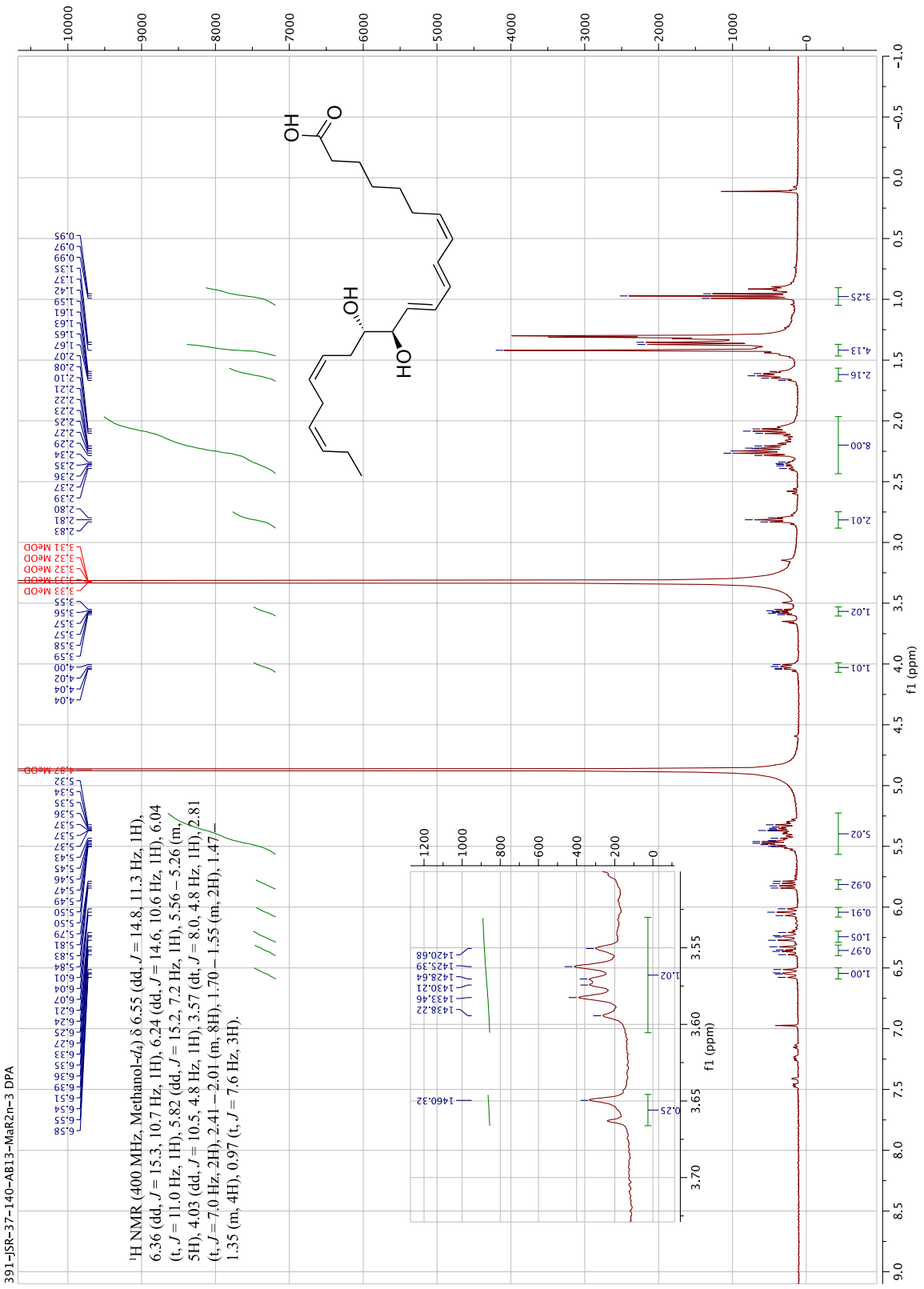

Figure A-31. ^{1}H NMR spectrum of compound **20**.

6.2 MS spectra of synthesized compounds

MS Spectrum Report

Analysis Info

Sample Name	391-JSR-10-41-AS	Acquisition Date	10/11/2018 1:25:51 PM
Method	ESI_pos_50_1500.m	Analysis Name	D:\Data\maxis2018\14549.d

Acquisition Parameter

Source Type	ESI	Ion Polarity	Positive	Set Nebulizer	0.4 Bar
Focus	Not active	Set Capillary	3500 V	Set Dry Heater	200 °C
Scan Begin	50 m/z	Set End Plate Offset	-500 V	Set Dry Gas	4.0 l/min
Scan End	1500 m/z	Set Charging Voltage	2000 V	Set Divert Valve	Waste
		Set Corona	0 nA	Set APCI Heater	0 °C

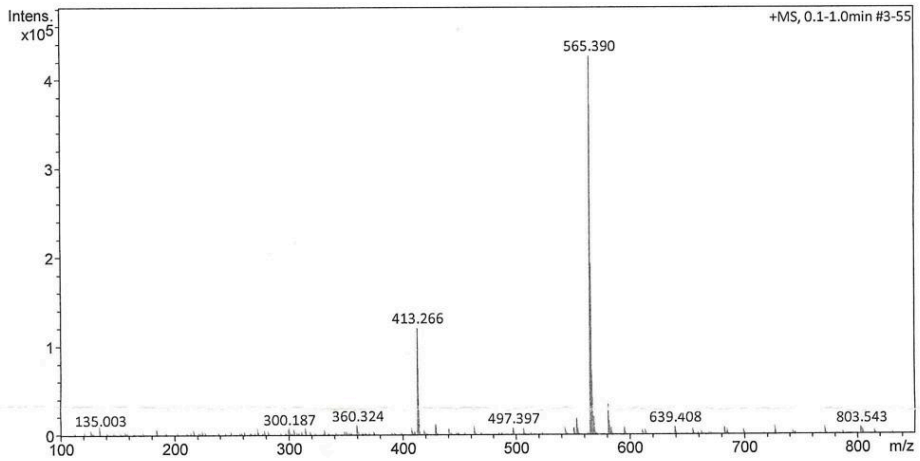

#	m/z	I %
1	360.324	2.5
2	413.266	28.2
3	414.270	7.3
4	429.240	3.0
5	497.397	1.8
6	507.329	1.6
7	551.356	1.8
8	553.459	4.4
9	554.463	1.7
10	565.390	100.0
11	566.392	45.0
12	567.390	15.9
13	568.391	4.9
14	581.364	8.0
15	582.366	3.5
16	583.364	1.8
17	595.382	1.9
18	639.408	2.1
19	683.434	1.8
20	803.543	1.8

14549.d
Bruker Compass DataAnalysis 4.3 printed: 10/11/2018 1:32:45 PM Page 1 of 1

Figure A-32. MS spectrum of compound **38**.

Elemental Analysis Report

Analysis Info

Sample Name	391-JSR-10-41-AS	Acquisition Date	10/11/2018 1:25:51 PM
Method	ESI_pos_50_1500.m	Analysis Name	D:\Data\maxis2018\14549.d

Acquisition Parameter

Source Type	ESI	Ion Polarity	Positive	Set Nebulizer	0.4 Bar
Focus	Not active	Set Capillary	3500 V	Set Dry Heater	200 °C
Scan Begin	50 m/z	Set End Plate Offset	-500 V	Set Dry Gas	4.0 l/min
Scan End	1500 m/z	Set Charging Voltage	2000 V	Set Divert Valve	Waste
		Set Corona	0 nA	Set APCI Heater	0 °C

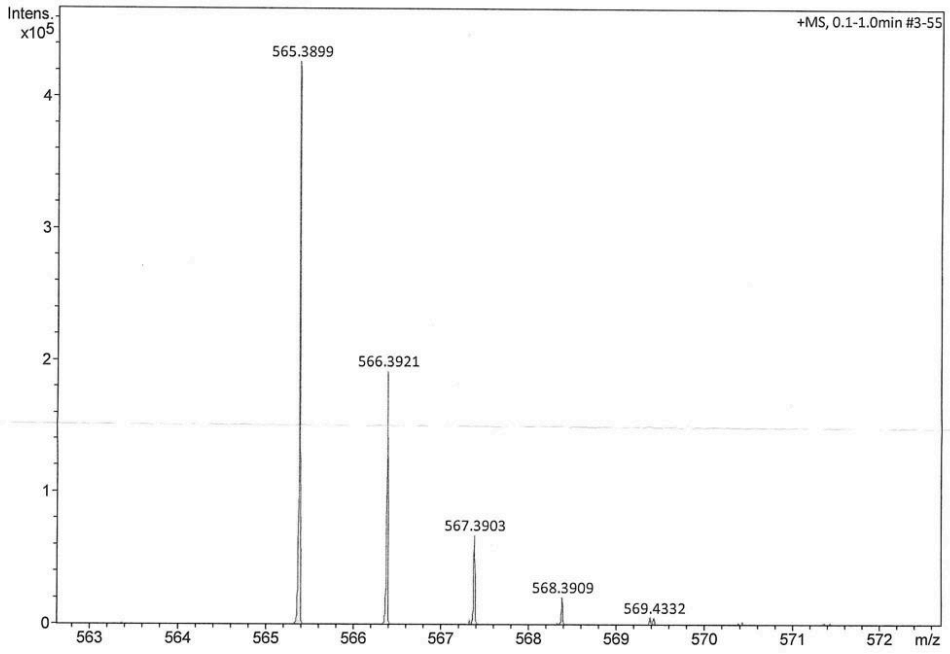

Meas. m/z	Ion Formula	m/z	err [ppm]
565.3899	C35H57O2Si2	565.3892	-1.3
	C27H57N6OSi3	565.3896	-0.5
	C29H62NaO3Si3	565.3899	-0.0
	C31H54N4NaO2Si	565.3908	1.6
	C29H49N10Si	565.3905	1.1
	C30H58NaO6Si	565.3895	-0.8
	C37H49N4O	565.3901	0.3
	C28H53N6O4Si	565.3892	-1.2
	C36H53O5	565.3888	-2.1

14549.d

Bruker Compass DataAnalysis 4.3 printed: 10/11/2018 1:31:39 PM Page 1 of 1

Figure A-33. HRMS spectrum of compound **38**.

MS Spectrum Report

Analysis Info

Sample Name	391-JSR-13-49-A6	Acquisition Date	10/25/2018 9:24:53 AM
Method	ESI_pos_50_1500_os.m	Analysis Name	D:\Data\maxis2018\14586.d

Acquisition Parameter

Source Type	ESI	Ion Polarity	Positive	Set Nebulizer	0.4 Bar
Focus	Not active	Set Capillary	3500 V	Set Dry Heater	200 °C
Scan Begin	50 m/z	Set End Plate Offset	-500 V	Set Dry Gas	4.0 l/min
Scan End	1500 m/z	Set Charging Voltage	2000 V	Set Divert Valve	Waste
		Set Corona	0 nA	Set APCI Heater	0 °C

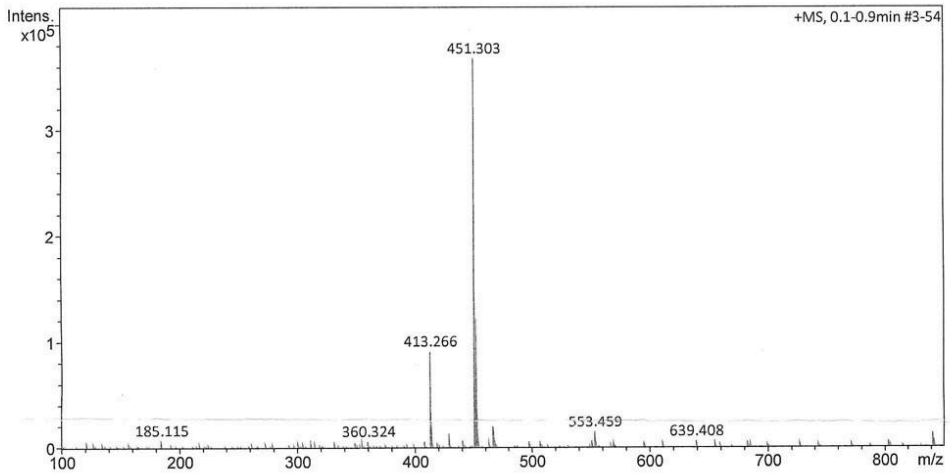

#	m/z	I %
1	185.115	2.0
2	360.324	1.6
3	413.266	24.9
4	414.270	6.5
5	429.240	3.5
6	441.298	1.9
7	451.303	100.0
8	452.306	33.2
9	453.303	8.8
10	454.305	2.2
11	467.277	5.4
12	468.280	1.7
13	507.329	1.7
14	551.355	1.8
15	553.459	4.2
16	595.382	1.7
17	639.408	1.7
18	803.543	1.7
19	841.580	3.6
20	842.583	2.2

Figure A-34. MS spectrum of compound **85**.

Elemental Analysis Report

Analysis Info

Sample Name	391-JSR-13-49-A6	Acquisition Date	10/25/2018 9:24:53 AM
Method	ESI_pos_50_1500_os.m	Analysis Name	D:\Data\maxis2018\14586.d

Acquisition Parameter

Source Type	ESI	Ion Polarity	Positive	Set Nebulizer	0.4 Bar
Focus	Not active	Set Capillary	3500 V	Set Dry Heater	200 °C
Scan Begin	50 m/z	Set End Plate Offset	-500 V	Set Dry Gas	4.0 l/min
Scan End	1500 m/z	Set Charging Voltage	2000 V	Set Divert Valve	Waste
		Set Corona	0 nA	Set APCI Heater	0 °C

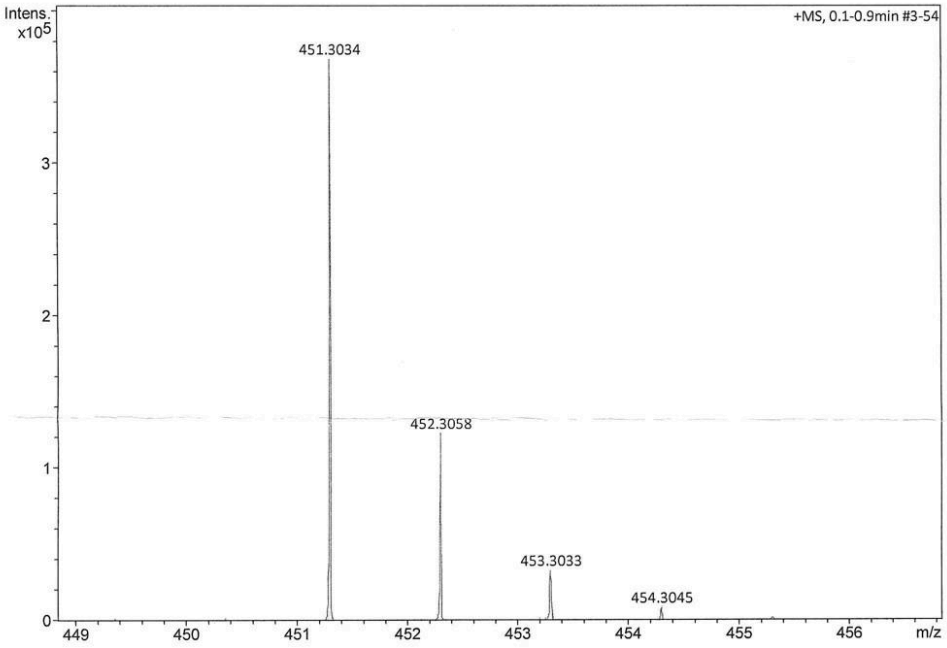

Meas. m/z	Ion Formula	m/z	err [ppm]
451.3034	C29H43O2Si	451.3027	-1.5
	C23H48NaO3Si2	451.3034	0.1
	C26H43O6	451.3054	4.5
	C25H40N4NaO2	451.3043	2.2
	C23H35N10	451.3041	1.6
	C24H44NaO6	451.3030	-0.8

14586.d
Bruker Compass DataAnalysis 4.3 printed: 10/25/2018 9:34:13 AM Page 1 of 1

Figure A-35. HRMS spectrum of compound **85**.

MS Spectrum Report

Analysis Info

Sample Name	391-JSR-18-67-A7	Acquisition Date	12/6/2018 9:10:01 AM
Method	ESI_pos_50_1500_os.m	Analysis Name	D:\Data\maxis2018\14762.d

Acquisition Parameter

Source Type	ESI	Ion Polarity	Positive	Set Nebulizer	0.4 Bar
Focus	Not active	Set Capillary	3500 V	Set Dry Heater	200 °C
Scan Begin	50 m/z	Set End Plate Offset	-500 V	Set Dry Gas	4.0 l/min
Scan End	1500 m/z	Set Charging Voltage	2000 V	Set Divert Valve	Waste
		Set Corona	0 nA	Set APCI Heater	0 °C

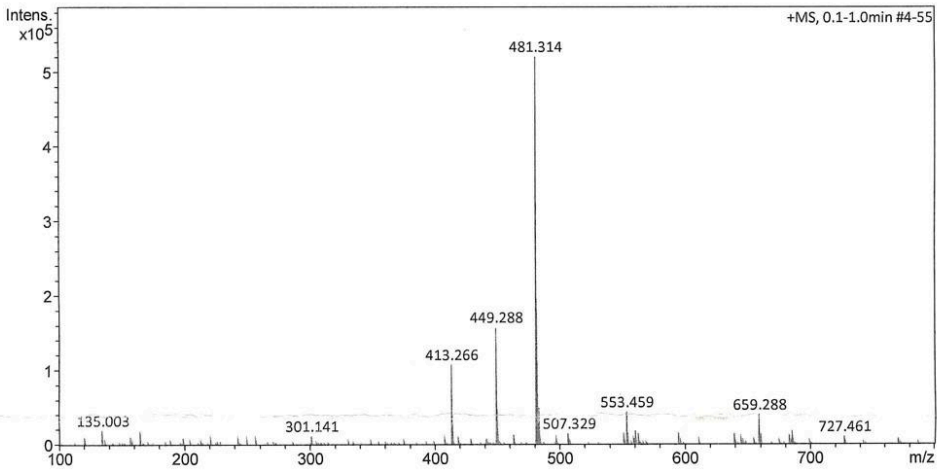

#	m/z	I %
1	135.003	3.8
2	164.920	3.6
3	413.266	20.8
4	414.270	5.6
5	449.288	30.3
6	450.290	9.9
7	481.314	100.0
8	482.316	34.9
9	483.314	9.7
10	507.329	3.0
11	551.356	3.2
12	553.459	8.5
13	554.463	3.3
14	560.892	3.6
15	562.890	2.8
16	595.382	3.1
17	639.408	3.0
18	659.288	7.8
19	660.291	2.8
20	685.436	3.5

Figure A-36. MS spectrum of compound **37**.

Elemental Analysis Report

Analysis Info

Sample Name	391-JSR-18-67-A7	Acquisition Date	12/6/2018 9:10:01 AM
Method	ESI_pos_50_1500_os.m	Analysis Name	D:\Data\maxis2018\14762.d

Acquisition Parameter

Source Type	ESI	Ion Polarity	Positive	Set Nebulizer	0.4 Bar
Focus	Not active	Set Capillary	3500 V	Set Dry Heater	200 °C
Scan Begin	50 m/z	Set End Plate Offset	-500 V	Set Dry Gas	4.0 l/min
Scan End	1500 m/z	Set Charging Voltage	2000 V	Set Divert Valve	Waste
		Set Corona	0 nA	Set APCI Heater	0 °C

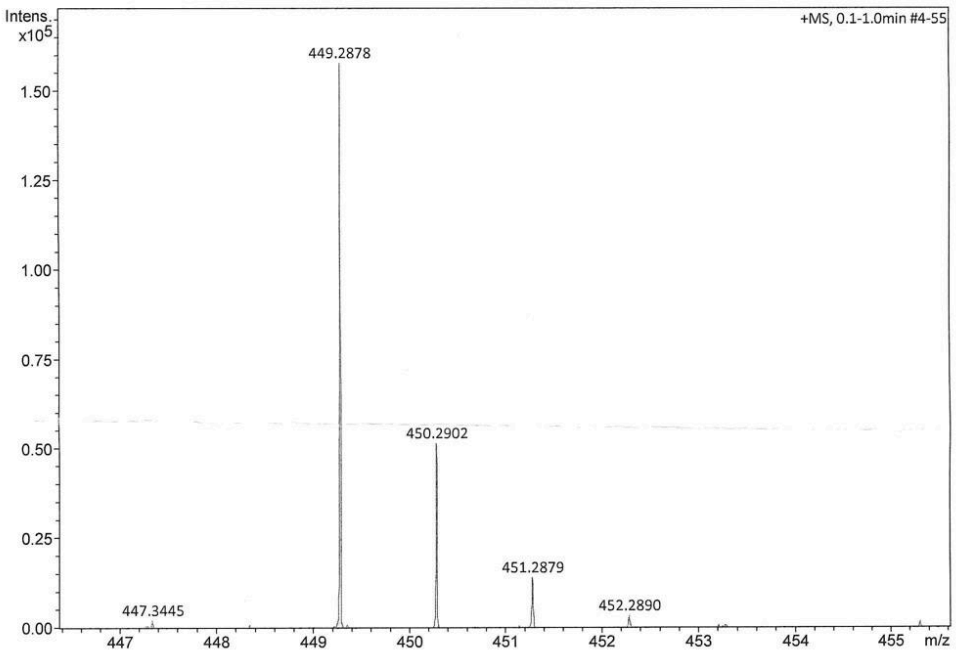

Meas. m/z	Ion Formula	m/z	err [ppm]
449.2878	C29H41O2Si	449.2870	-1.7
	C23H46NaO3Si2	449.2878	-0.0
	C26H41O6	449.2898	4.4
	C25H38N4NaO2	449.2887	2.0
	C23H33N10	449.2884	1.4
	C24H42NaO6	449.2874	-0.9

14762.d

Bruker Compass DataAnalysis 4.3 printed: 12/6/2018 9:15:15 AM Page 1 of 1

Figure A-37. HRMS spectrum of compound **37**.

MS Spectrum Report

Analysis Info

Sample Name	391-JSR-10-70-A8T	Acquisition Date	12/13/2018 1:47:34 PM
Method	ESI_pos_50_1500_os.m	Analysis Name	D:\Data\maxis2018\14797.d

Acquisition Parameter

Source Type	ESI	Ion Polarity	Positive	Set Nebulizer	0.4 Bar
Focus	Not active	Set Capillary	3500 V	Set Dry Heater	200 °C
Scan Begin	50 m/z	Set End Plate Offset	-500 V	Set Dry Gas	4.0 l/min
Scan End	1500 m/z	Set Charging Voltage	2000 V	Set Divert Valve	Waste
		Set Corona	0 nA	Set APCI Heater	0 °C

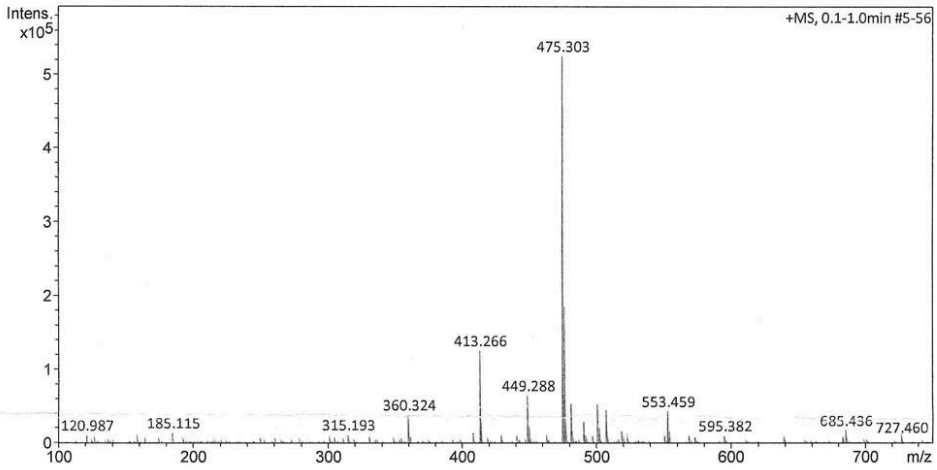

#	m/z	I %
1	360.324	7.4
2	408.309	2.6
3	413.266	23.9
4	414.270	6.5
5	449.288	12.3
6	450.290	4.1
7	475.303	100.0
8	476.306	35.6
9	477.304	9.7
10	481.314	10.3
11	482.316	3.7
12	491.277	5.5
13	501.319	10.0
14	502.322	3.9
15	507.330	8.6
16	508.332	3.0
17	519.330	3.1
18	553.459	8.3
19	554.463	3.2
20	685.436	3.3

14797.d
Bruker Compass DataAnalysis 4.3 printed: 12/13/2018 1:53:24 PM Page 1 of 1

Figure A-38. MS spectrum of compound **86**.

Elemental Analysis Report

Analysis Info

Sample Name	391-JSR-10-70-A8T	Acquisition Date	12/13/2018 1:47:34 PM
Method	ESI_pos_50_1500_os.m	Analysis Name	D:\Data\maxis2018\14797.d

Acquisition Parameter

Source Type	ESI	Ion Polarity	Positive	Set Nebulizer	0.4 Bar
Focus	Not active	Set Capillary	3500 V	Set Dry Heater	200 °C
Scan Begin	50 m/z	Set End Plate Offset	-500 V	Set Dry Gas	4.0 l/min
Scan End	1500 m/z	Set Charging Voltage	2000 V	Set Divert Valve	Waste
		Set Corona	0 nA	Set APCI Heater	0 °C

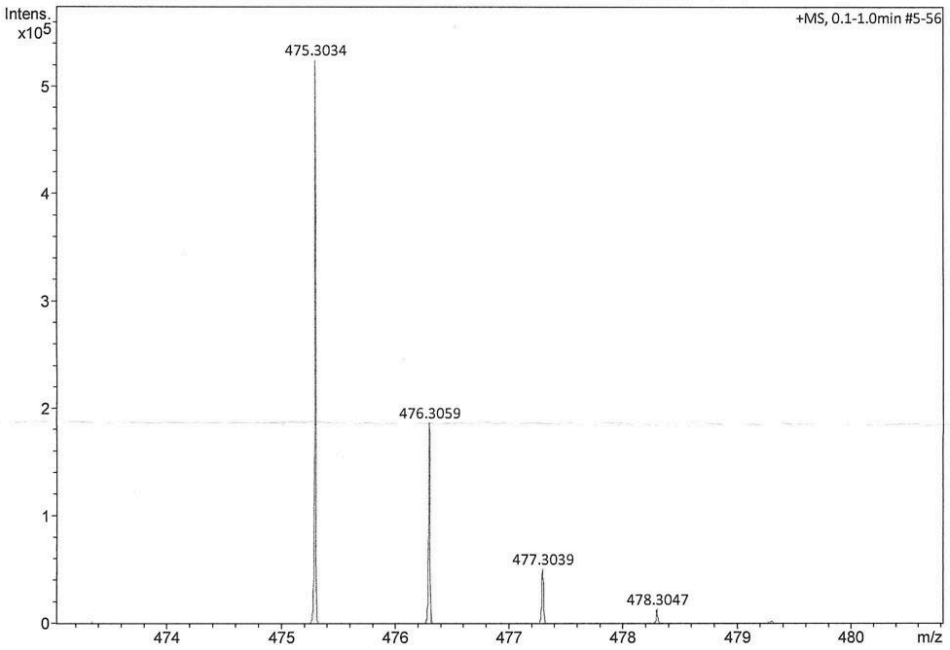

Meas. m/z	Ion Formula	m/z	err [ppm]
475.3034	C31H43O2Si	475.3027	-1.5
	C25H48NaO3Si2	475.3034	0.1
	C28H43O6	475.3054	4.3
	C27H40N4NaO2	475.3043	2.0
	C25H35N10	475.3041	1.4
	C26H44NaO6	475.3030	-0.8

14797.d

Bruker Compass DataAnalysis 4.3 printed: 12/13/2018 1:52:14 PM Page 1 of 1

Figure A-39. HRMS spectrum of compound **86**.

MS Spectrum Report

Analysis Info

Sample Name	391-JSR-23-80-A9T2	Acquisition Date	1/15/2019 10:43:06 AM
Method	ESI_pos_50_1500_os.m	Analysis Name	D:\Data\maxis2019\14896.d

Acquisition Parameter

Source Type	ESI	Ion Polarity	Positive	Set Nebulizer	0.4 Bar
Focus	Not active	Set Capillary	3500 V	Set Dry Heater	200 °C
Scan Begin	50 m/z	Set End Plate Offset	-500 V	Set Dry Gas	4.0 l/min
Scan End	1500 m/z	Set Charging Voltage	2000 V	Set Divert Valve	Waste
		Set Corona	0 nA	Set APCI Heater	0 °C

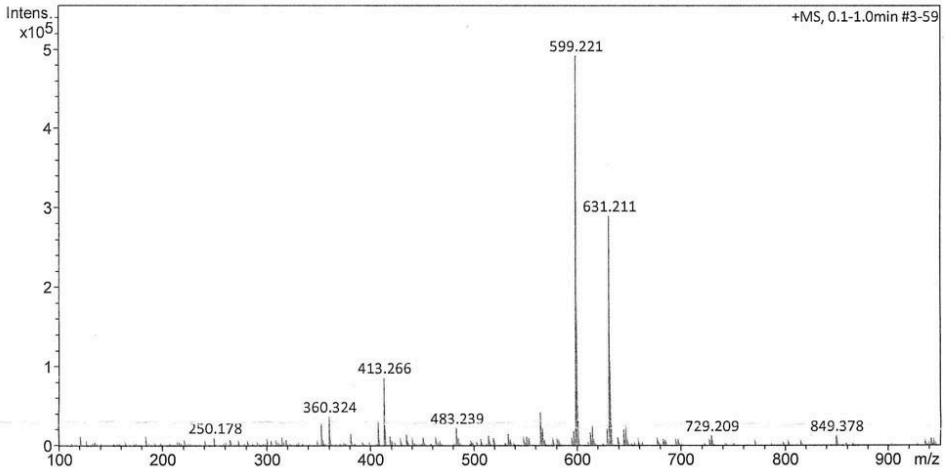

#	m/z	I %
1	353.266	5.8
2	360.324	7.6
3	408.308	6.3
4	413.266	17.4
5	414.270	4.7
6	483.239	4.6
7	565.335	8.6
8	567.315	4.6
9	597.325	3.9
10	599.221	100.0
11	600.223	36.8
12	601.221	10.4
13	615.195	5.1
14	629.195	4.5
15	629.231	4.3
16	631.211	58.9
17	632.213	21.9
18	633.212	6.5
19	645.226	4.2
20	647.185	5.5

Figure A-40. MS spectrum of compound **33**.

Elemental Analysis Report

Analysis Info

Sample Name	391-JSR-23-80-A9T2	Acquisition Date	1/15/2019 10:43:06 AM
Method	ESI_pos_50_1500_os.m	Analysis Name	D:\Data\maxis2019\14896.d

Acquisition Parameter

Source Type	ESI	Ion Polarity	Positive	Set Nebulizer	0.4 Bar
Focus	Not active	Set Capillary	3500 V	Set Dry Heater	200 °C
Scan Begin	50 m/z	Set End Plate Offset	-500 V	Set Dry Gas	4.0 l/min
Scan End	1500 m/z	Set Charging Voltage	2000 V	Set Divert Valve	Waste
		Set Corona	0 nA	Set APCI Heater	0 °C

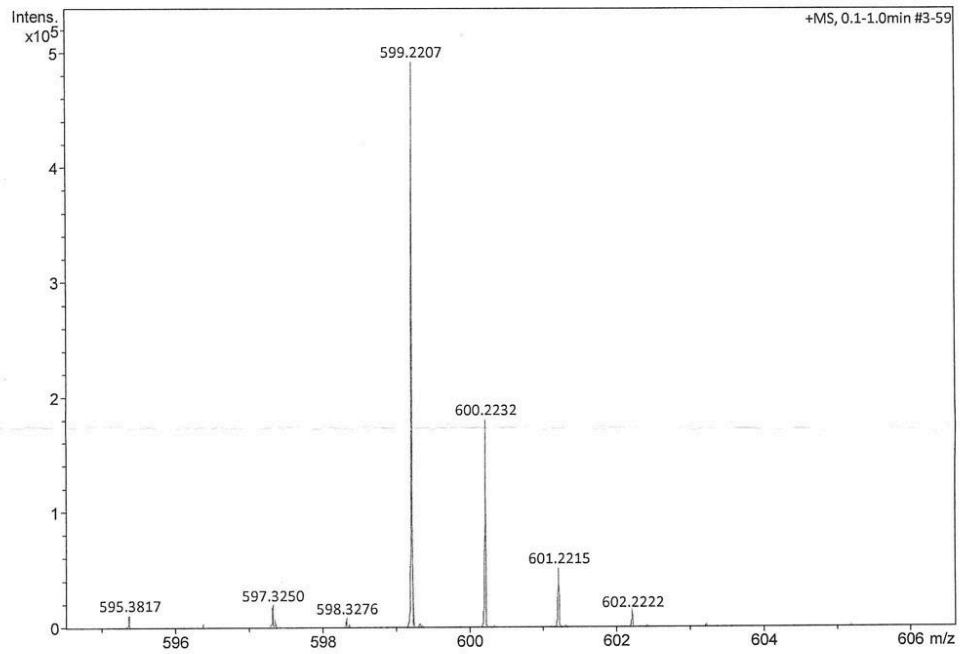

Meas. m/z	Ion Formula	m/z	err [ppm]
599.2207	C32H44IOSi	599.2201	-1.1
	C26H49INaO2Si2	599.2208	0.2
	C30H27N12OSi	599.2195	-2.1
	C26H24N16NaO	599.2211	0.7
	C32H32N6NaO3Si	599.2197	-1.6
	C28H36N2NaO11	599.2211	0.7
	C33H35N2O7Si	599.2208	0.2
	C26H31N8O9	599.2209	0.2
	C27H40N2NaO8Si2	599.2215	1.4
	C28H41IN4NaO	599.2217	1.7
	C27H45INaO5	599.2204	-0.5
	C42H31O4	599.2217	1.6
	C41H28N4Na	599.2206	-0.1
	C39H36NaOSi2	599.2197	-1.7

14896.d
Bruker Compass DataAnalysis 4.3 printed: 1/15/2019 10:53:55 AM Page 1 of 1

Figure A-41. HRMS spectrum of compound **33**.

MS Spectrum Report

Analysis Info

Sample Name	391-JSR-33-117-AB10.0P	Acquisition Date	2/13/2019 11:06:49 AM
Method	ESI_pos_50_1500_os.m	Analysis Name	D:\Data\maxis2019\15002.d

Acquisition Parameter

Source Type	ESI	Ion Polarity	Positive	Set Nebulizer	0.4 Bar
Focus	Not active	Set Capillary	3500 V	Set Dry Heater	200 °C
Scan Begin	50 m/z	Set End Plate Offset	-500 V	Set Dry Gas	4.0 l/min
Scan End	1500 m/z	Set Charging Voltage	2000 V	Set Divert Valve	Waste
		Set Corona	0 nA	Set APCI Heater	0 °C

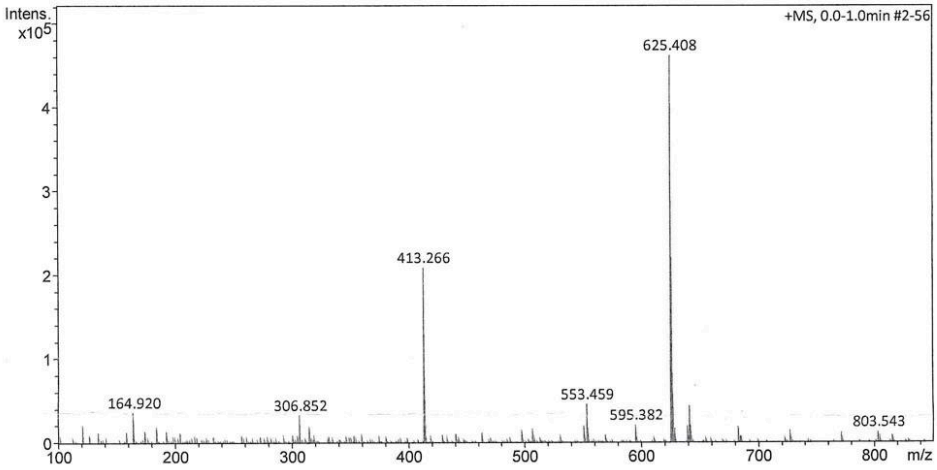

#	m/z	I %
1	120.987	4.6
2	164.920	8.0
3	185.115	4.0
4	306.852	7.3
5	315.193	4.3
6	413.266	45.3
7	414.270	12.2
8	507.329	3.6
9	551.356	4.4
10	553.459	10.0
11	554.463	3.8
12	595.382	4.7
13	625.408	100.0
14	626.410	47.8
15	627.410	14.4
16	628.410	3.8
17	639.408	4.5
18	641.382	9.7
19	642.384	4.6
20	683.434	4.2

Figure A-42. MS spectrum of compound **88**.

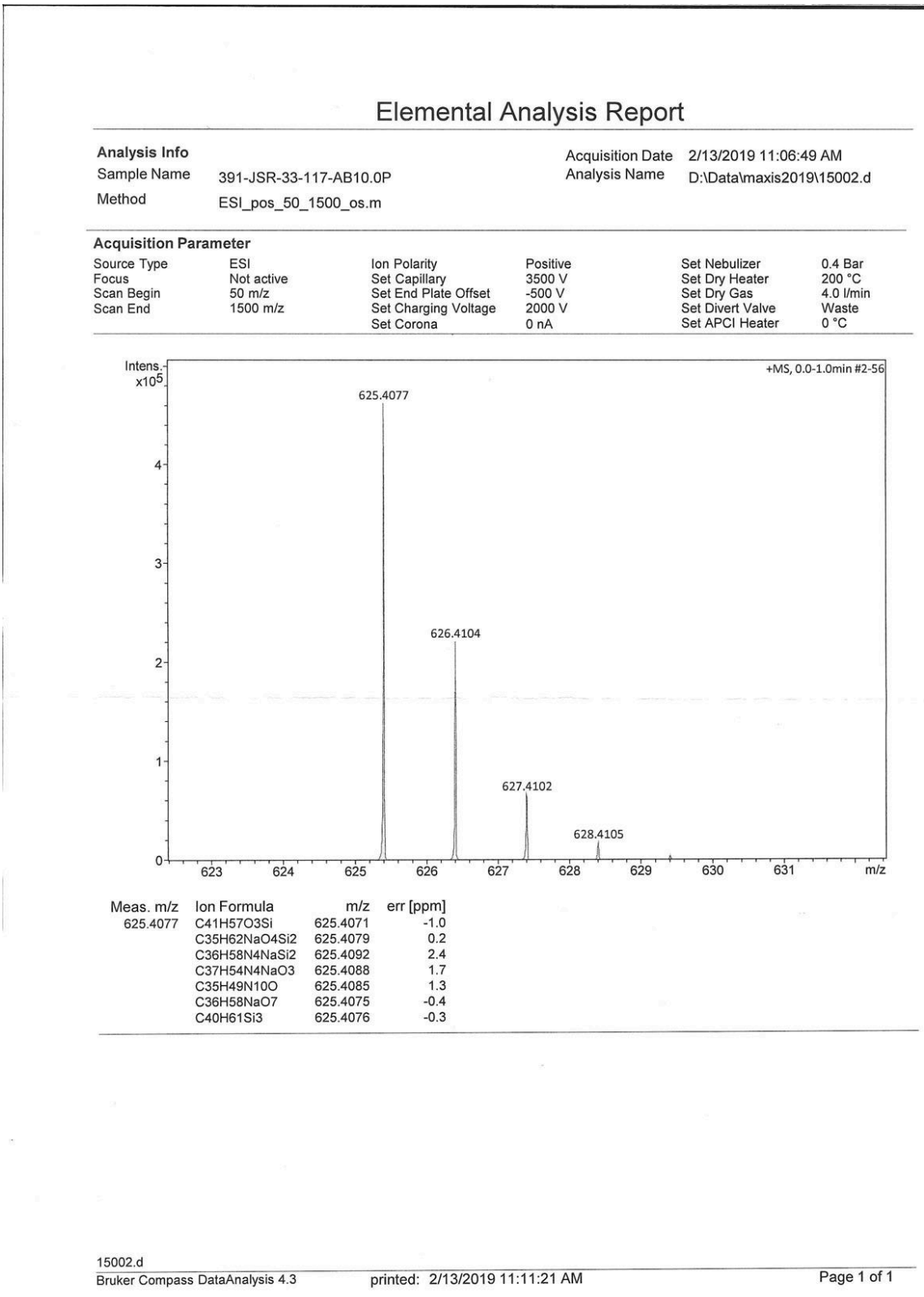

Figure A-43. HRMS spectrum of compound **88**.

MS Spectrum Report

Analysis Info

Sample Name	391-JSR-34-123-AB11	Acquisition Date	3/4/2019 9:25:02 AM
Method	ESI_pos_50_1500_os.m	Analysis Name	D:\Data\maxis2019\15089.d

Acquisition Parameter

Source Type	ESI	Ion Polarity	Positive	Set Nebulizer	0.4 Bar
Focus	Not active	Set Capillary	3500 V	Set Dry Heater	200 °C
Scan Begin	50 m/z	Set End Plate Offset	-500 V	Set Dry Gas	4.0 l/min
Scan End	1500 m/z	Set Charging Voltage	2000 V	Set Divert Valve	Waste
		Set Corona	0 nA	Set APCI Heater	0 °C

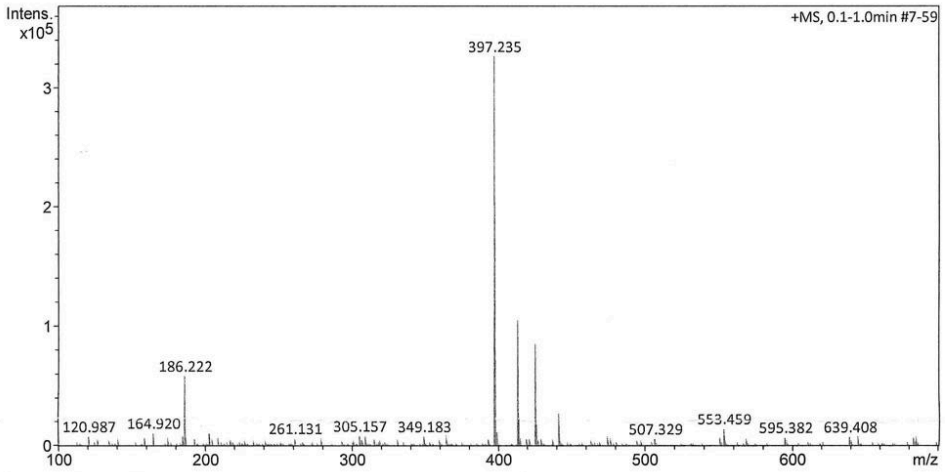

#	m/z	I %
1	120.987	2.4
2	164.920	3.3
3	185.115	2.7
4	186.222	18.0
5	187.225	2.5
6	203.053	3.3
7	305.157	2.6
8	349.183	2.4
9	397.235	100.0
10	398.238	25.2
11	399.241	3.7
12	413.209	8.2
13	413.266	32.3
14	414.270	8.6
15	425.287	26.4
16	426.291	6.6
17	441.298	8.7
18	442.301	2.5
19	553.459	4.4
20	639.408	2.3

15089.d
Bruker Compass DataAnalysis 4.3 printed: 3/4/2019 9:38:45 AM Page 1 of 1

Figure A-44. MS spectrum of compound **89**.

Elemental Analysis Report

Analysis Info

Sample Name	391-JSR-34-123-AB11	Acquisition Date	3/4/2019 9:25:02 AM
Method	ESI_pos_50_1500_os.m	Analysis Name	D:\Data\maxis2019\15089.d

Acquisition Parameter

Source Type	ESI	Ion Polarity	Positive	Set Nebulizer	0.4 Bar
Focus	Not active	Set Capillary	3500 V	Set Dry Heater	200 °C
Scan Begin	50 m/z	Set End Plate Offset	-500 V	Set Dry Gas	4.0 l/min
Scan End	1500 m/z	Set Charging Voltage	2000 V	Set Divert Valve	Waste
		Set Corona	0 nA	Set APCI Heater	0 °C

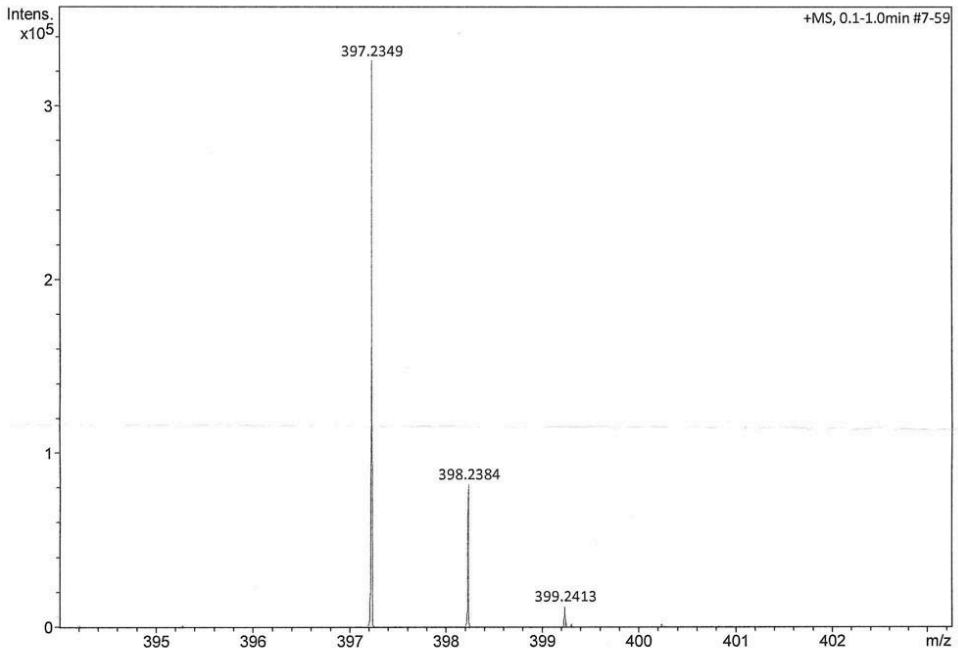

Meas. m/z	Ion Formula	m/z	err [ppm]
397.2349	C21H29N6O2	397.2347	-0.6
	C23H34NaO4	397.2349	0.1
	C19H30N6NaO2	397.2322	-6.7
	C20H33N2O6	397.2333	-4.0
	C25H33O4	397.2373	6.1
	C24H30N4Na	397.2363	3.5

15089.d
Bruker Compass DataAnalysis 4.3 printed: 3/4/2019 9:37:33 AM Page 1 of 1

Figure A-45. HRMS spectrum of compound **89**.

MS Spectrum Report

Analysis Info

Sample Name	391-JSR-34-126-AB12T	Acquisition Date	3/11/2019 11:55:40 AM
Method	ESI_pos_50_1500_os.m	Analysis Name	D:\Data\maxis2019\15144.d

Acquisition Parameter

Source Type	ESI	Ion Polarity	Positive	Set Nebulizer	0.4 Bar
Focus	Not active	Set Capillary	3500 V	Set Dry Heater	200 °C
Scan Begin	50 m/z	Set End Plate Offset	-500 V	Set Dry Gas	4.0 l/min
Scan End	1500 m/z	Set Charging Voltage	2000 V	Set Divert Valve	Waste
		Set Corona	0 nA	Set APCI Heater	0 °C

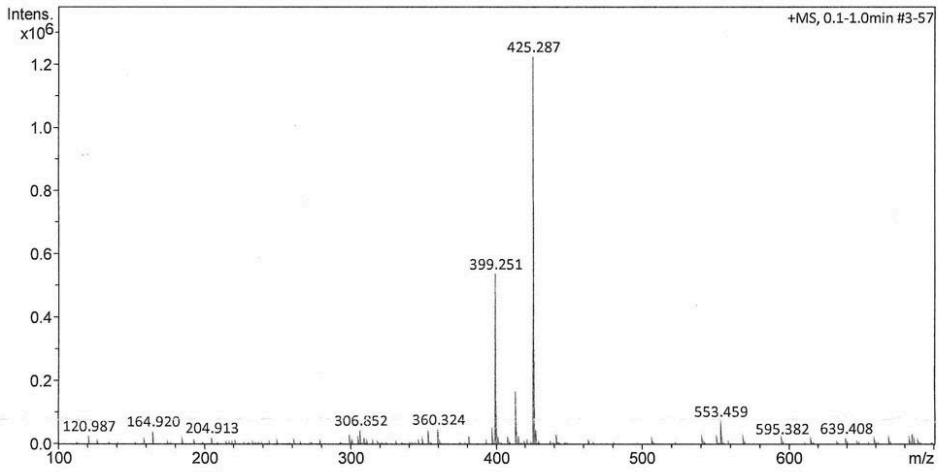

#	m/z	I %
1	120.987	2.2
2	164.920	3.4
3	299.183	2.5
4	306.852	3.6
5	353.266	3.6
6	360.324	3.9
7	397.235	4.3
8	399.251	43.9
9	400.254	11.3
10	408.309	2.1
11	413.266	13.8
12	414.270	3.7
13	415.225	2.0
14	425.287	100.0
15	426.291	24.9
16	427.293	3.9
17	441.262	2.6
18	553.459	6.1
19	554.463	2.4
20	685.436	2.6

15144.d

Bruker Compass DataAnalysis 4.3 printed: 3/11/2019 12:05:23 PM Page 1 of 1

Figure A-46. MS spectrum of compound **90**.

Elemental Analysis Report

Analysis Info

Sample Name	391-JSR-34-126-AB12T	Acquisition Date	3/11/2019 11:55:40 AM
Method	ESI_pos_50_1500_os.m	Analysis Name	D:\Data\maxis2019\15144.d

Acquisition Parameter

Source Type	ESI	Ion Polarity	Positive	Set Nebulizer	0.4 Bar
Focus	Not active	Set Capillary	3500 V	Set Dry Heater	200 °C
Scan Begin	50 m/z	Set End Plate Offset	-500 V	Set Dry Gas	4.0 l/min
Scan End	1500 m/z	Set Charging Voltage	2000 V	Set Divert Valve	Waste
		Set Corona	0 nA	Set APCI Heater	0 °C

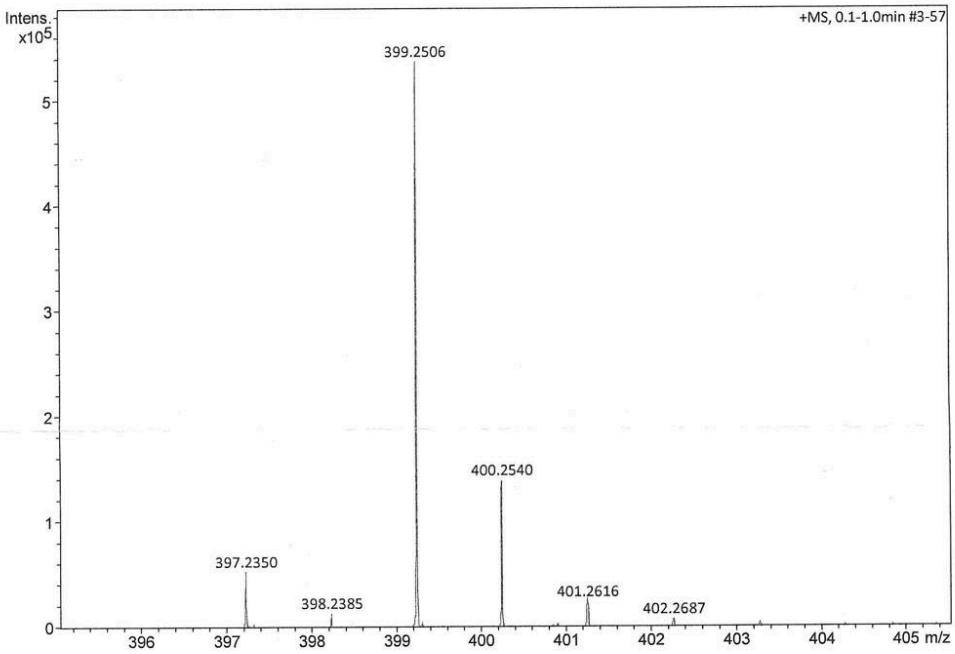

Meas. m/z	Ion Formula	m/z	err [ppm]
399.2506	C23H36NaO4	399.2506	0.1
	C21H31N6O2	399.2503	-0.6
	C25H35O4	399.2530	6.1
	C24H32N4Na	399.2519	3.4
	C20H35N2O6	399.2490	-4.0
	C19H32N6NaO2	399.2479	-6.7
	C17H27N12	399.2476	-7.4

15144.d
Bruker Compass DataAnalysis 4.3 printed: 3/11/2019 12:00:32 PM Page 1 of 1

Figure A-47. HRMS spectrum of compound **90**.

MS Spectrum Report

Analysis Info

Sample Name	391-JSR-37-140AB13	Acquisition Date	3/21/2019 2:02:15 PM
Method	ESI_pos_50_1500_os.m	Analysis Name	D:\Data\maxis2019\15214.d

Acquisition Parameter

Source Type	ESI	Ion Polarity	Positive	Set Nebulizer	0.4 Bar
Focus	Not active	Set Capillary	3500 V	Set Dry Heater	200 °C
Scan Begin	50 m/z	Set End Plate Offset	-500 V	Set Dry Gas	4.0 l/min
Scan End	1500 m/z	Set Charging Voltage	2000 V	Set Divert Valve	Waste
		Set Corona	0 nA	Set APCI Heater	0 °C

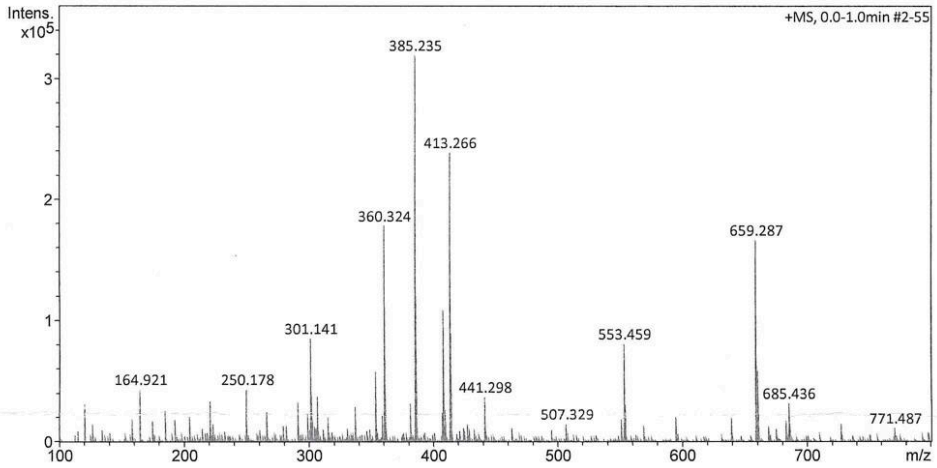

#	m/z	I %
1	164.921	13.6
2	221.175	10.5
3	250.178	13.7
4	291.193	10.4
5	301.141	26.7
6	302.245	12.2
7	306.852	11.9
8	353.266	18.4
9	360.324	55.7
10	361.327	13.6
11	381.298	10.0
12	385.235	100.0
13	386.238	24.2
14	408.308	33.9
15	413.266	74.7
16	414.270	20.4
17	441.298	11.7
18	553.459	25.3
19	659.287	52.1
20	660.291	18.6

15214.d
Bruker Compass DataAnalysis 4.3 printed: 3/21/2019 2:05:55 PM Page 1 of 1

Figure A-48. MS spectrum of compound **20**.

Elemental Analysis Report

Analysis Info

Sample Name	391-JSR-37-140AB13	Acquisition Date	3/21/2019 2:02:15 PM
Method	ESI_pos_50_1500_os.m	Analysis Name	D:\Data\maxis2019\15214.d

Acquisition Parameter

Source Type	ESI	Ion Polarity	Positive	Set Nebulizer	0.4 Bar
Focus	Not active	Set Capillary	3500 V	Set Dry Heater	200 °C
Scan Begin	50 m/z	Set End Plate Offset	-500 V	Set Dry Gas	4.0 l/min
Scan End	1500 m/z	Set Charging Voltage	2000 V	Set Divert Valve	Waste
		Set Corona	0 nA	Set APCI Heater	0 °C

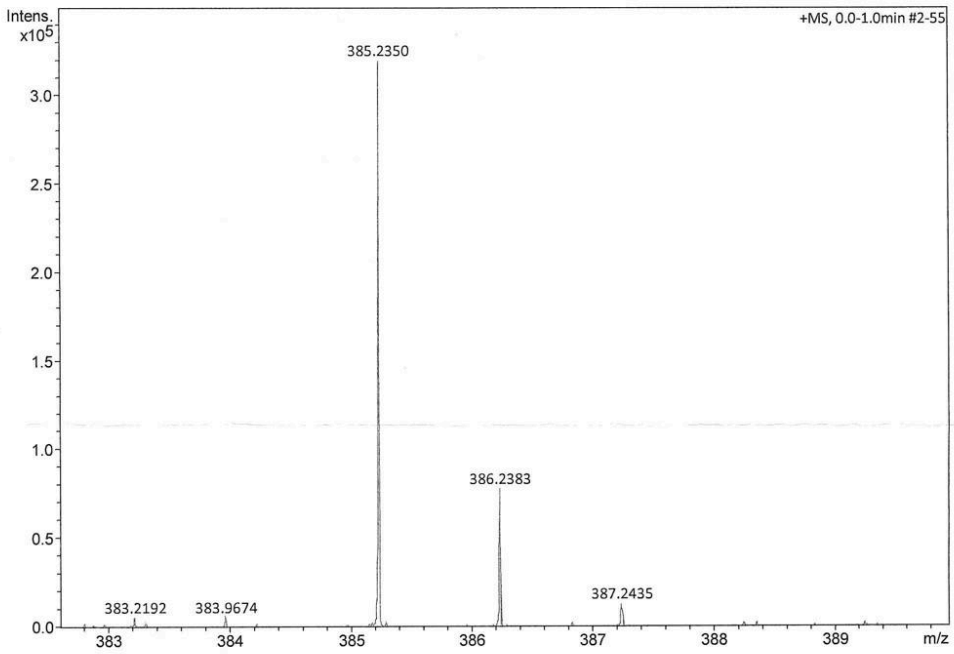

Meas. m/z	Ion Formula	m/z	err [ppm]
385.2350	C22H34NaO4	385.2349	-0.1
	C20H29N6O2	385.2347	-0.8
	C19H33N2O6	385.2333	-4.3
	C23H30N4Na	385.2363	3.4

Figure A-49. HRMS spectrum of compound **20**.

6.3 HPLC spectra of the synthesized compounds

```
Data File C:\CHEM32\1\DATA\JEANNE\ME-ESTER-MAR2N-3DPA_01.D
 Sample Name: ME-ESTER-MaR2n-3DPA_01

    ======================================================================
    Acq. Operator   : JEANNE
    Acq. Instrument : Instrument 1                    Location : Vial 1
    Injection Date  : 25.03.2019 16:02:44
                                                    Inj Volume : 20 µl
    Acq. Method     : C:\CHEM32\1\METHODS\MARIE_STABILITET_ISOKRATISK.M
    Last changed    : 25.03.2019 16:00:48  by JEANNE
                      (modified after loading)
    Analysis Method : C:\CHEM32\1\METHODS\MARIE_STABILITET_ISOKRATISK.M
    Last changed    : 26.03.2019 12:26:06  by RENATE
                      (modified after loading)
```

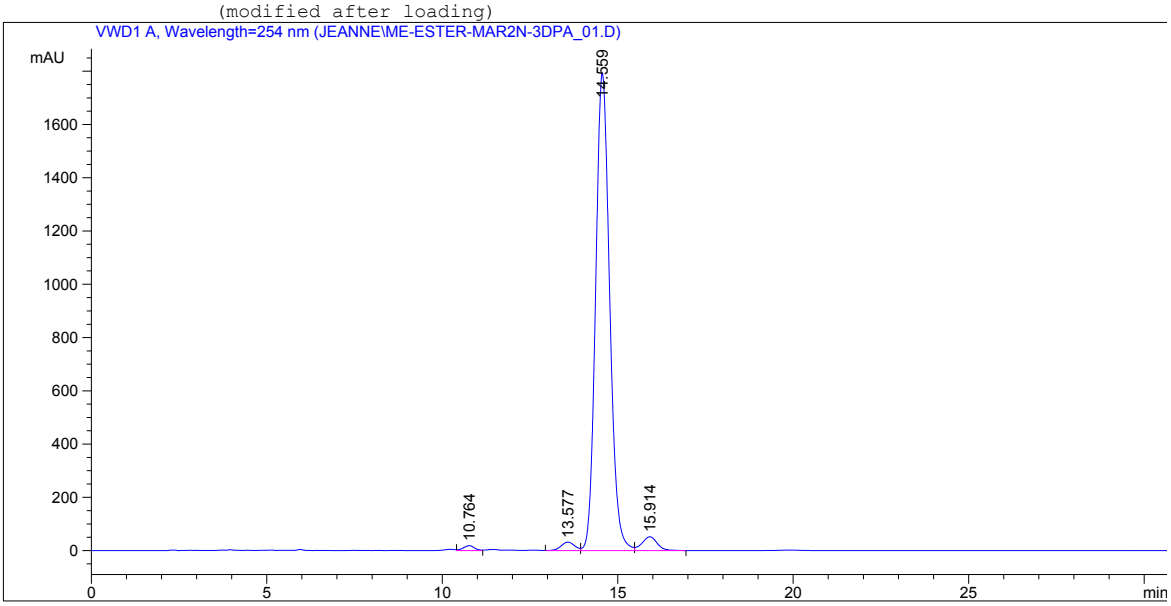


```
    ======================================================================
                              Area Percent Report
    ======================================================================

    Sorted By             :      Signal
    Multiplier            :      1.0000
    Dilution              :      1.0000
    Use Multiplier & Dilution Factor with ISTDs


    Signal 1: VWD1 A, Wavelength=254 nm

    Peak RetTime Type  Width     Area      Height     Area
      #   [min]        [min]  mAU   *s    [mAU   ]      %
    ----|-------|----|-------|----------|----------|--------|
       1  10.764 VV    0.3366  406.35724   18.37789   0.7740
       2  13.577 VV    0.4131  843.81006   31.64031   1.6072
       3  14.559 VV    0.4295 4.96954e4  1793.79358  94.6526
       4  15.914 VB    0.4584 1557.35388   51.81688   2.9662

    Totals :                  5.25029e4  1895.62866


    ======================================================================
                              *** End of Report ***


Instrument 1 26.03.2019 12:26:37  RENATE                    Page   1 of 1
```

Figure A-50. HPLC spectrum of compound **90**.

6.4 UV spectra of synthesized compounds

Spectrum/Peak Report Date 3/26/2019 Time 09:38:21 Page 1 of 1

Method file : <method not saved>
Information : Default Method
Data File : <data not saved>

Overlaid Spectra:

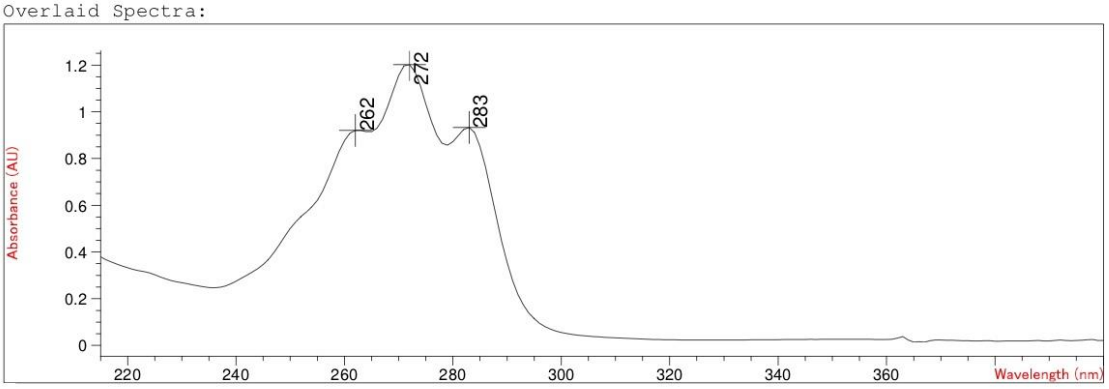

#	Name	Peaks(nm)	Abs(AU)
1		272.0	1.20180
1		283.0	0.93226

#	Name	Peaks(nm)	Abs(AU)
1		262.0	0.92076

Report generated by : Signature: .....

*** End Spectrum/Peak Report ***

Figure A-51. UV spectrum of compound **90**.

Spectrum/Peak Report Date 3/27/2019 Time 10:29:46 Page 1 of 1

Method file : <method not saved>
Information : Default Method
Data File : <data not saved>

Overlaid Spectra:

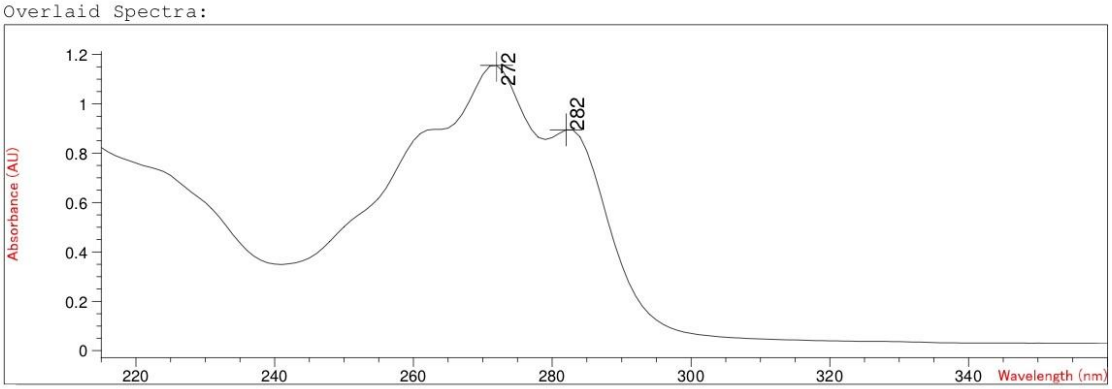

#	Name	Peaks(nm)	Abs(AU)	#	Name	Peaks(nm)	Abs(AU)
1		272.0	1.15580	1		***	***
1		282.0	0.89456	1		***	***
1		***	***	1		***	***
1		***	***	1		***	***
1		***	***	1		***	***

Report generated by : Signature: .....

*** End Spectrum/Peak Report ***

Figure A-52. UV spectrum of compound **20**.

Norges miljø- og biovitenskapelige universitet
Noregs miljø- og biovitskapelege universitet
Norwegian University of Life Sciences

Postboks 5003
NO-1432 Ås
Norway